ABSTRACT

NATZKE, JACE MICHAEL. Ethylene Production by *Azotobacter vinelandii*: Microbial Physiology, Bioprocess Development, and Other Unique Insights (Under the direction of José M. Bruno-Bárcena).

Azotobacter vinelandii is a Gram-negative, aerobic bacterium that has long been studied for its production of many industrially relevant compounds. Recently, it was discovered that its' vanadium nitrogenase is capable of reductively coupling molecules of carbon monoxide into ethylene and other hydrocarbons of various lengths. However, the cultivation methods currently employed severely restrict the production potential of this technology. Therefore, we aimed to re-design and optimize this process with the overall goal of generating a system capable of continuous bio-ethylene generation.

In order to accomplish this goal, we developed a unique method to monitor real-time nitrogenase activity from uptake hydrogenase, PHB deficient mutants of *A. vinelandii* by measuring hydrogen evolution. Using these insights, we optimized a two-stage chemostat system for the continuous cultivation of *A. vinelandii* in the presence of air enriched with 5% carbon monoxide; which was a major breakthrough considering that concentrations of carbon monoxide above 0.2% normally cause complete cessation of cell proliferation in batch cultures. Utilizing our system, we were able to continuously generate ethylene at a yield of 302 μg g^{-1} glucose consumed.

Additionally, we generated a stable *A. vinelandii* mutant carrying a translational fusion complex between the poly3-hydroxybutryate synthase gene and the ethylene-forming enzyme gene. Once expressed, these recombinant nanobeads acted as a proof-of-concept for both heterologous enzyme expression to generate bio-functional PHB nanobeads as well as a new metabolic pathway for *in vivo* ethylene production by *Azotobacter vinelandii*.

In total, the advances entailed in this work have significantly increased the economic potential of this microorganism.

Ethylene Production by *Azotobacter vinelandii*: Microbial Physiology, Bioprocess Development, and Other Unique Insights

by
Jace Michael Natzke

A dissertation submitted to the Graduate Faculty of
North Carolina State University
in partial fulfillment of the
requirements for the degree of
Doctor of Philosophy

Microbiology

Raleigh, North Carolina
2020

APPROVED BY:

_____	_____
José M. Bruno-Bárcena Committee Chair	Amy M. Grunden
_____	_____
Mari S. Chinn	Kelly D. Zering

BIOGRAPHY

Jace Natzke was born in Colorado and spent much of his childhood exploring the surrounding Rocky Mountain landscape. In the early 2000s, he moved to east Tennessee where he completed grade school and enrolled at the University of Tennessee. In his first year, he became interested in studying the complex metabolisms of microorganisms. It was amazing to him that no matter how toxic a compound was, there always seemed to be a bacterium out there capable of degrading it. In order to pursue these interests, he participated heavily in undergraduate research opportunities; studying yeast cell receptors and ocean-dwelling oil-degrading microorganisms. In the Spring of 2014, he finished his Bachelor of Science degree in Microbiology and graduated Summa Cum Laude.

After graduation, he received the unique opportunity to work at Oak Ridge National Laboratory investigating the interaction between *Clostridium thermocellum* and biomass crops, like switchgrass and poplar, for the production of second-generation biofuels. It was during this time he realized he needed a higher level of training if he wanted to make an impact in the field. Therefore, he decided to pursue a doctoral degree in Microbiology at North Carolina State University. Once enrolled, he began working in the Bruno-Bárcena lab; studying the physiology of *Azotobacter vinelandii*. His work during his time is detailed herein.

ACKNOWLEDGMENTS

Completing the research and writing requirements necessary for a dissertation is not an easy task and one person could not do it alone. First, I would like to thank my dad, Michael. None of this would have been possible without him. He raised me to question the way things are and always provided me with a positive example of how to live life. I would also like to thank the rest of my family (Rachel, Diana, Mom, Grammy and Grampy, the Nelsons, the Hansens, Wayne and Patty, Annette, and many others) for always being there for me.

To my mentor, José, thank you for always challenging me. Your constant mentorship over the past four years has allowed me to grow both as a scientist and as a person. Finally, to Stephanie and Hunter, thank you for your steadfast friendship and for all the laughs we shared together. I would not have made it through graduate school without you two.

TABLE OF CONTENTS

LIST OF TABLES

LIST OF FIGURES

CHAPTER 1. *Azotobacter vinelandii*: A Promising Biocatalyst for the Production of many Industrially Relevant Compounds

Introduction

Since the beginning of the industrial revolution, mankind has been dependent on finite petrochemicals to power everyday life and to provide a high standard of living. From gasoline to plastics, the petrochemical industry is involved in almost every aspect of day-to-day life. As global reserves for these materials are depleted, the demand for alternative renewable replacements will only increase[1,2]. As scientists, we are tasked with anticipating these future problems and developing solutions in advance.

Several renewable strategies (including wind, solar, and hydro) have been developed over the past century as a replacement for gasoline and coal-burning electricity with varying degrees of economic success[3]. Alternatively, there has been limited consideration for renewable generation of petrochemical precursors, such as ethylene, which are used in the production of many important consumer products including: plastics, pharmaceuticals, textiles, and electronics. Production of ethylene has traditionally been accomplished by pyrolyzing crude oil in a process called thermal cracking. However, the advent of hydraulic fracturing of shale rock has allowed production to increase immensely over the past decade[4]; along with a host of environmental problems[5-7].

Microorganisms have long been studied for their potential as 'biorefineries' for the industrial production of bulk chemicals and fuels, with some commercial success[8-10]. These methods are attractive because they usually do not require high temperatures or pressures to operate and generally are able to produce high purity products with minimal environmental impact. Therefore, one potential alternative for the industrial production of ethylene could be microbial biorefineries. One organism that has recently gained interest in this respect is *Azotobacter vinelandii*; which has shown the potential to produce ethylene, as well as many other industrially-relevant compounds.

General Characteristics of *Azotobacter vinelandii*

Central metabolism, cellular respiration, and respiratory protection

Azotobacters are generally root-colonizing microorganisms that are found in cool, temperate soils throughout the world[11]. These environments are typically limited by carbon

availability[12] which has resulted in these organisms developing the capability of utilizing a wide range of carbon sources including: sugars, alcohols, and phenolic acids[13-17]. For the more common carbohydrates, like glucose, the cells utilize a H^+-coupled symporter (*gluP*) to bring the sugar monomers into the cell[18]. Once inside the cell, the glucose is primed by glucokinases to form glucose-6-phosphate which enters glycolysis through the Entner-Doudoroff pathway and is ultimately converted into two molecules of pyruvate[19]; releasing 2 molecules of ATP, NADH, and NADPH[20]. Each pyruvate is then converted into acetyl-CoA, using a pyruvate dehydrogenase complex[21], which then enters the TCA cycle where 3 molecules of NADH, 1 molecule of $FADH_2$, and 1 molecule of GTP are formed. Finally, the electron carrying molecules, $FADH_2$ and NADH, move to the electron transport chain (ETC) where the electrons are donated to flavin-dependent dehydrogenases which then transfer electrons down the ETC; ultimately being donated to oxygen. This transfer of electrons is coupled with the translocation of protons across the cell membrane which generates a proton motive force (PMF) that is used for ATP production via an ATP synthase[22]. Thus, *A. vinelandii* is capable of converting a single molecule of glucose into approximately 28-30 molecules of ATP.

$$C_6H_{12}O_6 + 6\ O_2 \rightarrow 6\ CO_2 + 6\ H_2O + 28 - 30\ ATP$$

The ETC in *A. vinelandii* is made up of three major stages: (1) electron transfer from NADH / $FADH_2$ to dehydrogenases, (2) electron transfer from dehydrogenases to a ubiquinone-8 pool, and finally (3) electron transfer from the ubiquinone pool to terminal cytochrome oxidases where oxygen is reduced to water[23]. While seemingly straight-forward, there are actually two distinct branches of this ETC in *A. vinelandii* and their expression is regulated by the state of oxygen stress the cell is experiencing[24]. Under oxygen limiting conditions, the NADH dehydrogenase I and cytochrome c_4/c_5 branch is active and the cells generate PMF and ATP as expected. However, when oxygen stress is high, the cells switch expression of the ETC to the NADH dehydrogenase II and cytochrome *bd* oxidase branch. This branch is virtually decoupled from proton translocation but maintains high O_2 consumption rates and acts as a 'vacuum' sucking up any available intracellular O_2 at the cost of PMF and ATP production[25-27]. This defensive maneuver by the cells is commonly referred to as respiratory protection and is thought to be responsible for facilitating the somewhat unique ability of Azotobacters to fix nitrogen in aerobic environments. Furthermore, these cells are capable of sustaining incredibly high rates of

respiration which increases the effectiveness of the system; rapidly converting any harmful intracellular O_2 into water[28].

Poly-3-hydroxybutryate production and regulation

Another aspect of *A. vinelandii* physiology that is tightly controlled by the presence or absence of oxygen is the production of poly-3-hydroxybutyrate (PHB). This polyester acts as a carbon / energy storage mechanism for *A. vinelandii* and is produced by three main enzymes: β-ketothiolase (PhbA), acetoacetyl-CoA reductase (PhbB), and PHB synthase (PhbC). Under oxygen limiting conditions and upon entering the late exponential growth phase, acetyl-CoA is diverted away from central metabolism by PhbA; condensing two molecules of acetyl-CoA into acetoacetyl-CoA. This condensation is then followed by a reduction of the primary carbonyl group of acetoacetyl-CoA by PhbB to form hydroxybutyryl-CoA monomers; which are then polymerized by PhbC[29-32]. At the beginning of polymer formation, the PHB granules are localized at the inner site of the cytoplasmic membrane and gradually diffuse throughout the cell overtime[33]. As nutrients become scarce and time in stationary phase is prolonged, *A. vinelandii* utilizes several PHB depolymerases and the succinyl-CoA transferase to revert PHB granules back into acetyl-CoA in order to increase flux through the TCA cycle for ATP generation[34,35] (Figure 1.1).

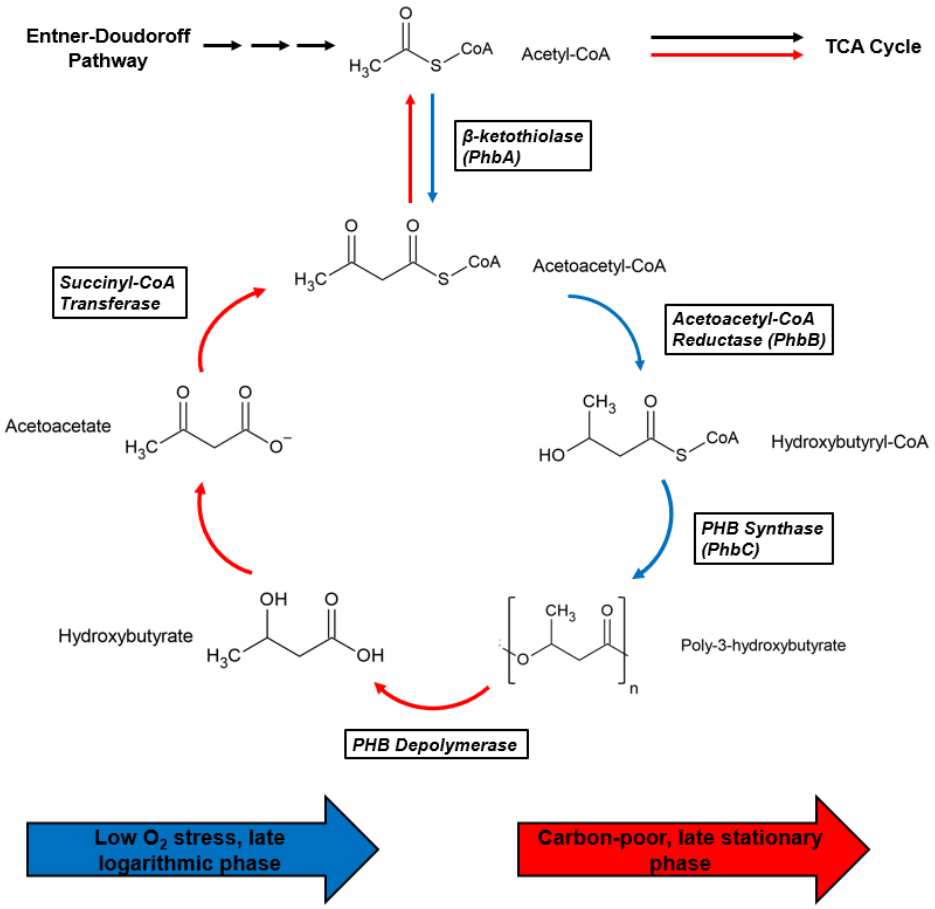

Figure 1.1. Schematic depicting the PHB metabolic pathway in *Azotobacter vinelandii*. Blue arrows indicate the path for PHB synthesis, which occurs during the late logarithmic growth phase under low oxygen stress. Red arrows show the path for PHB re-assimilation into central metabolism, which occurs in late stationary phase when carbon sources are exhausted.

Due to this polymer's importance to overall cellular physiology and carbon metabolism, the process is heavily regulated at both the transcriptional and translational levels. Two of the major transcriptional activators of PHB production in *A. vinelandii* are RpoS and PhbR. At the end of the exponential growth phase, sigma factor RpoS is induced which promotes the expression of the AraC-family transcriptional activator PhbR[36,37]. This activator then binds to the direct repeated sequence, TGTCACCAA-N_4-CACTA, in the *phbB* promoter region which recruits RNA polymerase to drive transcription through the PHB synthesis gene cluster[37,38]. For transcriptional repression, *A. vinelandii* utilizes CydR, an FNR-like global regulator. This protein

contains oxygen-responsive Fe-S metal clusters and acts as a repressor to *phbB* and *phbA* transcription[24,38,39].

For translational regulation, *A. vinelandii* utilizes both the Gac/Rsm and ArrF systems to control PHB production. The Gac/Rsm system is a 'light switch' mechanism that is balanced between the translational repressor RsmA, which sequesters and prevents translation of *phbR* and *phbB* transcripts under normal growth conditions, and the GacA-induced small interfering RNAs that prevent RsmA activity during stationary phase[40,41]. The ArrF system, which is the most potent method for post-transcriptional repression of PHB synthesis, consists of the iron-responsive small RNA ArrF[42] that prevents translation of several key PHB-associated transcripts (*phbR, phbF,* and *phbP*) by binding to the Shine-Dalgarno sequences of the associated mRNAs[43,44]. Deletion of the *arrF* gene causes a decrease in the premature degradation of these transcripts which allows these mutants to produce over 300-fold more PHB than the wild-type[43].

Alginate production and regulation

In addition to PHB synthesis, *A. vinelandii* produces and exports alginate, which is a linear exopolysaccharide[45] (Figure 1.2) that is required for cyst formation in many Gram-negative microorganisms[46,47]. Cysts are endospore-like structures that are produced during times of stress and consist of a central body, containing the chromosome and other essential proteins, encapsulated by two protective coatings: a thick, rigid outer layer and a low-density, homogenous inner layer[47]. Once cyst formation is complete, which takes approximately five days[48], the metabolically-dormant cells become highly resistant to many environmental stresses including: heat, ultraviolet irradiation, sonication, and desiccation[49]. Furthermore, alginate production seems to be correlated with low transformation efficiencies in *A. vinelandii*; likely due to the 'gummy' nature of the exported alginate polymer which prevents exogenous DNA molecules from reaching the cell surface[50,51].

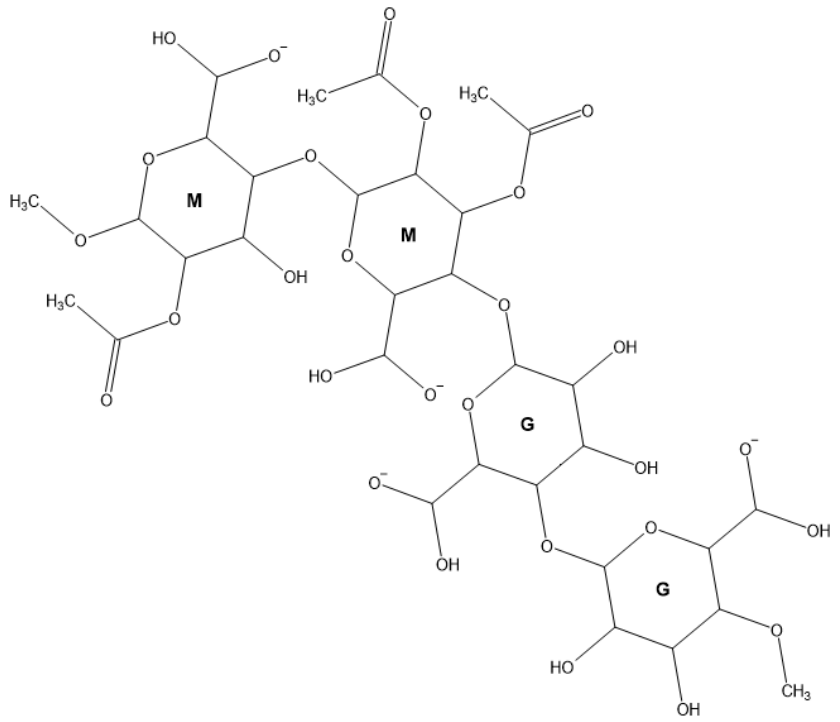

Figure 1.2. General structure of the alginate polymer that *A.vinelandii* produces; which consists of alternating mannuronic (M) and guluronic (G) acid residues.

The generation of alginate in *A. vinelandii* occurs in two complementary stages: (1) synthesis and polymerization of the substrate precursor and (2) modification and exportation of the final product[52,53]. To begin, fructose-6-phosphate is diverted away from central metabolism and is isomerized / phosphorylated by phosphomannose isomerase and phosphomannomutase to form GDP-mannose. This precursor is then converted to GDP-mannuronic acid by GDP-mannose dehydrogenase and is subsequently polymerized and transferred to the periplasmic space. During translocation, specific residues on the poly-mannuronic molecule become acetylated by an acetylase enzymatic complex. The degree of acetylation is dependent on environmental factors like oxygen availability and its result greatly impacts the physical properties of the final product[54,55]. Once in the periplasm, the second stage begins in which non-acylated mannuronic acid residues are converted to guluronic acid by an epimerase[56]; resulting in the completed alginate polysaccharide which is then exported through the outer membrane via a porin[57]. In addition to synthesis, *A. vinelandii* can depolymerize alginate using a series of lysases in order to prevent periplasmic accumulation and cell bursting[58].

Regulation of alginate production in *A. vinelandii* is similar to PHB; utilizing the same Gac/Rsm and CydR regulatory mechanisms previously mentioned. Additionally, expression of many of the alginate biosynthetic gene clusters in *A. vinelandii* is controlled by the alternative sigma σ^E factor AlgU[59]. Under adverse environmental conditions, AlgU binds to the promoter regions of *algD* and *algC* and recruits the σ^{70} RNA polymerase to initiate transcription of the associated operons[60]. Additionally, AlgU controls transcription of its own gene, *algU*, and any disruption to this gene or promoter region results in a non-mucoid phenotype[61,62]. The membrane-bound MucAB system provides a counter-balance to AlgU activity, acting as an anti-sigma factor and repressing alginate production[62].

Genetic manipulation and expression of foreign DNA

One of the key characteristics shared amongst nearly all industrially-relevant microorganisms is the ability to receive and maintain exogenous DNA. This capability allows these organisms to acquire new genetic information from their environment that can result in beneficial phenotypes. In the 1980s, researchers attempted to develop a functional molecular cloning system for *Azotobacter vinelandii* in which broad-range host plasmids could be transformed at a high frequency and be maintained for successive generations[63]. While the initial results were promising, these researchers eventually discovered that the presence of plasmids in *A. vinelandii* significantly impaired nitrogen fixation, cell size, and siderophore production[64]. Furthermore, transformation efficiency and overall maintenance of non-homologous extrachromosomal plasmids was reported to be low[65]. One explanation for this is that when plasmids are introduced into *A. vinelandii*, the 'metabolic load' increases which diverts cellular resources away from central metabolism and results in a decrease in specific growth rate and critical energy limitations; allowing plasmid-free cells to outcompete plasmid-containing cells which ultimately results in plasmid loss[66,67]. One of the plasmids that has previously been reported to be stable in *A. vinelandii* is pRK2501[63,68]; a derivative of the conjunctive RK2 plasmid that is known to confer tetracycline and kanamycin resistance[69]. This plasmid was sequenced by our lab and was found to carry genes for plasmid replication, plasmid maintenance, kanamycin resistance, and tetracycline resistance (Figure 1.3). Unfortunately, our attempts to replicate the work of the Glick group proved unsuccessful and plasmid stability could only be maintained for a maximum of two generations.

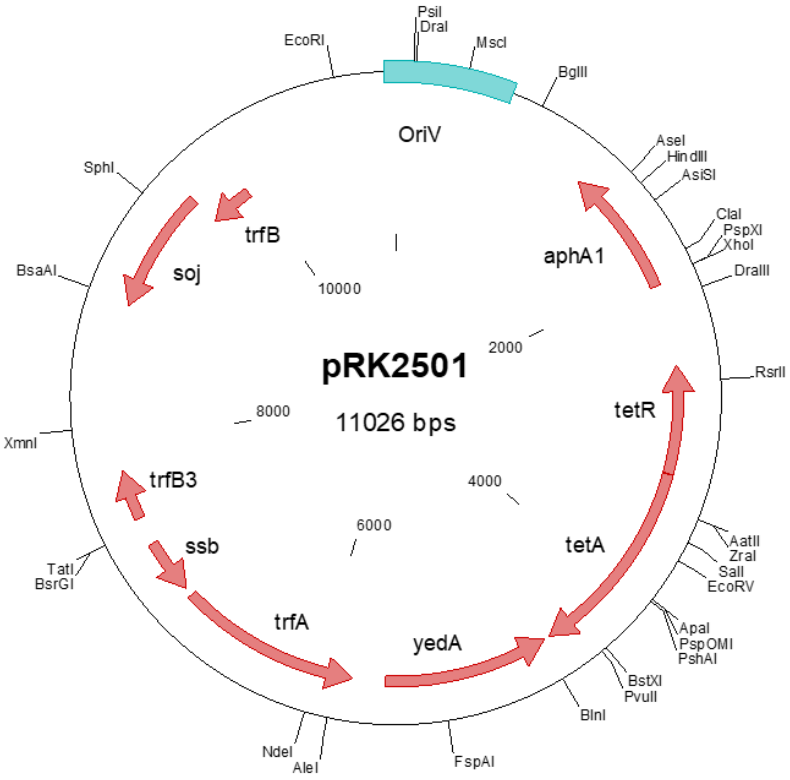

Figure 1.3 Genetic map of the pRK2501 plasmid sequenced by our group.

Instead of plasmids, recombinant expression of foreign genetic material in *A. vinelandii* is now typically accomplished by modifying the chromosome via double homologous recombination. The first step in this process is inducing DNA competence in *A. vinelandii* which requires the cells to be cultured under iron limiting conditions with an excess of magnesium ions[51,70,71]. Under these conditions, siderophore production is activated, indicated by the culture turning a bright green color, and linear DNA is able to cross the cell membrane and enter into the cytoplasm[72]. Once inside the cell, the foreign DNA, usually containing an antibiotic resistance cassette flanked by regions of DNA homologous to a gene in the host chromosome, is bound to the homologous pairing protein, RecA, which locates the regions of homology within the chromosome. Once these regions are found, strand invasion occurs and cross-shaped Holliday junctions are formed which then undergo branch migration and resolution; resulting in a 'spliced' chromosome containing the foreign DNA[73-75].

Nitrogen fixation and regulation

As mentioned previously, *A. vinelandii* has the ability to fix nitrogen aerobically using three independent nitrogenase isoenzyme systems with each isoenzyme consisting of a dinitrogenase reductase (DNR) and metal cofactor-containing dinitrogenase[76]. The three metal cofactors utilized in each dinitrogenase active site are either molybdenum (Mo), vanadium (V), or iron (Fe). Each nitrogenase isoenzyme participates in biological nitrogen fixation (BNF) which occurs when electrons are donated to the DNR from an electron carrier, such as flavodoxin, and then transferred onto a bound molecule of dinitrogen in the dinitrogenase active site[76-78]. For the Mo nitrogenase, two molecules of ATP are consumed for every cycle of electron transfer and these cycles continue until six electrons and protons have been dumped onto the dinitrogen molecule and two protons have been reduced to hydrogen. This results in the accepted equation for BNF as shown below:

$$\text{Mo nitrogenase: } N_2 + 8\ e^- + 8\ H^+ + 16\ ATP \rightarrow 2\ NH_3 + H_2 + 16\ ADP$$

However, this standard equation does not accurately depict the reactions for the V and Fe nitrogenases. These alternative nitrogenases are characterized for being able to evolve more hydrogen than the Mo version *in vitro* at the cost of efficiency[79-85]. This loss of efficiency is explained by the need for additional rounds of electron transfer to break the triple bond found in dinitrogen; resulting in higher ATP and proton input requirements.

Due to these differences, expression of each nitrogenase isoenzyme is highly regulated in *A. vinelandii* with priority given to the Mo nitrogenase[86-88]. For example, when molybdenum metal is present in the environment, at concentrations as low as 50 nM, the Mo nitrogenase is expressed and the V and Fe nitrogenases are repressed[82,89,90]. Likewise, if vanadium metal is present and molybdenum metal is absent, then the V nitrogenase is expressed and the other nitrogenases are repressed. If only iron metal is available, then the Fe nitrogenase is activated[91] (Table 1.1).

Table 1.1. Regulation of nitrogenase expression based on metal availability for wild-type strains of *A. vinelandii*.

Metal Cofactor Availability	Mo nitrogenase expression	V nitrogenase expression	Fe nitrogenase expression
(+) Mo, (+/-) V, (+/-) Fe	+	-	-
(-) Mo, (+) V, (+/-) Fe	-	+	-
(-) Mo, (-) V, (+) Fe	-	-	+

This is important because molybdenum-containing compounds are widely-distributed throughout the world's soils and are considered 'sticky'; meaning they are difficult to remove from the environment[92]. In fact, many researches have noted that once glassware has been exposed to molybdenum metal, those vessels can no longer be used to cultivate wild-type strains of *A. vinelandii* for the study of alternative nitrogenases[90,93,94]; unless intense acid-washing measures are implemented.

In addition to metal regulation, expression and maintenance of all the nitrogenase isoenzymes in *A. vinelandii* are strictly regulated by oxygen availability. This is because the nitrogenase enzyme complex is irreversibly inactivated by the presence of oxygen[95]. Therefore, *A. vinelandii* has developed several protective measures besides the previously mentioned respiratory protection to deal with this stress: including the NifL-NifA transcriptional regulatory system[96] and the FeSII/Shethna protein[97].

The NifL-NifA regulatory system is an atypical two-component system which combines a transcriptional repressor flavoprotein (NifL) and a σ^{54}-dependent transcriptional activator protein (NifA) that interact via protein-protein communication and not covalent modification[98,99]. When oxygen is present in the cells above a manageable level, NifL becomes oxidized and inhibits both the ATPase and GTPase activities of the NifA protein; preventing transcription of the nitrogen fixation genes in *A. vinelandii*[100]. Furthermore, this NifL protein is also thought to regulate nitrogenase expression based on fixed nitrogen availability in a similar manner; although the exact mechanism is still not fully understood[101,102].

The FeSII/Shethna protein protects nitrogenase from oxygen by post-translational modification. When intracellular oxygen is present, the Fe-S clusters in the Shetna protein become oxidized[103] which allows it to bind to a negatively charged pocket near the DNR /

dinitrogenase interface[104]; forming a three-component nitrogenase complex. This complex, while non-functional, is oxygen-stable because it causes a conformational change to the dinitrogenase that prevents oxygen from destroying the metal cofactors in its active site. Upon returning to a reduced state, the Shethna protein disassociates from the nitrogenase complex and allows *A. vinelandii* to resume diazotrophic growth[28].

Biotechnological applications for nitrogenases

Ammonium production

As discussed previously, the biological purpose of the nitrogenase enzyme is to fix atmospheric, inert dinitrogen gas into bioavailable ammonium so that living organisms can produce essential nitrogen-containing compounds such as DNA and amino acids. Roughly half of all global fixed nitrogen is produced from BNF while the other half is fixed industrially using the Haber-Bosch process[105]. This synthetic reaction combines atmospheric dinitrogen with hydrogen gas over a metal catalyst to form ammonium under intense temperature (350 – 550 °C) and pressure (250 – 300 atm); resulting in the consumption of 1 – 2 % of the world's energy sources[105,106].

Even including these inefficiencies, this process is still absolutely vital for maintaining global agricultural output and sustaining the world's ever-expanding human population[107]. However, there is a strong case to be made for increasing the role of the BNF reaction in industrial ammonium production because it occurs under standard temperatures and pressures and does not require immense energy inputs.

As stated previously, *A. vinelandii* would be an ideal candidate for the production of this important compound because it grows diazotrophically under aerobic conditions while utilizing cost-effective sources of carbon[14,91,108]. Unfortunately, the wild-type strains of *A. vinelandii* do not export meaningful amounts of ammonium under physiological growth conditions and therefore, researchers still need to elucidate the underlying mechanisms of BNF and nitrogen metabolism in order to develop an industrially-relevant ammonium-excreting strain.

One promising development in this area has been the discovery that specific disruptions of the *nifL* gene results in the excretion of 15 – 35 mM ammonium into the culture medium during late logarithmic and early stationary growth phases[109-112]. Furthermore, the disruption to the *nifL* gene has polar effects on *A. vinelandii* physiology which results in the continuous

expression of the Mo nitrogenase in the presence of exogenous ammonium[112]; implying that it is possible to culture *A. vinelandii* diazotrophically in media containing fixed nitrogen compounds. This is important because this would allow these mutants to be used in an agricultural setting where the presence of nitrogen-containing residues is inevitable. As a rhizobacterium, *A. vinelandii* natively colonizes the roots of many plants[113] and these *nifL* mutants should be capable of transferring fixed nitrogen to their plant symbionts; potentially increasing crop yields without the need for inorganic ammonium application. In fact, there have already been field trials using these strains assessing their effectiveness in replacing chemical fixed nitrogen additives for the cultivation of wheat[114]. While promising, more work still needs to be done to increase exported ammonium yields and correct the growth impairments observed in these strains[112,115].

One of the newest developments in biological ammonium production research has been the creation of nitrogenase-mediated enzymatic fuel cells (EFC)[116] that mimic the Haber-Bosch process. These EFCs operate as bio-batteries that continually recycle protons and electrons between hydrogenases and nitrogenases to generate ammonium and electricity. Each enzyme type is compartmentalized and separated from each other by a proton exchange membrane (PEM) to generate an electron current. In the hydrogenase compartment, methyl viologen (MV) is used an electron mediator between the uptake hydrogenase and the anode, allowing for continuous hydrogen oxidation. The generated protons then traverse the PEM into the nitrogenase compartment where MV is again used as an electron mediator between the Mo nitrogenase and the cathode. This allows the Mo nitrogenase to reduce dinitrogen into ammonium and hydrogen; which acts as a substrate for the hydrogenase. The ATP supply required by the Mo nitrogenase is continually regenerated through a creatine phosphokinase / creatine phosphate system[117].

Hydrogenase Anode: $H_2 + 2\ MV^{2+} \rightarrow 2\ H^+ + 2\ MV^{\bullet+}$

Nitrogenase Cathode: $16\ ATP + 8\ MV^{\bullet+} + 8\ H^+ + N_2 \rightarrow 16\ ATP + 2\ NH_3 + H_2 + 8\ MV^{2+}$

For each cycle of hydrogen oxidation and nitrogen reduction, two molecules of ammonium are generated along with a small electric current. Researchers have also been successful in utilizing whole cells of nitrogen-fixing and hydrogen-oxidizing bacteria to generate ammonium in a similar manner[118]; although the productivity values remain low (5.2 picomoles $NH_4^+\ s^{-1}\ cm^{-2}$).

Hydrogen production

Another product of BNF that has immense biotechnological implications is hydrogen. Hydrogen has long been investigated for its use as a clean alternative fuel source because it is energy-dense[119] and its combustion, unlike gasoline, does not emit toxic byproducts like carbon monoxide, carbon dioxide, and heavy metals[120]. Traditionally, this gas has been produced chemically from either steam reformation of natural gas or the splitting of water through the use of an electrical current[121]. Hydrogen can also be produced biologically using either phototrophic microorganisms that utilize the energy from sunlight to convert water into hydrogen[122] or anaerobic organisms that utilize fermentation and hydrogenases to convert excess protons and electrons into hydrogen[123]. However, the costs associated with culturing these organisms at industrial scales are prohibitive because of the requirement for either high surface areas (phototrophic production) or maintenance of strict anaerobiosis (fermentative production). Therefore, the possibility of nitrogenase-mediated hydrogen production from an aerobic microorganism, like *A. vinelandii*, that can be cultured in minimal media would be highly appealing and could provide a future path for biological hydrogen production.

Unfortunately, the wild-type *A. vinelandii* does not evolve significant amounts of hydrogen into the atmosphere when growing diazotrophically[124,125] because of the presence of a membrane-bound uptake hydrogenase which converts nearly all nitrogenase-derived hydrogen into protons and electrons under physiological conditions[126,127]. This uptake hydrogenase, which is encoded and regulated by the *hox* and *hyp* operons, acts as an alternative site for proton translocation and electron transfer resulting in an increase in PMF and nitrogenase activity[125,128]; although researchers disagree about the impact this increase has on overall cellular physiology[124,129,130]. There is also another putative soluble hydrogenase encoded in the genome of *A. vinelandii*[131] but it is not considered to be active and shows no signs of hydrogen oxidation activity under nitrogen-fixing conditions[132-134]. Luckily, removal of uptake hydrogenase activity, either through targeted *hoxK* deletion or a natural deletion encompassing the entire *hox* and *hyp* operons, results in a hydrogen-evolving phenotype in *A. vinelandii*[129]; although the productivity values still lag behind other fermentative and phototrophic processes.

Alternative substrate catalysis

In addition to ammonium production and hydrogen evolution, nitrogenases have also been investigated for their promiscuous characteristics which allow them to reduce many compounds besides dinitrogen. MJ Dilworth was one of the first researchers to discover that the nitrogenase enzyme complex had these alternative functionalities when he observed that acetylene, a two-carbon alkyne, could be reduced to ethylene by nitrogenase-containing *Clostridium pasteurianum* cell lysates[135]. While this process did not make sense economically, it ignited interest in the study of nitrogenase for alternative substrate catalysis and provided a method for measuring *in vitro* nitrogenase activity. Over the years, there have been a variety of other carbon-containing compounds that have been found to be substrates for the nitrogenase isoenzymes; sharing the characteristics of being small molecules with double or triple bonds[136]. Each nitrogenase isoenzyme is somewhat unique in regards to which compounds it can reduce and the differences are likely due to the variance of physical characteristics in the metal-containing dinitrogenase active sites.

The Mo nitrogenase is the most-widely distributed nitrogenase isoenzyme in nature, present in nearly all nitrogen-fixing bacteria, and its active site is well characterized; consisting of two P clusters and two FeMo cofactors[137]. Each P cluster consists of 4 iron atoms and 4 sulfur atoms bridged by cysteine thiol ligands which work together to shuttle electrons from the DNR to the FeMo-cofactor cluster in the dinitrogenase[137,138]. The FeMo-cofactor cluster (containing 7 iron atoms, 9 sulfur atoms, 1 molybdenum atom, 1 carbon atom, and 1 R-homocitrate compound) is the location where substrates are bound and reduced by accumulated electrons[136,139]. Together, these metal centers allow the Mo nitrogenase to reduce a variety of chemical motifs including: C-C, C-O, C-S, and C-N bonds[136]. Of particular interest is the capability to break down environmental toxins like hydrogen cyanide into safer, less toxic hydrocarbons like ethylene and ethane[140,141]. However, many of these alternative reactions either completely inhibit enzyme activity or involve the reduction of highly valuable compounds into other valuable compounds; which limits the overall economic upside of utilizing Mo nitrogenases for these purposes.

The Fe nitrogenase, which is encoded by the *anfHDGK* genes, is the least well-characterized version of the nitrogenase enzyme complex and contains an extra gamma subunit in its FeFe-cofactor cluster[81,142]. This variant of nitrogenase is found in approximately 9 % of nitrogen-fixing bacteria[143,144] and its alternative substrate catalysis capabilities are still under

investigation. However, recently it has been demonstrated that Fe nitrogenases, isolated from several different microorganisms, have the unique capability to reduce soluble CO_2 into methane[143]; an economically-relevant hydrocarbon normally purified from natural gas. While the Fe nitrogenase-mediated production values for methane are limited from an industrial perspective, this process likely plays a role in microbial community interactions with methane being utilized as a carbon source for methane-oxidizing bacteria like *Methylomonas*[143].

Finally, the V nitrogenase, which is encoded by *vnfHDGK*, has an active site that is similar to the FeMo-cofactor cluster but is proposed to contain a carbonate substitution for one of the bridging sulfide atoms[93]. This seemingly minor difference provides the V nitrogenase with perhaps the most economically-relevant alternative substrate catalysis capability: carbon monoxide (CO) reduction to ethylene and other hydrocarbons[145,146]. This process, which was discovered in 2010, presents the possibility of converting toxic, industrial waste gas into value-added hydrocarbons that are currently sourced through non-renewable resources like oil and natural gas. However, CO has traditionally been considered toxic to diazotrophic growth and concentrations of CO as low as 0.2 % can have severe negative effects on nitrogen fixation and cell proliferation[147]. Furthermore, the methods for *in vivo* ethylene production have relied on small-scale, hermetically sealed batch systems which are unsuitable for proper process development and industrial scale-up[148].

Chemical and microbial methods for ethylene production

Chemical: Hydrocarbon cracking

As stated previously, ethylene is a valuable commodity used in the production of a variety of polymers, fibers, and chemicals and is mainly produced by hydrocarbon cracking[149]. The first thermal cracking process was developed and patented in 1891 by Vladimir Shukhov as a means to convert heavy petroleum crude oils into useful gasolines and short chain olefins[150]. The process works by heating up hydrocarbon feedstocks to extremely high temperatures (800-850°C) under pressure, which causes the covalent bonds to fracture and recombine; resulting in shorter chain molecules such as ethylene and propylene[151]. However, this pyrolysis technology has several major drawbacks related to its energy consumption and greenhouse gas emissions. The inherent intense temperature requirements for cracking reactors results in an estimated

energy consumption of 26 megajoules per kilogram ethylene produced and, alone, accounts for nearly 2% of worldwide CO_2 emissions[149,152].

Chemical: Fischer-Tropsch

Shortly after World War I, two scientists at the Kaiser Wilhelm Institute for Coal Research in Germany, Hans Tropsch and Franz Fischer, developed an alternative method for the production of liquid hydrocarbons independent of petroleum crude oil, denoted the Fischer-Tropsch (F-T) synthesis reaction. In short, the original experiment combined carbon monoxide (CO) and hydrogen (H_2) gases, derived from steam reformation of coke-oven gas, into aliphatic straight-chain hydrocarbons of various lengths[153]. While the technology could not compete economically with cracking at the time, scientists around the world were astounded at the ability to transform gases into liquid fuels. Over the years, there have been many advancements to the F-T process which has led to the industrial adoption of the technology for production of high quality, low sulfur transportation fuels and commodity chemicals from a variety of feedstocks, including renewable biomass residues.

There are still a host of challenges associated with the F-T process with the biggest obstacle being the inherent inefficiency[154,155]. F-T fluid bed reactors typically operate under high pressures and usually require tremendous amounts of heat exchange in order to function. Furthermore, the process requires large inputs of H_2 gas as a substrate, which is a valuable product in itself[156]. Even under favorable conditions, the F-T reaction is somewhat unpredictable with possible products ranging from fuel gases (C_1-C_4) to hard waxes (C_{35+}) depending on the temperature, catalyst, syngas composition, and many other factors[157,158]. Finally, the F-T synthesis reaction still generates greenhouse gas emissions comparable to levels produced from hydrocarbon cracking[159].

While researchers continue to search for ways to increase the efficiency, predictability, and cleanliness of the F-T process; there are practical limitations to the amount of money that can be spent in the pursuit of these goals. Furthermore, the most profitable products of the F-T technology moving forward are the longer chain, high quality diesel fuels. Therefore, investigation into alternative methods for the production of short chain hydrocarbons, such as ethylene, is still needed[153,160,161].

Microbial: KMBA pathway

The first microbial ethylene production pathway described was the 4-methylsulfanyl-2-oxobutanoate (KMBA) pathway which was discovered in plants and fungi but was also found to be active in several *Escherichia coli* strains. In the early stages of this research, bio-ethylene formation was thought to be catalyzed by an NADH:Fe(III) EDTA oxidoreductase enzyme[162,163]. It was later discovered that the production of ethylene through this pathway was not actually a direct product of enzyme catalysis, but instead was a spontaneous reaction between KMBA and a reactive oxygen species. In short, the oxidoreductase enzyme reduces L-malate into KMBA which then reacts with oxygen; forming a free hydroxyl radical through Fenton chemistry[163]. This hydroxyl radical then reacts with KMBA to form ethylene, although only in trace amounts[164]. Because the values are so low and the process is non-enzymatic, the KMBA pathway is not considered to be a viable candidate for the industrial production of ethylene.

Microbial: Nitrogenase-like reductases

While the KMBA pathway is not viable for large-scale ethylene production, it is not the only ethylene-generating process involved in microbial sulfur metabolism. Recently, it has been discovered that anaerobic, sulfur-limited environments (like freshwater and soils) contain photosynthetic Alphaproteobacteria that produce ethylene and methane at higher levels than expected[165]. The production of these hydrocarbons was traced back to the reduction of volatile organic sulfur compounds, like (2-methylthio)ethanol and dimethyl sulfide, by a nitrogen fixation-like methylthio-alkane reductase (*marBHDK*) which likely follows the below equations:

$$C_3H_8OS \rightarrow CH_4S + C_2H_4 + H_2O$$

$$C_2H_6S \rightarrow CH_4S + CH_4$$

Expression of this enzyme is induced under sulfate limiting conditions and is phylogenetically related to traditional nitrogenase enzymes; although the native enzyme cannot reduce atmospheric dinitrogen. Furthermore, nitrogenase and methylthio-alkane reductase are independently regulated and can be activated either separately or simultaneously. In these initial experiments, the researchers reported a specific productivity of approximately 20 µg C_2H_4 g^{-1} biomass h^{-1} [166].

Microbial: 2-oxoglutarate dependent pathway

Another microbial ethylene production pathway that exists in nature is the 2-oxoglutarate (2OG) dependent pathway which is catalyzed by a single enzyme, the ethylene-forming enzyme (EFE)[167]. This protein is found natively in several microbial plant pathogen species within the *Pseudomonas* and *Penicllium* genera and belongs to the superfamily of Fe^{2+}/ascorbate oxidases[168,169]. The enzymatic reaction occurs in a dual-circuit mechanism, with the first reaction being the formation of ethylene and CO_2 from 2OG, L-arginine, and oxygen and a second reaction resulting in 1-pyrroline-5-carboxylate (P5C), guanidine, CO_2, and succinate[170,171]. The stoichiometry of the overall reaction follows the equation below:

$$2OG + 3\ O_2 + \text{arginine} \rightarrow 2\ C_2H_4 + \text{succinate} + 7\ CO_2 + \text{guanidine} + P5C$$

Recently, researchers have been successful with recombinant expression of this enzyme in a variety of host organisms, such as *Saccharomyces cerevisiae* and *E. coli*, with varying degrees of success[169,172]. The highest reported yield to date was in *Pseudomonas putida* KT2440 carrying the *efe* gene from *P. syringae* pv. *glycinea* grown in glucose-supplemented LB media with a yield of 21.7 mg ethylene per gram glucose consumed[173]. The main issues currently preventing wider adoption of the EFE enzyme as a replacement for industrial ethylene production is that the enzyme is unstable above 30°C, it requires a high gene copy number to be effective, and it needs expensive reagent supplements to achieve high productivities[174,175]; making it difficult to scale.

Microbial: Nitrogenase-mediated CO reductive coupling pathway

The final known bacterial pathway for ethylene production is the V nitrogenase-mediated CO reductive coupling pathway. This pathway is thought to occur in four major steps: (1) CO outcompeting dinitrogen for the V nitrogenase active site, (2) hydrogenation of CO to HCO, (3) hydrogenation of HCO to HCOH, and (4) elimination of H_2O to form the C-C bond[176]. This reaction does not occur naturally in the other nitrogenase isoenzymes, although single amino acid substitutions can confer the same ability to the Mo nitrogenase to a lesser degree[177]; indicating that it is not a unique characteristic of VFe metal clusters but rather an issue of substrate access. Unfortunately, the *in vivo* ethylene production values reported have been underwhelming due to reliance on small-scale, hermetically sealed batch systems which severely restricts the diazotrophic growth potential of *A. vinelandii*; making it unsuitable for industrial scale-up in its current state[148]. Therefore, the bulk of the work entailed in this dissertation will be focused on

solving these issues for the achievement of continuous, microbial ethylene production from nitrogenase activity.

Conclusions

As detailed above, *A. vinelandii* has long been the focus of researchers for the production of many industrially-relevant compounds in a cost-effective manner. Of particular interest to this endeavor is the unique ability of *A. vinelandii* to convert carbon monoxide, a toxic industrial waste gas, into ethylene using its V nitrogenase enzyme complex; although there are still a host of problems with the current methodologies that limit overall productivity. Therefore, we wanted to focus our efforts on redesigning and optimizing the process for *A. vinelandii* cultivation while developing novel techniques for monitoring real-time catalytic capacity. Furthermore, we wanted to explore the possibility of generating additional value by producing bio-functional ethylene-forming nanobeads. These efforts will be discussed in detail in the following chapters.

Chapter 2. *Azotobacter vinelandii* Nitrogenase Activity, Hydrogen Production, and Response to Oxygen Exposure

Introduction

Azotobacter species are archetypes of aerobic diazotrophic heterotrophy, studied for over 100 years for their ability to fix nitrogen in the presence of oxygen[178-181] and their physiology has been discussed in detail by our group previously[91,182]. *A. vinelandii* encodes for three versions of the nitrogenase complex, each employing a different metal-containing cofactor in its active site. These isoenzymes all convert dinitrogen into ammonia coupled with hydrogen production that is recaptured *in vivo* by a membrane-bound uptake hydrogenase (*hoxKG*)[183]. There are homologous genes for a soluble hydrogenase in *A. vinelandii* that do not participate in hydrogen re-oxidation, as membrane-bound hydrogenase knock-out mutants show no hydrogen oxidation activity[132-134]. Various factors can affect molar yields of hydrogen generation from nitrogenase including electron flux and oxygen exposure. As supported by *in vitro* measurements, the alternative vanadium (V) and iron-only (Fe) nitrogenases have a lower affinity for dinitrogen with more electrons being fluxed to hydrogen. As a result, the V nitrogenase (*vnfHGDK*) produces three to five moles of H_2 per mole of N_2 fixed *in vitro*[79,83] and the Fe nitrogenase (*anfHGDK*) produces between three and eleven moles of H_2 per mole of N_2 fixed *in vitro*[81,82,184]. The molybdenum (Mo) nitrogenase (*nifHDK*) has consistently been shown to produce one mole of H_2 per mole of N_2 fixed, which accounts for 25% of its electron flux[79,81,84,85].

It is well established that oxygen and its reactive species are incompatible with active nitrogenase enzymes, capable of irreversibly inactivating them and preventing diazotrophic growth[179,180,185-188]. Therefore, Azotobacters' employ a multifaceted approach for tolerating oxygen when fixing nitrogen. The most important facet is called respiratory protection, an increase in respiration resulting in so-called "wasting" of oxygen[28,95,178-181,189-192]. The cells redirect electron flux through the cytochrome *bd* branch of their electron transport chain, starting from NADH dehydrogenase II[25,26], in which respiration is virtually decoupled from phosphorylation[22,95,187,193,194]. Maximum specific growth rate and apparent molar biomass yield are also affected, as cells devote carbon and energy to respiratory protection rather than to biosynthesis[181,189,191,192].

In contrast, in the case of oxygen limitation, which results in an excess of reducing equivalents, *Azotobacter* species have other adaptations. Chief among these is the production of polyhydroxyalkanoates as storage polymers, especially poly-β-hydroxybutyrate (PHB). Oxygen limitation induces its production in *Azotobacter*, and PHB can represent up to 70% of the cells' dry weight[29,181,195-197]; when the limitation is lifted, cells assimilate the PHB[196,197]. Formation of this polymer also acts as an electron sink, accepting excess reductants when insufficient oxygen is present[197,198]. Production and consumption of this polymer changes metabolic patterns and the composition of cellular dry weight, affecting the quantification of apparent molar yields and parameters that assume constant cellular composition. Therefore, by creating PHB-deficient strains, a true linear relationship between biomass and product molar yields could be obtained for all oxygen exposure conditions.

To study the impact of oxygen exposure on hydrogen generation driven by each nitrogenase isoenzyme *in vivo*, three unique offspring of *A. vinelandii* CA were tested: CA6, DJ Δ*hoxK*, and CA11.6. *Azotobacter vinelandii* CA6 was selected under directed evolution as capable of overcoming tungsten poisoning of the Mo nitrogenase[199]. This phenotype is ideal for this type of study, since its nitrogenase regulation system is disrupted, allowing for cell growth utilizing the alternative nitrogenases, even in conditions in which wild-type CA would maintain them repressed[200]. *Azotobacter vinelandii* DJ Δ*hoxK* was used as a comparison control because this strain has an active nitrogenase regulation system, ensuring expression of only the Mo nitrogenase when exposed to molybdenum[89], and a deletion of the uptake hydrogenase gene resulting in a hydrogen-evolving phenotype. *Azotobacter vinelandii* CA11.6 was constructed by introducing the same deletion from CA6 into CA11, which additionally lacks a functional Mo nitrogenase due to a deletion in the *nifHDK* genes[81]. CA11.6 is ideal for studying the alternative nitrogenases since molybdenum is difficult to remove from glassware and the residuals could potentially skew results[90,93,94].

Strain CA6 was previously sequenced and characterized by our group to understand why these strains show a deregulated nitrogenase phenotype. This analysis revealed a large ~42kb deletion encompassing the molybdate uptake operon, several regulation operons, and the entire uptake hydrogenase operon[129,131]. This same 42 kb deletion is also present in strain CA11.6. Without the uptake hydrogenase operon, these strains have the same hydrogen producing phenotype driven by nitrogenase activity as the *hoxK* knock-out mutants[129]. Therefore, hydrogen

gas released by cells growing under nitrogen fixing conditions can be used as a means to estimate the *in vivo* nitrogenase activity of each isoenzyme under various oxygen exposure conditions.

Almost all studies of dissolved oxygen impact on *Azotobacter* growth have focused on the evaluation of the Mo nitrogenase, but how much these results could be extrapolated to the alternative isoenzymes has not been well characterized. In addition, most studies of nitrogenase have relied on *in vitro* measurements to estimate enzyme activity, which is less accurate than *in vivo* direct measurements. Based on the *in vitro* data, it is plausible to conclude that expression of the alternative nitrogenases would be preferable for hydrogen production applications. In this paper, we investigated the impact of dissolved oxygen on biomass and hydrogen molar yields in chemostat cultures by uptake hydrogenase/PHB-deficient, de-repressed nitrogenase synthesis mutants of *Azotobacter vinelandii* and propose a real-time method for quantifying *in vivo* nitrogenase activity for each isoenzyme.

Materials and Methods

Strains and Media

Escherichia coli and *A. vinelandii* strains utilized in this study are listed in Table 2.1, along with plasmids and primers. *A. vinelandii* CA6 and CA11.6 are part of the NCSU's Department of Microbial Biology Culture Collection.

E. coli strains were grown in lysogeny broth (LB) (with 1.5% w/v agar added for solid medium). Unless otherwise noted, *A. vinelandii* strains were grown in modified nitrogen-free Burk broth, which contained, per liter, 0.2 g $MgSO_4 \cdot 7H_2O$, 90 mg $CaCl_2 \cdot 2H_2O$, 0.2 g KH_2PO_4, 0.8 g K_2HPO_4, 5 mg $FeSO_4 \cdot 7H_2O$, 0.5 g $C_6H_7NaO_7$, and 10 g sucrose. For molybdenum and vanadium conditions, $NaMoO_4 \cdot 2H_2O$ (0.25 mg/L) and $NaVO_3$ (30µM final concentration) were added, respectively. Sucrose and iron solutions were filter-sterilized with 0.2 µM filters; other solutions were autoclaved and the various components were combined after cooling. Inocula were cultured by incubating at 30°C, shaking at 150 rpm.

Antibiotics were added to media as needed: 100 µg mL^{-1} ampicillin for *E. coli* or 50 µg mL^{-1} for *A. vinelandii*.

Table 2.1. Strains, plasmids, and primers. Primers with added restriction sites, **bold** sequence indicates added restriction site, and <u>underlined</u> sequence indicates homology to target.

Name	Relevant Characteristics	Reference or Source
A. vinelandii		
DJ *ΔhoxK*	DJ with *hoxK*-knockout, utilizes Mo nitrogenase in presence of molybdenum, kan^r	This study
DJ *ΔhoxK ΔphbC*	DJ *ΔhoxK* with *phbC*-knockout, amp^r	This study
CA6	Tungsten-tolerant, natural hydrogen-evolving mutant (42kb deletion including entire *hox* operon), utilizes Mo nitrogenase in presence of molybdenum	[200]
CA6 *ΔphbC*	CA6 with *phb*C-knockout, amp^r	This study
CA11.6	CA11 (Δ*nif*HDK, knock-out of Mo nitrogenase) with CA6 mutation (42kb deletion), utilizes V nitrogenase in presence of vanadium and Fe nitrogenase in presence of iron-only (no vanadium or molybdenum present in media)	[195]
CA11.6 *ΔphbC*	CA11.6 with *phb*C-knockout, amp^r	This study
E. coli		
TOP10	F$^-$ *mcr*A Δ(*mrr-hsdRMS-mcrBC*) Φ80*lacZ*ΔM15 Δ*lacX*74 *rec*A1 *araD*139 Δ(*araleu*)7697 *galU galK rpsL* (StrR) *end*A1 *nup*G	Invitrogen
Thunderbolt GC10	F$^-$ *mcr*A Δ(*mrr-hsdRMS-mcrBC*) Φ80*lacZ*ΔM15 Δ*lacX*74 *end*A1 *rec*A1 Δ(*araleu*)7697 *araD*139 *galU galK nupG rpsL* λ$^-$ T1R	GeneChoice
DH5α	*supE*44 Δ*lacU*169 *hsdR*17 *end*A1 *rec*A1 *gyrA*96 *hi*-1 *relA*1	Invitrogen
Plasmids		
pUC19	ampR, *lacZ* α-subunit, pMB1 origin	New England Biolabs
pUC-phb	pUC19 + *A. vinelandii* inserted at multi-cloning site	This study
pUC-phb+amp	pUC-phb with ampR cassette inserted in *A. vinelandii phbC* region	This study
Primers		
pUCphbCF (HindIII site)	AGATGT-**AAGCTT**-<u>TATGGTCCTTGCTGCCTTGAG</u>	This study
pUCphbCR (EcoRI site)	TGAACA-**GAATTC**-<u>GCCTTTCGCCCTATGTTCTTC</u>	This study
pUCampF (PstI site)	AGTAGT-**CTGCAG**-<u>TGGTCTGACAGTTACCAATG</u>	This study
pUCampR (SacI site)	AGTACA-**GAGCTC**-<u>GCCTCGTGATACGCCTATTT</u>	This study
ampTestF	GTCAGCTCAGACGCCCTTCGTAG	This study
ampTestR	TATGCAGCCAGCGAGCCGAACAG	This study

Polymerase Chain Reactions and Restriction Digestions

Primers were designed using Clone Manager 9 software (Sci-Ed Software, Cary, NC) and ordered from Integrated DNA Technologies (IDT, Coralville, IA); see Table 2.1 for oligo sequences. Polymerase chain reactions (PCR) were performed using Qiagen Taq polymerase (Qiagen, Valencia, CA) or Phusion High-Fidelity polymerase (Bio-Rad, Hercules, CA) according to manufacturer's instructions.

Restriction digests were performed as specified later with HindIII, EcoRI, PstI, SacI (Promega, Madison, WI), Sau3AI (Thermo Fisher Scientific, Waitham, MA), or NdeI (New England Biolabs, Ipswich, MA) according to manufacturers' instructions.

Preparation of Competent E. coli Cells

E. coli Thunderbolt electrocompetent cells were grown shaking in LB at 37°C up to an optical density (OD_{600}) of 0.5 to 1. The cells were then chilled on ice for 30 minutes and pelleted in chilled rotor at 4000 x *g* for 20 minutes, resuspended in cold water, pelleted and resuspended again. The cells were then pelleted and resuspended in sterile 10% (v/v) glycerol to approximately 3×10^{10} cells per mL. Fifty-microliter aliquots were frozen on dry ice and stored at -80°C. *E. coli* DH5α competent cells were prepared as described previously[201].

Plasmid Construction

E. coli TOP10 competent cells (Invitrogen, Carlsbad, CA) were transformed with plasmid pUC19 (Invitrogen) by the heat-shock method according to manufacturer's instructions and plated on LB with ampicillin to select for transformants. Plasmid was extracted from transformant cultures by the alkaline lysis method using a Qiagen Miniprep kit according to manufacturer's instructions, and plasmid size was determined by 1% agarose gel electrophoresis with ethidium bromide staining. Plasmid identity was further confirmed by band pattern analysis by electrophoresis after cutting plasmid with restriction enzyme Sau3AI (Fisher) according to manufacturer's instructions.

A region of *A. vinelandii* CA6 genome spanning from within *phb*C to within *phb*A was amplified by PCR with HindIII and EcoRI sites incorporated into forward and reverse primers, respectively (primers pUCphbCF and pUCphbCR; see Table 2.1). PCR and pUC19 plasmid were digested with HindIII and EcoRI according to manufacturer's instructions and purified by gel

extraction with Zymo Research Zymoclean Gel DNA Recovery kit (Zymo Research, Irvine, CA) according to manufacturer's instructions. Products were ligated with Promega T4 DNA Ligase according to manufacturer's instructions. Electrocompetent *E. coli* Thunderbolt cells were transformed with ligation using electroporation: 1 µl ligation was mixed with 50 µl cells, then a ECM399 electroporator (BTX, San Diego, CA) applied 2.5 kV at 25 µF to an electroporation cuvette containing the mixture. One milliliter LB was added, the mixture was transferred to a centrifuge tube, and the tube was incubated at 37°C for 20 minutes. Cells were plated onto LB agar with ampicillin and 800 µg 5-bromo-4-chloro-3-indolyl-β-D-galactopyranoside (X-gal) and incubated at 37°C for 24 h, then white colonies were screened by PCR with *pUCphbCF* and *pUCampF* primers on extracted plasmids.

The resulting pUC-phb plasmid, as well as an ampicillin resistance cassette amplicon generated by PCR with pUCamp primers with pUC19 as template, was cut with SacI and PstI; these enzymes remove a 201-bp section of gene from *phb*C. After purification by gel-extraction, restricted plasmid was treated with Antarctic Phosphatase (New England Biolabs, Ipswich, MA) according to manufacturer's instructions for a 3' overhang and ligated together with the ampicillin resistance cassette amplicon. Competent *E. coli* DH5α cells were transformed with this ligation by the heat-shock method[201] except that the heat-shock interval was one minute and 300 µl LB was added; transformants were plated on LB with ampicillin and incubated at 37°C for 24 h. Colonies were screened by colony PCR using pUCphbC and phbInt primers, and a positive was saved as pUC-phb+amp.

Transformation of A. vinelandii

A. vinelandii competence was induced and cells were transformed using previously described methods[70,71]. In brief, *A. vinelandii* strains were grown on transformation (TF) medium (Burk agar with 10-fold increased magnesium, 28 mM ammonium acetate, and no added iron or molybdenum) for 3-4 days until green pigment appeared. Growth was washed off with 1 mL sterile Burk buffer (0.2 g L^{-1} KH_2PO_4 and 0.8 g L^{-1} K_2HPO_4), mixed with 50 µL of linearized plasmid and incubated at 30°C for 1 h. It was then plated onto selective *Azotobacter* growth (AG) agar (Burk with 0.5 g L^{-1} yeast extract added) and incubated at 30°C. Colonies were screened by PCR to confirm mutants.

Bioreactor Setup and Oxygen Requirement Chemostats

Chemostat experiments were performed as described previously[129], in a constant working volume of 700 mL. Temperature was held at 30°C; pH was allowed to vary; filtered compressed air was sparged at a rate of 0.315±0.05 liters per minute (lpm) using a mass flow control system. The system was open to gas exchange with the atmosphere through a filter. Culture turbidity was monitored and recorded in real-time using an in-house device that continuously measures light transmittance through a section of glass tubing through which culture is recirculated (United States Patent 6975403). Arbitrary Unit (AU) measurements from this device can be converted to OD_{600} units with the following formula: OD_{600} units = 0.0177*(AU)-1.9583.

Medium was prepared in 20 L glass carboys and consisted of modified Burk medium, described previously. Samples of each batch of medium were saved at -20°C for later analysis. To begin an experiment, the reactor, set to maintain the appropriate temperature (30°C) and dissolved oxygen concentration (30%), was inoculated with pre-grown batch cell. When the reactor culture reached mid-log phase, the inflow of fresh medium and removal of excess culture volume were initiated. Steady state was achieved before starting any sampling.

System parameters were defined as follows: dilution rate (D) is the value obtained after reaching equal feed and harvest flows (F) that allows for obtaining a constant volume (V) of culture in the reactor (D = F/V). Yield is defined as the ratio of product generated to limiting substrate (sucrose) consumed. Productivity is the value of product generated per limiting substrate consumed per unit of time. The dilution rate for these experiments was set to 0.066 h^{-1}. Once steady-states were achieved, at least three samples were taken and analyzed before the agitation rate was changed. At least one retention period was allowed to pass between each sample; at D=0.066 h^{-1}, 700 mL pass through the system in approximately 15 h.

Gas Analysis

Exhaust gases (O_2, N_2, CO_2, H_2, and Ar) were monitored and recorded redundantly in real-time using in-line O_2/CO_2 EasyLine Continuous Gas Analyzers, Model EL3020 (ABB, Germany) and a Pfeiffer OmniStar quadrupole mass spectrometer. Dissolved oxygen was measured with an in-line Ingold InPro 6820 amperometric oxygen probe (Mettler-Toledo, Columbus, OH, USA), calibrated from 0% (anoxic) and 100% (saturated).

Oxygen consumption and hydrogen and CO_2 production were calculated from the difference between environmental/baseline levels (as measured by the sensors) and levels measured in gas exhausting from the reactor. Culture steady-state was confirmed when these gas values, along with biomass concentration, did not change measurably over time. Oxygen transfer rate was calculated from oxygen consumption and dissolved oxygen, and medium flow rate with the following equation:

$$R = C + kSF$$

where R is the oxygen transfer rate in milligrams per hour, C is the oxygen consumption rate by cells in milligrams per hour, k is a constant reflecting the amount of oxygen dissolved per liter of medium (7.456 mg L^{-1}), S is the dissolved oxygen saturation (0 to 1), and F is the flow rate of liquid in lph.

Sample Analysis

Biological and technical replicates were processed as previously described[129]. Culture volumes were spun down for 5 min at 10,000 rpm in a Centrifuge 5415C (Eppendorf, US), then the supernatant and pellet were saved at -20°C for later analysis. Dry weight was obtained by filtering a portion of sample through a 0.2µm filter of known mass (mixed cellulose esters, EMD Millipore, Germany) using vacuum suction; the filter was then dried at 60°C until constant weight to determine the dry weight of biomass per sample volume. Carbon-moles were calculated assuming a cellular composition of $C_6H_{10.8}N_{1.5}O_{2.9}$ as shown previously[202].

The initial and residual concentration of sucrose were determined into the initial medium and from supernatants of each reactor samples. They were analyzed by high-performance liquid chromatograph (Shimadzu, Japan) run under isocratic conditions at 65°C (mobile phase was water at 0.5 mL/min, Supercogel™ Ca column 300mm x 7.8mm). The column was coupled to a refractive index detector. Absolute values were obtained by measuring known quantities of sucrose to generate a standard curve.

Nile Blue Staining of PHB

Nile Blue A (Chem-Impex Int'l Inc, Wood Dale, IL, USA) was dissolved in water to a final concentration of 1% w/v. This solution was applied to *A. vinelandii* cells air-dried onto a glass slide and then was again air-dried for 10 min at 30°C. Any stained PHB granules were

viewed with an Axioskop2 oil immersion microscope with epifluorescence at 450nm, exciting fluorescence at approximately 600nm.

Results

Generation of phbC Knockout Strains

A. vinelandii exposure to excess dissolved oxygen limits nitrogenase activity and thus its hydrogen production, while dissolved oxygen limiting conditions induce the production of the storage polymer PHB. The accumulation of PHB granules has the potential to skew relationships between biomass and product yields – PHB production leads to increased cell size and weight without concurrent increase in catalytic capacity, resulting in lower apparent specific molar yields. To evaluate this relationship, we generated three mutants of *A. vinelandii*, all deficient in PHB production, one isogenic to strain CA6, a second isogenic to strain CA11.6, and a third isogenic to DJ Δ*hoxK*. The three new strains lacking a functional PHB synthase (PhbC) – CA6 Δ*phb*C, CA11.6 Δ*phb*C, and DJ Δ*hoxK* Δ*phb*C – were generated by inserting an ampicillin resistance cassette near the 5' end of *phbC* by double homologous recombination. The PHB-negative phenotype was confirmed by culturing cells under dissolved oxygen limiting conditions, high-sucrose medium and then staining PHB granules with Nile Blue A.

To confirm the absence of PHB production resulted in a true relationship between biomass and product molar yields, we conducted oxygen limited chemostat culture experiments under iron-sufficient and nitrogen-free medium (D = 0.066 h^{-1}, 30°C), as previously described[129]. Continuous measurements and samples at steady-state allow for the determination of carbon dioxide production yields and cell dry weight. The cessation of PHB production resulted in an increase of specific CO_2 yield and a decrease of cell dry weight when compared to values obtained for CA6 and DJ Δ*hoxK* (Table 2.2). These new PHB negative strains were exclusively used throughout the remainder of the study.

Table 2.2. Steady-state values of dry cell weight, carbon dioxide molar yield, and specific carbon dioxide yield for *A. vinelandii* strains cultured under hypoxic conditions (D = 0.066 h^{-1}, 250 rpm, 0% dO_2, 106 mg O_2 h^{-1}).

	Steady-State Values		
Strain	**Dry Cell Weight (g/L)**	**CO_2 Yield (mol/mol sucrose)**	**Specific CO_2 Yield (mol/mol sucrose/g dry BM)**
DJ Δ*hoxK*	0.69 (±0.04)	3.61 (±0.15)	7.47 (±0.04)
DJ Δ*hoxK*Δ*phbC*	0.61 (±0.04)	4.94 (±0.05)	11.57 (±0.02)
CA6	0.62 (±0.05)	3.88 (±0.03)	8.92 (±0.03)
CA6 Δ*phbC*	0.50 (±0.04)	4.55 (±0.24)	12.97 (±0.03)
CA11.6 Δ*phbC*	0.53 (±0.04)	4.28 (±0.02)	11.47 (±0.06)

Impact of oxygen exposure on biomass and product yields

The inability to recapture hydrogen and the deficiency in PHB formation by these *Azotobacter* strains allows for the kinetic monitoring of hydrogen generation *in vivo* that correlate with nitrogenase activity allowing for comparisons of the apparent molar hydrogen yields across various oxygen exposure conditions. Biological replicate chemostat culture experiments were conducted under iron-sufficient and nitrogen-free medium (D = 0.066 h^{-1}, 30°C), as previously described[129] with various metal cofactors added (Mo, V, or Fe only) to the media in order to measure hydrogen evolution by each particular nitrogenase system. Oxygen mass transfer was determined from experimental steady-state values of oxygen consumption and dissolved oxygen saturation. These rates were modified by adjusting the reactor agitation speed (250, 500, and 750 rpm, e.g. from 105.8 to 487.7 mg O_2 h^{-1}). Continuous measurements of the cultures and sample collection were performed at steady-state during each condition of oxygen exposure.

The measured oxygen mass transfer rates from gas to liquid phase did not increase proportionally to the change in agitation speed across the whole range of agitation settings. The largest change in rate was observed between 250 and 500 rpm (Figure 2.1). The lack of a linear relationship is expected because of the formation of a vortex, at agitation speeds above 500 rpm, which greatly increases oxygen transfer rates[130]. Oxygen remained the growth-limiting factor at agitation speeds below 500 rpm, so dissolved oxygen remained undetectable and significant residual sucrose was observed in the supernatant. At 500 rpm and above, carbon became the

limiting factor, so observed dissolved oxygen levels increased with increasing agitation (Figure 2.1).

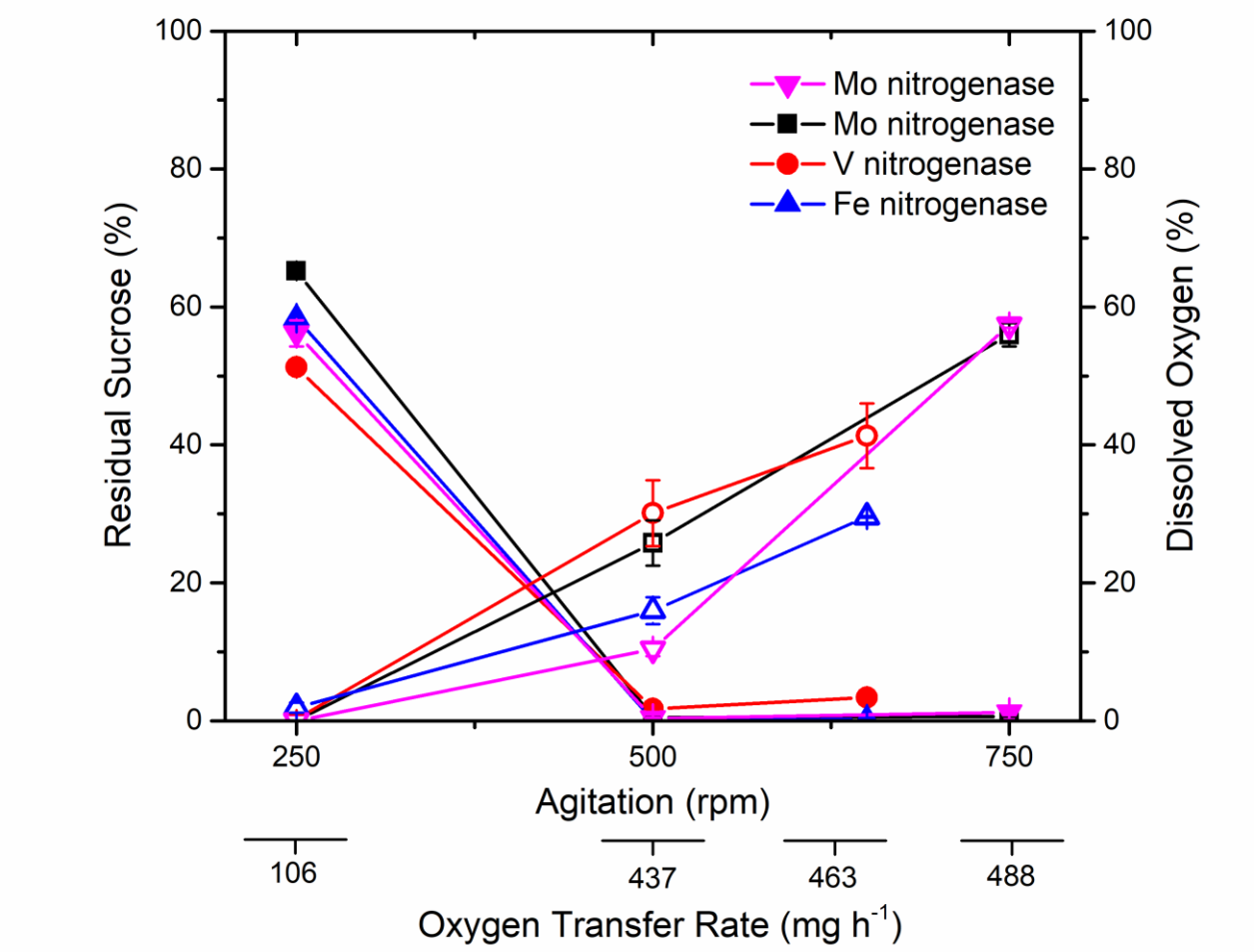

Figure 2.1. Steady-state values of residual sucrose (full symbols) and dissolved oxygen (empty symbols) as function of the increase of agitation speed/oxygen mass transfer rate. All *A. vinelandii* strains are negative for PHB production (Δ*phb*C) and have deletions of their uptake hydrogenase (Δ*hoxK* or natural CA mutation). Figure legend shows which nitrogenase system is active: purple triangles and black squares represent cells utilizing the Mo nitrogenase (DJ Δ*hoxK* Δ*phb*C and CA6 Δ*phb*C + molybdenum containing media), red circles represent cells utilizing the V nitrogenase (CA11.6 Δ*phb*C + vanadium containing media), and blue triangles represent cells utilizing the Fe nitrogenase (CA11.6 Δ*phb*C + iron-only media). All strains were cultured under D = 0.066 h^{-1} at 30°C. Supernatants of steady-state samples were taken at retention time intervals (~15h) for HPLC measurement while pO_2 measurements were constantly recorded. Error bars represent standard deviations from technical and biological replicates.

As predicted, increased cell exposure to oxygen resulted in decreased apparent hydrogen and biomass molar yields. As the cell exposure to oxygen was limited, the apparent hydrogen and biomass molar yields increased because of the reduction in adaptive respiration rates (Figure 2.2). Under all conditions of oxygen exposure, the cells utilizing the Fe nitrogenase showed the lowest values of apparent hydrogen molar yields, the cells using the Mo nitrogenase generated the highest, while the values of cells utilizing the V nitrogenase fell in the middle. The largest difference in apparent hydrogen molar yields between the isoenzymes occurred under the oxygen limiting condition (106 mg h^{-1}) with the Mo nitrogenase producing approximately 159 mmol H_2 mol^{-1} sucrose, the V nitrogenase producing 88 mmol H_2 mol^{-1} sucrose, and the Fe nitrogenase producing 75 mmol H_2 mol^{-1} sucrose (Figure 2.2). Comparable *in vivo* hydrogen yields were obtained for both strains utilizing the Mo nitrogenase (CA6 Δ*phbC*, DJ Δ*hoxK* Δ*phbC*). When cells employing either the V or Fe nitrogenases were cultured at the highest oxygen exposure level (488 mg h^{-1}), the cultures washed out due to the increased oxygen exposure and the limited nitrogenase activity was unable to sustain cell growth at the dilution rate tested. Therefore, cells using the alternative nitrogenases were cultured at a lower agitation rate (650 rpm) corresponding to an oxygen mass transfer rate of 463 mg h^{-1}.

Carbon dioxide molar yields increased concurrently with oxygen exposure, especially between 106 and 437 mg O_2 h^{-1} (Figure 2.2). These values correlated with oxygen consumption per unit of sucrose utilized, with coefficients of determination (R^2) between 0.748 and 0.999. There were no sustained differences in biomass or carbon dioxide molar yields between strains of *A. vinelandii* fixing nitrogen between the different nitrogenase isoenzymes, suggesting that the particular active nitrogenase utilized by the cell does not have a major impact on overall biosynthesis or respiration capabilities.

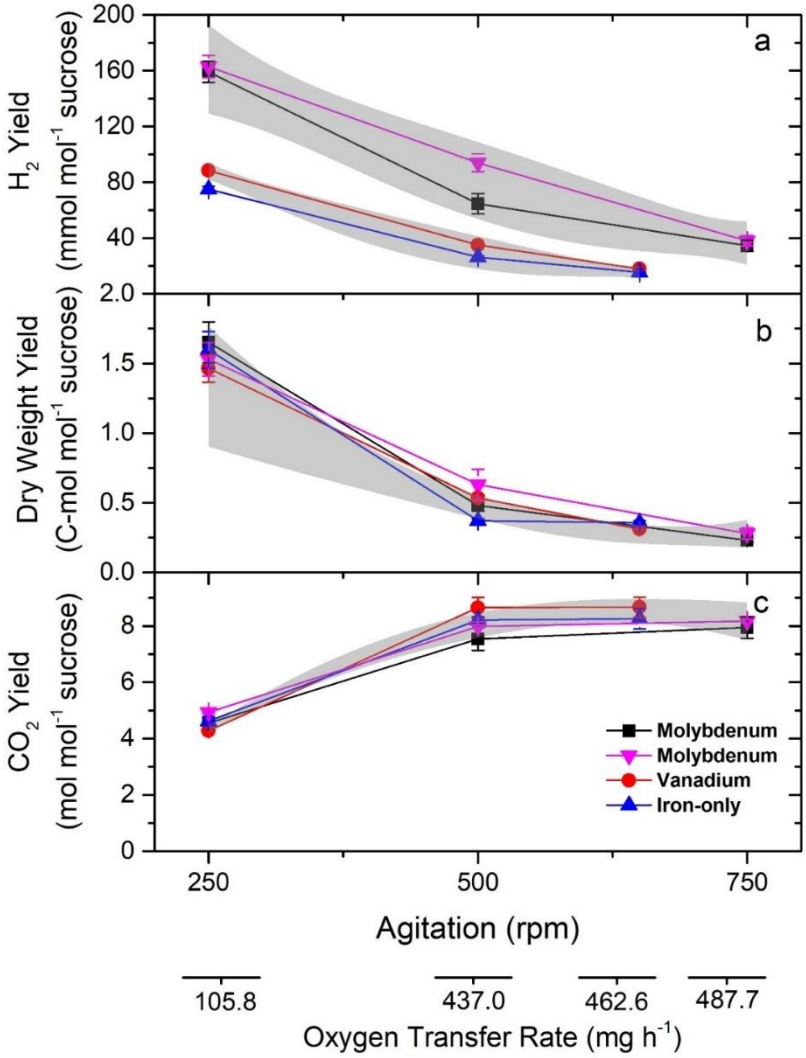

Figure 2.2. Steady-state apparent molar yields of hydrogen (a), biomass (b), and CO_2 (c) as function of the increase of agitation speed/oxygen mass transfer rate. All *A. vinelandii* strains are negative for PHB production (Δ*phb*C) and have deletions of their uptake hydrogenase (Δ*hoxK* or natural CA mutation). Figure legend shows which nitrogenase system is active: purple triangles and black squares represent cells utilizing the Mo nitrogenase (DJ Δ*hoxK* Δ*phb*C and CA6 Δ*phb*C + molybdenum containing media), red circles represent cells utilizing the V nitrogenase (CA11.6 Δ*phb*C + vanadium containing media), and blue triangles represent cells utilizing the Fe nitrogenase (CA11.6 Δ*phb*C + iron-only media). Grey areas represent confidence bands (95 % confidence) showing the best-fit line between data points. All strains were cultured under D = 0.066 h^{-1} at 30°C. Error bars represent standard deviations from technical and biological replicates.

Discussion

In this study we investigated the impact of dissolved oxygen on the growth and product molar yields of *Azotobacter vinelandii* using independently each of its nitrogenase systems. In addition to its lack of normal nitrogenase regulation, the mutants tested are deficient in uptake hydrogenase and PHB accumulation. The elimination of the PHB carbon storage mechanism allowed for measurable reduction in dry cell weight under oxygen limitation as well as increased values in specific CO_2 yields (Table 2.2). The above characteristics of these strains allow for *in vivo* direct measurement of the nitrogenase activity during active growth in chemostats leading to an accurate determination of product molar yields under all oxygen exposure conditions. Thus, a relationship between cell mass, hydrogen production, and catalytic capacity was achieved.

Our results verified the ability of *A. vinelandii* to fix nitrogen aerobically using each of the three nitrogenase isoenzymes independently. Hydrogen yield values generated by cells utilizing the Mo nitrogenase were comparable over the various oxygen exposure conditions tested (Figure 2.2); thus confirming that CA6 Δ*phbC* is primarily utilizing the Mo nitrogenase to fix nitrogen *in vivo* when molybdenum is bioavailable. The determined apparent molar yields demonstrate that increasing oxygen exposure reduce *in vivo* activity of all nitrogenase isoenzymes proportionally (Figure 2.2). This supports previous studies indicating that oxygen increases cause a higher proportion of electrons to directly combine with oxygen without contributing to ATP production essential for nitrogen fixation[187,193]. Under all tested conditions the highest apparent molar yields of hydrogen were generated by cells utilizing the Mo nitrogenase and the lowest from cells using the Fe nitrogenase while biomass between the strains remained constant (Figure 2.2). These variations may be a result of differences between the efficiencies of the nitrogenase isoenzymes. As mentioned previously, *in vitro* data suggests that the Mo nitrogenase has lower electron flux requirements than the alternative isoenzymes (11–17). This lower electron flux requirement results in a lesser demand for NADH through the nitrogenase complex and, therefore, cells utilizing the Mo nitrogenase *in vivo* are able to sustain higher enzyme activity levels and produce more hydrogen as a result. Future research targeting *A. vinelandii* for hydrogen production should focus on a Mo nitrogenase-utilizing strain.

These enzyme activity differences could also partially explain why Azotobacters and other diazotrophs prioritize the use of the Mo nitrogenase over the alternatives. In the wild-type, the membrane-bound uptake hydrogenase acts as an additional site for proton translocation and

generates a proton motive force, leading to increased ATP generation[125] and higher nitrogenase activity[128]. There has been some disagreement in the literature about whether or not the proton motive force (PMF) generated by the uptake hydrogenase confers a growth advantage for Azotobacters; with some studies supporting this idea[129,130] and one study refuting it[124]. In a recent publication, a wild-type strain of *A. vinelandii* was shown to have slightly better biomass and CO_2 productivities than similar strains without the uptake hydrogenase[129]. The data presented here indicates that wild-type cells, containing the uptake hydrogenase and utilizing the Mo nitrogenase, would generate more hydrogen, and thus a greater PMF, than cells utilizing the alternative isoenzymes. This difference in potential PMF would lead to a slightly larger ATP pool and, along with the lesser demand for NADH, may be the reason for the prioritization of the Mo nitrogenase in wild-type Azotobacters.

A. vinelandii is capable of adapting to a wide range of oxygen concentrations even when fixing nitrogen, which serves to enhance its fitness in nature, but makes study of its carbon metabolism more complex. When fixing nitrogen at high aeration, respiratory protection skews carbon flow toward CO_2, while at low aeration, a larger portion of the carbon assimilated goes toward biomass. Moderation in oxygen exposure is advisable to improve biomass and hydrogen molar yields. Here, we observed up to 4-fold increases in hydrogen and biomass molar yields under low aeration, although a large percentage of sucrose was left untouched (Figure 2.1, Figure 2.2). When oxygen provided was sufficient to allow complete consumption of carbon, biomass and hydrogen values were greatly reduced. The optimal conditions may require a compromise and fall in between these levels, controlling agitation to achieve the minimum detectable dissolved oxygen levels while still consuming a large percentage of the available carbon source.

Although the apparent hydrogen molar yields in this study are not yet competitive with commonly observed values from dark fermenters such as *Clostridium*, *Thermotoga*, and *Enterobacter* species[129], *A. vinelandii* has additional characteristics that make it valuable for various applications involving its nitrogenases. As one example, nitrogen fixation could be harnessed to provide fixed nitrogen fertilizer to plants or other industrially relevant microorganisms[203]. This paper provides researchers a tool for analyzing *in vivo* nitrogenase activity in real-time and will help streamline nitrogenase research in the future.

Chapter 3. Two-stage Continuous Conversion of Carbon Monoxide to Ethylene by Whole Cells of *Azotobacter vinelandii*

Introduction

Ethylene is a flammable, colorless gas used as a commodity feedstock in the production of a wide variety of commonly used polymers, fibers, and chemicals. Commercial production of this essential gas is currently accomplished by pyrolyzing non-renewable hydrocarbon feedstocks, such as crude oil and natural gas, under intense temperature and pressure[149]. The harsh process conditions cause the covalent bonds in heavy hydrocarbons to fracture and recombine, resulting in shorter-chain molecules such as ethylene[151]. This highly inefficient cracking process consumes an estimated 40% of the total energy used in the entire petrochemical industry and accounts for nearly 2% of global carbon dioxide (CO_2) emissions[149,152]. Alternatively, ethylene synthesis can be obtained by the Fischer-Tropsch (F-T) reaction, an industrial chemical method that combines carbon monoxide (CO) and hydrogen (H_2) gases over a metal catalyst under elevated temperature and pressure[157]. While this process is slightly more efficient than hydrocarbon cracking and can utilize renewable substrates like biomass-derived synthesis gas, the F-T synthesis reaction still generates greenhouse gas emissions at comparable levels[159]. Furthermore, the most profitable products of the F-T technology are the longer chain, high-quality diesel fuels and waxes, whereas ethylene production is not the primary objective[153,160,161]. As the world's governments become more carbon emissions conscious[1] and the global supply of non-renewable hydrocarbons becomes increasingly limited[2], a more sustainable approach for ethylene production will become necessary.

Microorganisms have long been studied as an alternative approach for the industrial production of many chemicals and fuels, with some commercial success[8-10]. These methods are attractive because they usually do not require high temperatures or pressures to operate and can utilize renewable substrates, such as corn and sugarcane as carbon sources. For the past several decades, researchers in this field have mainly been focused on fuel alcohol production, such as ethanol and butanol[204-207], while less attention has been given towards replacing, with biological alternatives, other petroleum-derived products such as ethylene. One reason for this discrepancy is that the few known biological ethylene production pathways described suffer from issues related to productivity, enzyme stability, and reagent cost; which limits overall commercial feasibility[164,174,175]. However, within the last decade, a new biological alternative was unveiled

involving the reduction and coupling of CO gas into ethylene and other hydrocarbons by the vanadium (V) nitrogenase from *Azotobacter vinelandii*[145,146]. While the exact mechanism is still under debate, the general reaction is similar to the industrial F-T process with the exception of H^+ ions being used as a substrate rather than H_2 gas (Equations 1 and 2).

Equation 1: $2CO + 8H^+ + 8e^{-1} \rightarrow C_2H_4 + 2H_2O$

Equation 2: $3CO + 14H^+ + 14e^{-1} \rightarrow C_3H_8 + 3H_2O$[176]

A. vinelandii is an aerobic, Gram-negative, diazotrophic bacterium that has long been recognized for its ability to produce many commercially-relevant compounds such as: alginate, polyhydroxybutyrate (PHB), H_2, and organic ammonium while utilizing cost-effective sources of carbon and molecular dinitrogen[14,91,108]. The wild-type strains encode three distinct versions of the nitrogenase complex, each employing a different metal cofactor, and regulation of each nitrogenase isoenzyme is based on the presence or absence of the associated metals[86-88]. For example, when molybdenum (Mo) is present, the Mo nitrogenase is expressed and the V and iron-only (Fe) nitrogenase isoenzymes are repressed[182].

To date, much of the research into the ethylene production capability of the V nitrogenase from *A. vinelandii* has been performed using small-scale, hermetically sealed systems[145,146,148,208]; which create critical oxygen limitations that negatively affect all aspects of *A. vinelandii* physiology (i.e. the finite amount of dissolved oxygen in these sealed systems is rapidly depleted by *A. vinelandii* cells which have extremely high rates of respiration)[209]. Compounding this issue, when CO is introduced into these closed systems, the additional stress that is created further impacts oxygen availability, nitrogen fixation, and redox generation[147,148,210-213]; resulting in complete cessation of cell proliferation. Nevertheless, we believe that when *A. vinelandii* is cultured in an open system with a continuous supply of both air and CO, nitrogen fixation and CO reductive coupling will be able to proceed simultaneously; resulting in a culture capable of continuous dynamic growth and ethylene generation.

Prior to testing such a continuous dynamic culturing system for *A. vinelandii* in the presence of air enriched with CO, it was necessary to have a reliable, real-time indicator for *in vivo* V nitrogenase activity. Traditional off-line acetylene reduction assays (requiring a multistep disruption to cells followed by data normalization)[214] generate inaccurate real-time data further skewed by the different affinities of each nitrogenase isoenzyme towards the substrate of the reaction [136,215]. Thus, to accomplish real-time monitoring of *in vivo* V nitrogenase activity, our

lab has previously studied specific mutants of *A. vinelandii*[129,216]. Particularly, the highly characterized strain CA11.6 Δ*phbC* was ideal for this purpose because, along with its previously reported absence of molybdenum (Mo) nitrogenase and PHB accumulation, the strain carries a natural 42 kb deletion eliminating the uptake hydrogenase activity and the overall nitrogenase regulation system found in the wild-type[80,129,131-133,199,200,216]. Strains carrying these disruptions show no evidence of growth impairment and allow CA11.6 Δ*phbC* to solely express its V nitrogenase in vanadium containing medium, even when molybdenum and iron metals are also present [200,216]. The absence of uptake hydrogenase activity in this mutant allows for the predictable release of H_2 gas evolving solely from V nitrogenase activity (Equation 3)[79,80,82,216]. Thus, making H_2 production a highly correlated metric to *in vivo* V nitrogenase activity when culturing *A. vinelandii* CA11.6 Δ*phbC* diazotrophically in medium containing vanadium.

Equation 3: $N_2 + 14H^+ + 14e^- \rightarrow 2NH_4^+ + 3H_2$ [217]

In this work, we implemented and characterized a robust and reliable two-stage continuous process for the cultivation of *A. vinelandii* in the presence of air enriched with CO. This methodology, in addition to determining accurate ethylene yield and productivity rates dynamically, allowed for the identification of specific culture conditions and bottlenecks that impact *in vivo* V nitrogenase-mediated ethylene production.

Materials and Methods

Strains and media

Azotobacter vinelandii CA11.6 Δ*phbC* was used throughout this work by taking advantage of its unique properties regarding deficiency of Mo nitrogenase (Δ*nifHDK*), deregulated capability to solely express its V nitrogenase, and inability to recapture the H_2 gas resulting from nitrogenase activity (CA6 natural mutation)[81,131,216]. Additionally, previous work demonstrated a linear relationship between biomass and product molar yields across all oxygen exposure conditions (*phbC* deletion)[216]; making this strain ideal for studying the continuous *in vivo* ethylene production capability from the V nitrogenase.

A. vinelandii CA11.6 Δ*phbC* Δ*cooS* was generated through transformation and homologous recombination as previously described[216]. Briefly, a partial region of the *cooS* gene was amplified by PCR from *A. vinelandii* CA11.6 Δ*phbC* genomic DNA using *cooS* gDNA primers and ligated into the multicloning site (mcs) of a pUC19 plasmid hosted by *Escherichia*

coli DH5α to create the pUC*cooS* plasmid. Next, a new multicloning site was added into the middle of the partial *cooS* region in pUC19*cooS* using the pUC*cooS* mcs primers resulting in a new pUC*cooS*mcs plasmid. Finally, a spectinomycin resistance cassette, *aadA*, was amplified by PCR from a spectinomycin resistant *A. vinelandii* strain using *aadA* gDNA primers and inserted into the mcs within the *cooS* region of the pUC*cooS*mcs plasmid; resulting in the pUCSA plasmid. This pUCSA plasmid was then linearized with a *Bam*HI restriction enzyme and transformed into competent *A. vinelandii* CA11.6 Δ*phbC* cells and incubated at 30°C for 1 hour to allow for homologous recombination. This was then followed by plating on Burk's agar medium containing 20 µg mL^{-1} spectinomycin to select for the *A. vinelandii* CA11.6 Δ*phbC* Δ*cooS* mutant. Successful integration was further confirmed by PCR using integration confirmation primers that targeted the flanking genomic region upstream of *cooS* gene and the spectinomycin resistance cassette (Table 3.1).

Table 3.1. Plasmids and primers used in this study. Primers are shown with added restriction sites: boldface sequence indicates the added restriction site and underlined sequence indicates homology to the target. Primers were designed using Clone Manager 9 software (Sci-Ed Software) and ordered from Integrated DNA Technologies (IDT, Coralville, IA USA).

Plasmids and primers	**Relevant characteristic(s)**	**Source**
Plasmids		
pUC19	Amp^r, *lacZ* α-subunit, pMB1 origin	NEB
pUC*cooS*	pUC19 + *cooS* region inserted at multicloning site	This study
pUC*cooS*mcs	pUC*cooS* + new multicloning site added into *cooS* region	This study
pUCSA	pUC*cooS*mcs + spectinomycin cassette inserted into *cooS* mcs, Sp^r	This study
Primers		
cooS gDNA Fwd	AA**GGATCC**-AGTTCGGTCTGCGAGTTGTG	This study
cooS gDNA Rev	CCT**AAGCTT**-TCAAGGGCGTATCCAAGGTG	This study
pUC*cooS* mcs Fwd	GA**AGATCTCCATGGCTCGAGAG**-CATCAGTGAGACCGGATC	This study
pUC*coos* mcs Rev	GA**AGATCT**-CGTGCTGAAGATGAGCCTGATCG	This study
aadA gDNA Fwd	GA**AGATCT**-CACCGTGGAAACGGATGAAGG	This study
aadA gDNA Rev	CATG**CCATGG**-GCGTCGGCTTGAACGAATTG	This study
Integration Confirm Fwd	TGGTCAGCACCAGCACGTTC	This study
Integration Confirm Rev	GCTCGCCGCGTTGTTTCATC	This study

All experiments were performed using a glucose / vanadium modified Burk's medium recipe to culture *A. vinelandii*. In short, the medium contained (per liter) 10-20 g glucose, 0.2 g magnesium sulfate, 90 mg calcium chloride, 0.2 g potassium phosphate monobasic, 0.8 g potassium phosphate dibasic, 15 mg iron sulfate, 0.5 g sodium citrate, and 4 mg sodium metavanadate. The glucose, iron, and salts were mixed together and autoclaved separately from the potassium phosphate buffer solution in order to prevent precipitation. After cooling, the two solutions were combined under sterile conditions. Inocula were prepared by incubating cells at 30°C, shaking at 150 rpm in 150 mL shake flasks.

Definitions and mathematical expressions

Dilution rate (D) is the value of inflow of fresh medium divided by the volume of culture. When the reactor is maintained at a constant culture volume by maintaining equal feed and harvest flows the dilution rate is constant and equals specific growth rate. The overall dilution rate for a two-stage system is calculated by dividing the media flow rate by the constant volumes from each reactor ($D_{overall}$ = Flow/[$Volume_1$+$Volume_2$]).

Retention time (RT) is the time required for an entire culture volume to be replaced. This value is calculated by taking the inverse of the dilution rate (RT = 1/D).

A steady-state is defined as a condition in which all the monitored variables' values remain unchanging with time. For example, a steady-state condition in our system was achieved when all physical and biological parameters (biomass concentration, residual glucose concentration, H_2 and CO_2 yields) remained constant after at least three retention times. In contrast, a transient state is defined as a condition in which at least one parameter is changing over time.

In our system, we define the mass oxygen transfer rate (MOTR) as the mass of O_2 transferred to, and consumed by, the bacterial cells per unit of time. We calculated this value using the following equation, as previously described[216].

Equation 4: MOTR = C + kSF

MOTR is the oxygen transfer rate in milligrams per hour, *C* is the oxygen consumption rate by cells in milligrams per hour, *k* is a constant reflecting the amount of oxygen dissolved per liter of medium (7.456 mg per liter), *S* is the measured dissolved oxygen saturation, and *F* is the flow rate of gas in liters per hour.

Yield is defined as the ratio of product generated to the amount of substrate consumed. Specific productivity is the value of product generated per amount of biomass generated per unit of time. Volumetric productivity is the value of product generated per culture volume per unit of time.

Two-stage bioreactor setup

A two-stage continuous process consisting of a 2-liter stirred tank reactor generating biomass containing active V nitrogenase and a second reactor dedicated to reductive coupling of CO were connected in series and each controlled by Biostat Bplus control units (Sartorius). In the seed tank: temperature was held at 30°C, pH was allowed to freely vary, constant volume was maintained at 0.7 L, and filtered compressed air was sparged at a constant rate of 0.315 ± 0.05 liters per minute (lpm) using a mass flow control system. In the reaction vessel the temperature was held at 30°C, pH was allowed to freely vary, constant volume was maintained at 1.75 L, and filtered compressed air and/or 5% CO-enriched air (AirGas, Raleigh, NC) was sparged at a rate of 0.315 ± 0.05 lpm using a mass flow control system. In the cases where a lower concentration of CO was needed, two mass flow control systems were used to mix the 5% CO / 95% air gas mixture with 100% compressed air.

To begin each experiment, both reactors were sterilized separately and then assembled and connected together under sterile conditions. Both reactors were filled with modified Burk's medium and were set to maintain appropriate temperature (30°C) with slow mixing from the impellers (200 rpm). The seed tank was inoculated with pregrown batch cells that were allowed to proliferate under similar batch conditions until the culture reached mid-log phase. At this point, inflow of fresh medium and removal of excess culture was initiated while maintaining constant volume. The effluent volume from the seed tank (containing biomass and residual Burk's medium) was continuously pumped to the reaction vessel, and the excess culture volume from the reaction vessel was then sent to a harvest tank. Once steady-state conditions were achieved, at least three samples were collected at different retention times.

Gas analysis

Several exhaust gases (O_2, CO_2, H_2, and CO) were monitored and recorded in real-time using in-line EasyLine Continuous Gas Analyzers, Model EL3020 (ABB, Germany) and a

Pfeiffer OmniStar quadrupole mass spectrometer. For ethylene gas monitoring, samples were manually collected from the reaction vessel headspace using a gas-tight syringe and immediately analyzed on an Agilent 7890A – FID gas chromatograph with prior separation using a 6-foot Restek Porapak Q80/100 stainless steel packed column. Briefly, the samples were injected into a split/splitless injector held at 200°C with an oven temperature maintained at 40°C while using nitrogen as the carrier gas at a constant flow rate of 10 mL min^{-1}. The column was coupled to a flame-ionization detector operated at 200°C. Absolute values were obtained by measuring known quantities of pure ethylene gas (Airgas, USA), as well as propane and butane, to generate standard curves which had a limit of detection of 1ppm.

Liquid sample analysis

Each culture sample was processed as previously described[129,216]. Briefly, during steady-state conditions, approximately 10 mL of culture volume was collected at independent retention time intervals and a small volume from each sample was pelleted and frozen at -20°C for later HPLC analysis. Biomass concentration values were quantified by filtering (using vacuum suction) a fixed sample volume (1 to 4 mL depending on culture turbidity) through a 0.2 µm filter of a known mass (mixed cellulose ester membranes, EMD Millipore, Germany). The filter was then dried at 60°C until constant weight to determine the dry weight of biomass per filtered volume.

Initial and residual concentrations of glucose were determined by a high-performance liquid chromatograph (Shimadzu, Japan) operated under isocratic conditions at 65°C and 5mM H_2SO_4 mobile phase flowing at 0.5 mL min^{-1} through a Rezex™ ROA-Organic Acid H+ column (Phenomenex, USA). The column was coupled to a refractive index detector and absolute values were obtained by measuring known quantities of glucose to generate a standard curve.

Results

Configuration of the two-stage continuous culture system

As stated previously, culturing *A. vinelandii* diazotrophically using hermetically sealed systems exposed to a concentration of CO gas greater than 0.2% creates a critical oxygen limitation that significantly impairs nitrogen fixation and cell proliferation[147,148]. To mitigate this problem, we implemented a continuous two-stage open system operated with continuous flow of

air enriched on different concentrations of CO. These types of culturing systems have traditionally been utilized to mitigate the negative impacts of inhibitory compounds on microbial growth[218,219] while increasing product generation[220,221].

For our application, the first stage (seed tank) was dedicated to the continuous generation of dense *A. vinelandii* biomass with maximal content in active V nitrogenase. The biomass from this stage was subsequently fed, along with residual medium components, into a second vessel (reaction vessel) exposed to air enriched with CO. Gas and volume flows were identical in both tanks while cell retention time in the reaction vessel was increased. This strategy allowed for continuous supply of active *A. vinelandii* cells from the seed tank to the reaction vessel while maximizing biomass production and catalytic potential, thereby preventing culture washout and extending growth in an air enriched with CO atmosphere.

Determining the optimal physiological state to maximize in vivo V nitrogenase activity and biomass production

To maximize the potential of the continuous two-stage system, we identified the optimal seed tank reactor conditions that would result in the continuous transfer of dense *A. vinelandii* biomass containing catalytically active V nitrogenase. Previously published single-stage chemostat experiments tested a reduced number of mass oxygen transfer rate (MOTR) conditions with *A. vinelandii* and found that oxygen growth limitation allows for higher steady-state H_2 yields and maximal biomass yields while controlling residual sugar levels[216]. Oxygen limiting growth conditions allow *A. vinelandii* to utilize its electron transport chain cytochrome c_4 / c_5 branch, which correlates with higher rates of proton translocation, ATP generation, and biomass production. On the contrary, carbon-limited cultures sacrifice ATP generation when utilizing the cytochrome *bd* branch as a way of protecting nitrogenases from irreversible inactivation by oxygen, commonly referred to as respiratory protection[25,178,179,216,222]. While the effects of low and high oxygen exposure conditions on biomass molar yield and *in vivo* nitrogenase activity are well understood, the intermediate range of MOTR conditions required further testing. Therefore, we performed new single-stage chemostat experiments culturing *A. vinelandii* CA11.6 Δ*phbC* and tested a wider range of oxygen exposure conditions and physiological states (dilution rates).

Throughout this process, we found that increasing the MOTR in the seed tank, up to 283 mg O_2 h^{-1}, had a positive effect on both biomass concentration and H_2 yield. Under these

conditions, the culture maintained a steady-state value of biomass concentration of over 1.0 g L^{-1} dry weight biomass and a H_2 yield of at least 1,150 μg H_2 g^{-1} glucose consumed. At this optimal MOTR, and as a function of the dilution rate, roughly 10-40 % of the initial 10 g L^{-1} glucose was left unutilized (Figure 3.1). Also, when the cells were exposed to increasingly higher MOTRs (>300 mg O_2 h^{-1}), the culture rapidly became carbon-limited and a precipitous drop in both steady-state biomass concentration and H_2 yield was observed; indicating the physiological state at which respiratory protection was activated and the cytochrome branch switched from the c_4 / c_5 branch to the *bd* branch. Increasing the dilution rate, and by definition the specific growth rate, from 0.055 h^{-1} to 0.077 h^{-1} while maintaining constant MOTR had a negative effect on overall biomass concentration, little effect on H_2 yield, and an expected decrease in the levels of glucose utilization (Figure 3.1).

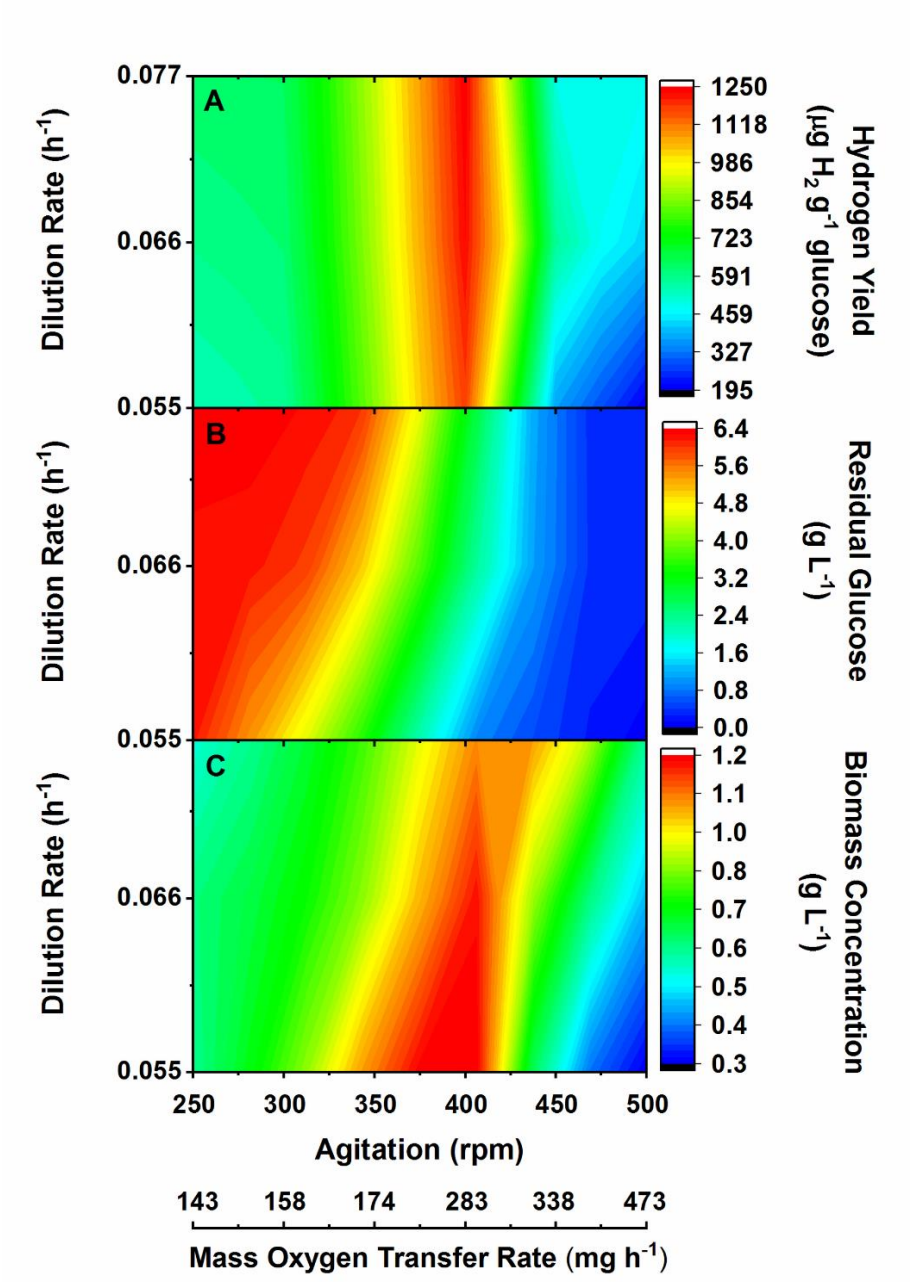

Figure 3.1. Interpolation of 18 experimental steady-state values of [A] hydrogen yield (µg H2 g^{-1} glucose), [B] residual glucose concentration (g L^{-1}), and [C] biomass concentration (g L^{-1}) obtained from *A. vinelandii* CA11.6 Δ*phbC* cultured in a single-stage chemostat reactor with 10 g L^{-1} initial glucose Burk's medium at various dilution rates (0.55 h^{-1} to 0.77 h^{-1}) and oxygen exposure conditions (143 to 473 mg O_2 h^{-1}). All cultures were grown at 30°C with an air flow rate of 315 mL min^{-1} and a constant volume of 0.7 L. Dilution and oxygen transfer rates were altered by changing the inflow rate of the media and agitation of the impeller, respectively.

Even though H_2 yield and biomass production were maximal under the MOTR of 283 mg O_2 h^{-1} steady-state condition, the amount of residual glucose was an insufficient carbon and energy source for the cells present in the reaction vessel. After careful consideration, we selected a MOTR of 210 mg O_2 h^{-1} and a dilution rate of 0.077 h^{-1} in the seed tank; ensuring a constant flow of approximately 0.9 g L^{-1} dry weight biomass containing catalytically active V nitrogenase (1,000 μg H_2 g^{-1} glucose consumed) to the reaction vessel while also transferring sufficient redox power (residual glucose ≥5.4 g L^{-1}) (Figure 3.1).

Transient production of ethylene; baseline yield and productivity rates

Once the seed tank culture reached steady-state under the desirable operational conditions, a harvest tube was connected in series with the reaction vessel to complete the two-stage system. The volumes of the seed tank (0.7 L) and the reaction vessel (1.75 L) were maintained at a constant level to maximize both the retention time of our system and the absolute amount of catalyst participating in CO reductive coupling. The catalytically active biomass and residual medium components from the seed tank were constantly fed into the reaction vessel and allowed to reach steady-state values under the same oxygen growth limiting conditions at a dilution rate of 0.031 h^{-1} (Table 3.2). Under these steady-state conditions, it was found that the active biomass concentration in the reaction vessel was 1.1 g L^{-1}, H_2 yield was 695 μg H_2 g^{-1} glucose, while 97% of the initial glucose had been consumed while still maintaining oxygen as the growth limiting factor (Table 3.2). A decrease in H_2 yield was expected as any changes in culturing conditions (i.e. the change in physiological state from the seed tank to the reaction vessel) results in a disruptive effect on *A. vinelandii* physiology that manifests itself as lower biomass and product molar yields[129]. The measured value of reaction vessel MOTR for this new condition was 280 mg O_2 h^{-1} and adjustments to this parameter, either higher or lower, resulted in further reduced steady-state H_2 yield values and biomass concentrations. Thus, these initial conditions were chosen to test the cultures' continuous CO reductive coupling capacity.

Once steady-state conditions were achieved in the two-stage system, the 100% air stream in the reaction vessel was replaced with a 5% CO / 95% compressed air gas mixture at constant flow. This is near the highest allowable concentration for safe laboratory research as the lower explosion limit (LEL) for CO vapor in air is 12.5% by volume, and standard practice recommends operations at concentrations below 50% LEL.

Samples taken over one-hour time intervals were used to monitor transient ethylene production using off-line GC-FID chromatography. After each hour of CO exposure, the 100% air stream was reestablished and the culture was allowed to return to its initial steady-state conditions that were confirmed by returning to prior constant values of H_2 yield and biomass production. The CO pulsing and sampling process was repeated followed by at least three retention time intervals to ensure reversible V nitrogenase activity recovery, overall system reproducibility, and statistical significance.

Experiments using repetitive one-hour air enriched with 5% CO gas flows generated an average transient ethylene yield of 353 µg g^{-1} glucose consumed corresponding to a volumetric ethylene productivity of 57 µg L^{-1} h^{-1} (Table 3.2). No major deleterious effects in the culture's turbidity or changes in CO_2 production were observed.

Table 3.2. Key process parameters and steady-state values from *A. vinelandii* CA11.6 Δ*phbC* cultured in the two-stage continuous system. Operative conditions in the seed tank were identified in Figure 1 while conditions in the reaction vessel were set to ensure near complete sugar utilization (>90%) while maintaining an oxygen-limited culture (<1% pO_2). During continuous CO exposure, gas samples were taken from the headspace every 20 minutes for one hour and measured off-line by GC-FID. The * symbol indicates transient production values.

Parameters / Steady-state values	**Seed tank**	**Reaction vessel**
Initial Glucose Concentration (g L^{-1})	9.6	5.9
Residual Glucose Concentration (g L^{-1})	5.9	0.3
Gas Flow Rate (mL min^{-1})	315	315
Dissolved Oxygen (%)	0	0
Volume (L)	0.70	1.75
Dilution Rate (h^{-1})	0.077	0.031
Agitation (rpm)	350	350
Mass Oxygen Transfer Rate (mg h^{-1})	210	280
Biomass Concentration (g L^{-1})	0.9 ± 0.1	1.1 ± 0.1
H_2 Yield (µg H_2 g^{-1} glucose)	1000 ± 9	695 ± 3
C_2H_4 Yield (µg g^{-1} glucose)	-	353 ± 34*
Sp. C_2H_4 Productivity (µg g^{-1} dry weight h^{-1})	-	54 ± 7*
Volumetric C_2H_4 Productivity (µg L^{-1} h^{-1})	-	57 ± 7*

Identifying the reaction limiting factors of V nitrogenase-mediated CO reductive coupling

After determining the baseline transient values of ethylene yield and productivity under the above culture conditions, further CO pulse experiments were conducted to identify reaction-limiting factors for ethylene generation. It was hypothesized that absolute catalyst abundance and/or CO mass transfer would be responsible for limiting the ethylene generation of the system.

To evaluate whether these factors limited ethylene generation, we tested a range of biomass concentrations (i.e. absolute catalyst abundance) and input CO concentrations (i.e. CO mass transfer) while maintaining constant *in vivo* V nitrogenase activity (monitored as H_2 yield). To accomplish this task, the initial glucose concentration was increased sequentially leading to new steady-state values of biomass concentration under oxygen limiting growth conditions. Later, the reaction vessel was transiently exposed to air enriched with CO concentrations ranging from 0 to 5%. During these experiments, the seed tank parameters were fixed as previously described and the steady-state values (maintaining oxygen limiting growth conditions) were monitored to ensure consistency (Table 3.2). Since the seed tank's growth limiting factor was oxygen, all additional glucose was transferred to the reaction vessel, and the MOTR in the reaction vessel was increased to allow for maximal glucose utilization while also ensuring equivalent steady-state H_2 yields (Figure 3.2). Once steady-state values were established, under 100% airflow, and after at least three retention times had occurred for each biomass concentration, the constant gas flow rate of 315 mL per minute of air in the reaction vessel was transiently replaced with air enriched with CO ($3 \rightarrow 4 \rightarrow 5$ % CO) for one hour intervals at each concentration as previously described.

Ethylene production was monitored off-line by GC-FID during each transient CO exposure. The averaged data showed increases of volumetric ethylene productivity proportional to biomass and CO concentrations, at constant H_2 yield (reaching a maximum rate of 118 µg C_2H_4 L^{-1} h^{-1}); while the transient ethylene yield values (reaching a final yield of 289 µg C_2H_4 g^{-1} glucose consumed) remained proportional to the input CO concentration and H_2 yield, and was not limited by the biomass concentration (Figure 3.2). These trends are indicative of a reaction limited by CO mass transfer and not by the biomass abundance (i.e. absolute catalyst abundance). Therefore, this reaction follows traditional Michaelis Menten kinetics where a higher substrate concentration under constant *in vivo* V nitrogenase activity will lead to a higher reaction rate until reaching maximum velocity (V_{max}) and product saturation[223].

Furthermore, to confirm that the V nitrogenase was responsible for all observed ethylene production, ammonium acetate was added to the medium at the end of each run; resulting in the inactivation of the V nitrogenase along with elimination of ethylene production (Figure 3.2).

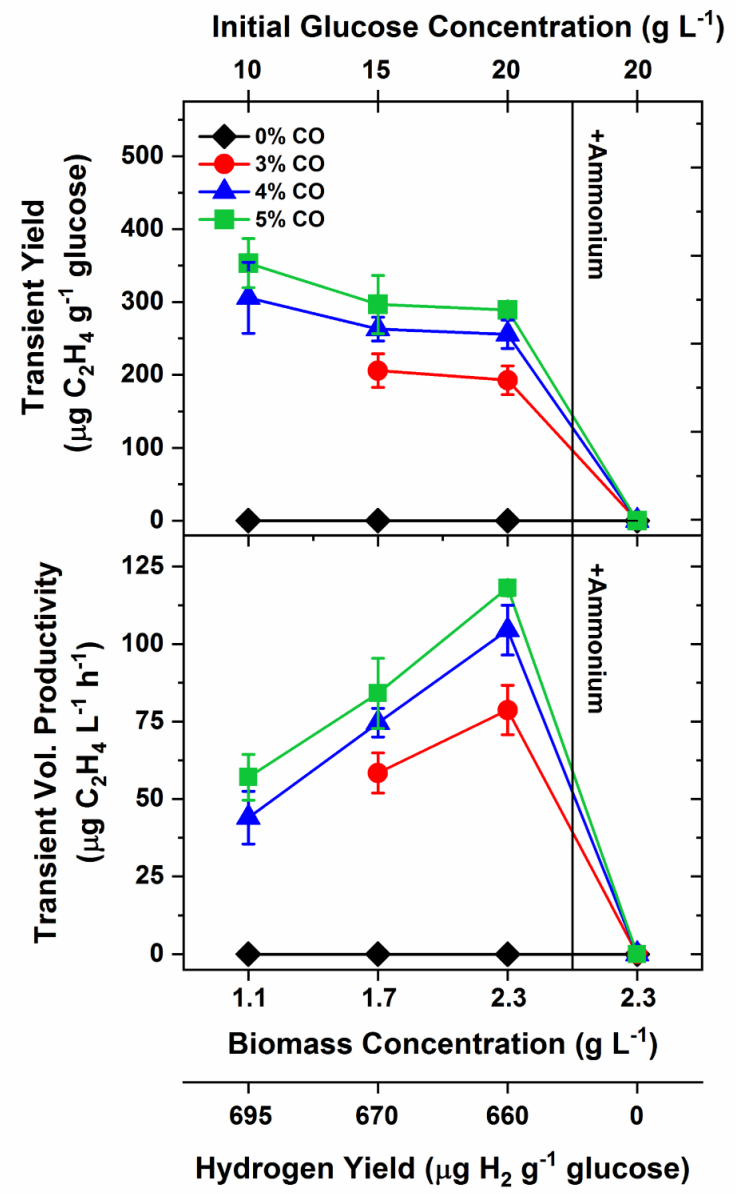

Figure 3.2. Transient ethylene yield and volumetric productivity values obtained after the reaction vessel was continuously exposed to various CO concentrations for one-hour intervals. Conditions in the reaction vessel were set to maximize consumption of the available glucose (>90% glucose consumption) while still remaining oxygen limited (<1% pO_2) and maintaining constant hydrogen yield values across conditions. At the end of the experiment, ammonium acetate was added to the input medium to a final concentration of 15 mM.

Increased CO mass transfer corresponds to increased transient ethylene production

To further prove that *in vivo* V nitrogenase-mediated ethylene production is governed by Michaelis Menten kinetics, we decided it was necessary to increase either *in vivo* V nitrogenase activity or CO solubility in an attempt to reach V_{max}. Since we were already operating at near maximum steady-state H_2 yields (V nitrogenase activity) under our culturing conditions, increasing CO mass transfer was targeted. There are several physical parameters that can alter CO mass transfer in stirred tank reactors including: gas bubble size, reactor temperature, impeller design, agitation speed, and gas flow rate[224-227]. Of these potential options, we chose to decrease the input gas bubble size by replacing the previously used ring sparger in the reaction vessel with a 0.5 µm pore size stone microsparger; which reportedly reduces gas rise velocity and increases gas-liquid contact times[224,228]. The two-stage reactor was operated in a similar manner as before (20 g L^{-1} glucose Burk's broth) but the agitation parameter in the reaction vessel was reduced (470 rpm → 450 rpm) to account for the increased MOTR caused by the smaller bubbles while ensuring equivalent steady-state values for residual glucose concentration, H_2, CO_2, and biomass yields (Table 3.3). Once the culture reached steady-state conditions under 100% air flow and at least three retention times had passed, the air enriched with 5% CO was microsparged for one-hour intervals and transient ethylene production in the exhaust gas was again monitored as previously described.

As expected, the results confirmed that increased CO gas-liquid contact time resulted in statistically significant increases in transient ethylene yield and productivity (p-values > 0.05) (Table 3.3). Thus, providing additional evidence that CO mass transfer is a key bottleneck under our experimental conditions. However, product saturation does not appear to have been reached, demonstrated by a proportional increase in volumetric ethylene productivity. Therefore, further efforts to increase this parameter should result in additional ethylene production until the reaction reaches V_{max}.

Table 3.3. Kinetic and yield parameters from *A. vinelandii* CA11.6 Δ*phbC* cultured in two-stage continuous system. Pulsed CO experiments containing a 5% CO / 95% compressed air was performed into the reaction vessel during one-hour intervals and then allowed to return to steady-state conditions under 100% air flow. Reported steady-state values of H_2 and CO_2 for these experiments were obtained during 100% airflow. Exhaust H_2 gas was not measured during times of CO exposure for safety reasons. Experiments under continuous flow of air enriched with 5% CO were performed for over 80+ hours. Reported values of CO_2 and ethylene were obtained during the CO exposure period once the culture achieved a new steady-state equilibrium. The * symbol indicates transient production values.

Parameters / Steady-state values (Reaction vessel only)	**Pulsed CO**	**Pulsed CO**	**Continuous CO**
Gas Sparger	Ring	Microsparger	Microsparger
Gas Flow Rate (mL min^{-1})	315	315	315
Agitation (rpm)	470	450	450
Mass Oxygen Transfer Rate (mg h^{-1})	705	916	930
5% CO Exposure Time (h)	1	1	84
Glucose Transfer from Seed Tank (g L^{-1})	16.9	17.3	17.3
Residual Glucose (g L^{-1})	0.6	1.7	4.5
Dissolved Oxygen (%)	0	0	15
Biomass Concentration (g L^{-1})	2.3 ± 0.2	2.3 ± 0.1	1.2 ± 0.1
H_2 Yield (μg H_2 g^{-1} glucose)	657 ± 5	663 ± 2	Not measured
Exhaust CO_2 Production (%)	3.27 ± 0.05	3.23 ± 0.05	2.65 ± 0.02
C_2H_4 Yield (μg g^{-1} glucose)	289 ± 9*	319 ± 18*	302 ± 9
Sp. C_2H_4 Productivity (μg g^{-1} dry weight h^{-1})	45 ± 6*	60 ± 2*	90 ± 3
Volumetric C_2H_4 Productivity (μg L^{-1} h^{-1})	118 ± 3*	140 ± 8*	106 ± 3

Continuous two-stage system allows for steady-state culturing in the presence of CO

To investigate whether our two-stage culturing mode of operation could successfully mitigate the previously reported negative effects of CO on diazotrophic growth and allow for continuous dynamic culturing of *A. vinelandii* in an air enriched CO atmosphere, the reaction vessel was continuously sparged with air enriched with 5% CO for over 80 hours. During the initial 24 hours of CO exposure, the *A. vinelandii* CA11.6 Δ*phbC* culture exhibited a slight increase in CO_2 production and ethylene productivity with little effect on biomass compared to steady-state values, followed by an asymptotic decline in CO_2, biomass, and ethylene production. However, the culture did not washout and instead approached a new steady-state condition, as indicated by stabilizing ethylene and CO_2 production values, after approximately 48 hours of

exposure (Figure 3.3, black squares). Over the next 30+ hours, this new equilibrium condition maintained constant production of approximately 1.2 g L^{-1} dry biomass, 2.7% CO_2, and an ethylene yield of 302 µg g^{-1} glucose consumed (Table 3.3). Interestingly, the growth-limiting factor for this new equilibrium was neither oxygen nor carbon availability, as in all of our previous reactor runs, since both were found to be in excess in the reaction vessel (Table 3.3). One explanation that aligns with previously collected *in vitro* data[229], is that CO is competing with N_2 for the active site of the V nitrogenase which would likely result in reduced intracellular ammonium production; potentially making nitrogen availability the key growth-limiting factor for *A. vinelandii* when continuously cultured in air enriched CO atmospheres.

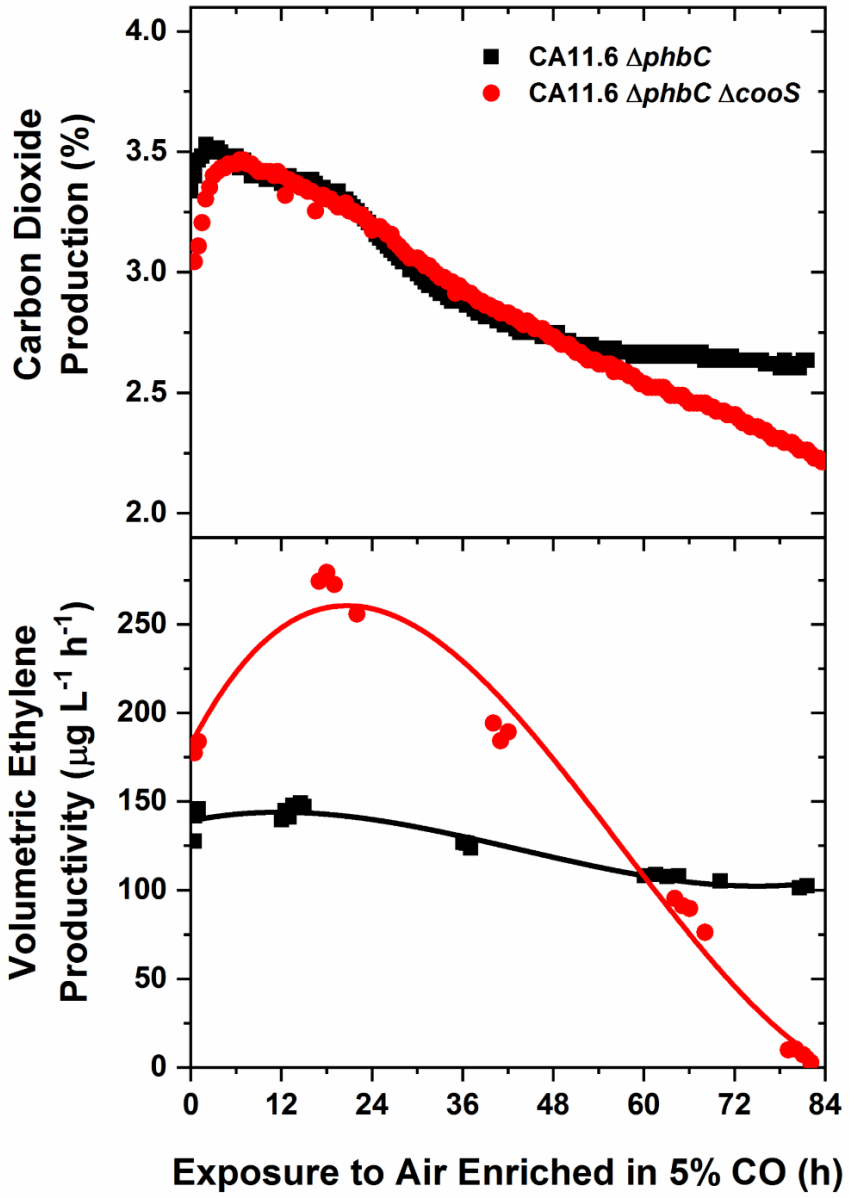

Figure 3.3. CO_2 and ethylene production values monitored over time from independent cultures of *A. vinelandii* CA11.6 Δ*phbC* (black squares) and *A. vinelandii* CA11.6 Δ*phbC* Δ*cooS* (red circles) exposed to a continuous inflow of air enriched with 5% CO for over 80 hours. Each reaction vessel was outfitted with a 0.5 µm pore-size stone microsparger and operated with 20 g L^{-1} initial glucose Burk's medium and identical seed tank parameters. During CO exposure, exhaust CO_2 was continuously monitored by an in-line EasyLine Continuous Gas Analyzer while ethylene in the headspace was monitored off-line periodically by a GC-FID.

CO dehydrogenase role on continuous dynamic growth and ethylene formation

While our data clearly shows *A. vinelandii* CA11.6 Δ*phbC*'s ability to sustain dynamic growth while reductively coupling CO into ethylene using its V nitrogenase, it may not be the only enzyme participating in CO catalysis. In fact, there are predicted genes in the *A. vinelandii* genome that may relate to CO metabolism[131,230]. For example, the most relevant is an annotated operon with high sequence similarity to a membrane-bound anaerobic CO dehydrogenase (*cooFSCJT*), which oxidizes molecules of CO into CO_2 (Equation 5).

Equation 5: $CO + H_2O \leftrightarrow CO_2 + 2e^- + 2H^+$ [231]

Furthermore, unrelated RNA-sequencing experiments with *A. vinelandii* have shown presence of transcripts from this operon when cultured under aerobic conditions[112]. If this putative CO dehydrogenase (CODH) is produced and active during times of CO exposure, then V nitrogenase-mediated ethylene production may be limited by a decrease of intracellular soluble CO gas caused by competition with CODH. Therefore, we decided to knock out the main subunit of the putative CODH complex, *cooS*, and culture this new strain (*A. vinelandii* CA11.6 Δ*phbC* Δ*cooS*) in the two-stage continuous system as previously described.

Culturing the new strain under 100% air flow resulted in no observable deleterious effects on cell proliferation or steady-state product yields as compared to the CA11.6 Δ*phbC* strain. During the initial 24 hours of exposure to air enriched with 5% CO, we observed a sharp increase in transient volumetric ethylene productivity compared to the CA11.6 Δ*phbC* strain, reaching a maximum rate of 279 µg ethylene L^{-1} h^{-1} representing a 62% relative increase in ethylene production (Figure 3.3). However, *A. vinelandii* CA11.6 Δ*phbC* Δ*cooS* was unable to reach equilibrium under these conditions and biomass began to washout of the reactor (i.e. values of biomass and CO_2 dropped precipitously and ethylene production was eliminated altogether) (Figure 3.3, red circles). This data points to an increased concentration of available CO that is able to outcompete N_2 for the active site of the V nitrogenase. A reduction to 3% CO concentration in gas flow provided further evidence of competitive inhibition. At this lower CO concentration, the culture reached equilibrium values comparable to those shown in Figure 3.3 (black squares), while continuously producing an increased amount of ethylene (143 ± 4 µg C_2H_4 L^{-1} h^{-1}). This genetic and physiological evidence further confirms that CO acts as a competitive inhibitor of the V nitrogenase and consequently the maintenance of a suitable soluble CO

concentration is a key factor in achieving simultaneous V nitrogenase-mediated nitrogen fixation and continuous CO reductive coupling.

Discussion

In this report, we achieved industrially relevant continuous ethylene production from a dynamically growing culture of *A. vinelandii*. To accomplish this, a continuous two-stage mode of operation system was implemented wherein controlled cell proliferation was physically separated from CO biotransformation. This type of culturing system, which has been thoroughly characterized over many decades[232,233], required prior process development to identify culture conditions and bottlenecks specific to *in vivo* V nitrogenase-mediated ethylene production.

First, we identified reactor process parameters specific to each stage, such as oxygen culture exposure, to maximize biomass production and *in vivo* V nitrogenase activity while also recognizing CO mass transfer as a key reaction limiting factor (Tables 3.2, 3.3 and Figures 3.1, 3.2). Second, we demonstrated the possibility of simultaneous cellular respiration, nitrogen fixation, and CO reductive coupling by cultures of *A. vinelandii* (Table 3.3, Figure 3.3). We also found that having an intact *cooS* gene was vital in maintaining dynamic growth and continuous ethylene generation in high concentrations of air enriched CO atmospheres (Figure 3.3).

Figure 3.4 shows a schematic representation of the important *A. vinelandii* CA11.6 Δ*phbC* physiology occurring in the continuous two-stage system. Overall, the dynamic production system was able to mitigate CO competitive inhibition of the V nitrogenase during diazotrophic growth and prevented culture washout while continuously producing 302 µg ethylene g^{-1} glucose consumed (Table 2). Moreover, the culturing system described in this study is suitable for scale up *in vivo* ethylene generation from CO; although further genetic modifications to the host organism may be required to reach relevant ethylene production values.

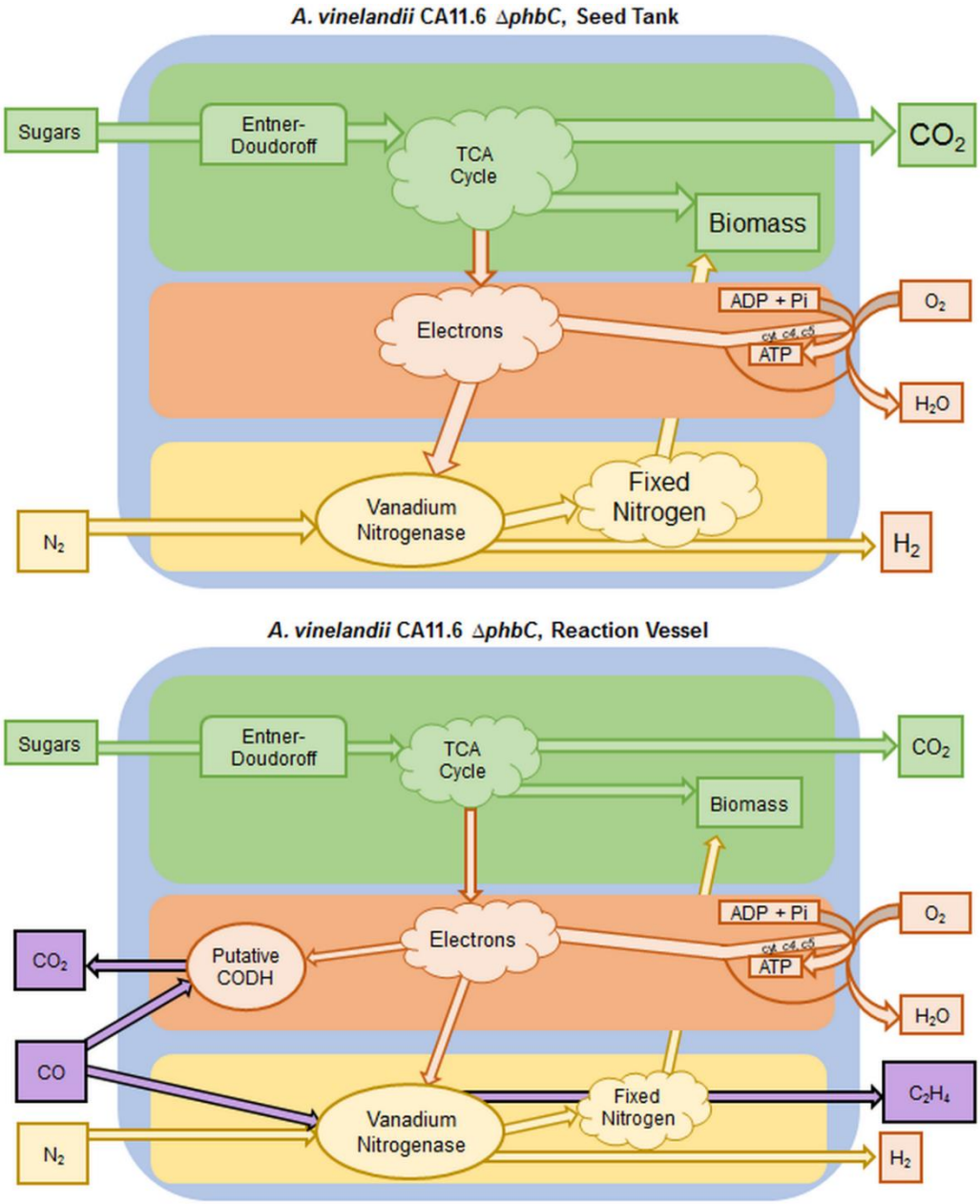

Figure 3.4. Broad overview of *A. vinelandii* CA11.6 Δ*phbC*'s metabolic pathways when cultured in our two-stage system: showing inputs, outputs, and pathways for carbon, nitrogen, and electrons. Shape size and arrow thickness represent the predicted relative abundance and flow of each component. Top: seed tank conditions. Bottom: reaction vessel conditions during continuous flow of air enriched with CO.

One such improvement could be the development of an *A. vinelandii* strain that is capable of diazotrophic growth in the presence of extracellular ammonium. Hypothetically, a deregulated

strain of *A. vinelandii* capable of diazotrophic growth in the presence of an exogenous organic nitrogen supply would allow the V nitrogenase to be completely dedicated to CO reductive coupling while the exogenous ammonium could support biomass production. Researchers focused on ammonium excretion by *A. vinelandii* have found many promising targets, such as disrupting the *nifL* gene (a regulator of the *nif* nitrogen assimilation genes). Unfortunately, these strains, while exhibiting constant expression and activity of the Mo nitrogenase in the presence of extracellular ammonium, manifest significant growth impairments[101,109-112,115]. Extending this physiology to cultures expressing the V nitrogenase, it is reasonable to assume that these hypothetical *A. vinelandii* strains may be able to continuously express the V nitrogenase in medium containing fixed nitrogen and produce higher ethylene yields. This assumption is stipulated on the ability to resolve the growth impairments.

Alternatively, potential increases in ethylene generation could be achieved by switching catalysts from the V nitrogenase to the Mo nitrogenase, as *A. vinelandii* strains expressing the Mo nitrogenase have demonstrated a capability to sustain nearly twice the specific activity compared to cells expressing the V nitrogenase under the same physiological conditions [216]. However, in order to secure ethylene production from the Mo nitrogenase, a modified version would be required as CO is not able to enter the active site of the native Mo nitrogenase enzyme; resulting in negligible *in vitro* hydrocarbon production[146]. Recently, researchers focused on modifying the Mo nitrogenase active site have found that substituting the $\alpha\text{-}70^{Val}$ amino acid with either alanine or glycine allows CO to enter the active site and be reductively coupled in a similar manner to the V nitrogenase[177]. Therefore, such a strain may be capable of producing nearly twice the ethylene reported in this paper; as long as the modification has no negative impacts on cell proliferation or *in vivo* enzyme activity.

While the baseline values reported in this work are not yet competitive with other bioethylene production strategies[169], we believe that the challenges are not insurmountable and implementation of the proposed solutions stated above could result in *A. vinelandii* strains capable of significant increases in ethylene production. The culturing system strategy proposed here provides the framework for future investigations of continuous nitrogenase-mediated CO-reductive coupling and, if eventually adopted at an industrial scale, has the potential to significantly lower the total energy and purification costs associated with current industrial ethylene production; while simultaneously lowering greenhouse gas emissions. Furthermore, the

production of ethylene could be incorporated with the other commodities that *A. vinelandii* naturally produces (such as H_2, PHB, alginate, and organic ammonium) to create a comprehensive sustainable microbial bio-factory.

Chapter 4. Production of Metabolic Ethylene by *Azotobacter vinelandii* Using Bio-functional PHB Nanobeads

Introduction

Polyhydroxyalkanoates (PHAs) are a class of polymers that act as a carbon and energy storage mechanism for many microorganisms when nutrients are limited and oxygen-related stress is low[32,234]. Under these conditions, acetyl-CoA is diverted away from central metabolism and is converted into hydroxyalkanoate-CoA monomers, which are later polymerized and self-assembled into cytoplasmic PHA nanobeads[30,31]. To date over 150 variants of PHA have been identified and investigated for their mechanical, sustainable, and biodegradable properties as an alternative to petroleum-derived plastics[30,235,236]. However, issues surrounding the economics of the process have limited their real-world application for this purpose[237]. More recently, alternative uses for these microbial reserve polymers have been developed, including the generation of translational chimeric proteins. Such proteins combine the enzyme responsible for polymerizing hydroxyalkanoate-CoA monomers, PhaC, with a functional protein or enzyme that remains bound to the PHA nanobead surface; resulting in bio-functional nanobeads[238,239]. This functionalization has expanded the use of tailored nanobeads into areas such as bioremediation and medicine[240-243] and has been explored for use as a drug delivery system targeting cancer cells[244,245]. Furthermore, these fusions between chimeric proteins and polymers have advantages such as the directional display of enzymes and a chromatography-free method for protein purification and recovery[238,246-248].

Azotobacter vinelandii is an obligate aerobic, Gram-negative bacteria that naturally produces the most common type of PHA polymer, poly-3-hydroxybutryate (PHB)[91]. Production of PHB by *A. vinelandii* is accomplished utilizing a three-protein pathway whose genes are predicted to be arranged in an operon: β-ketothiolase (*phbB*), acetoacetyl-CoA reductase (*phbA*), and PHB synthase (*phbC*)[38]. The expression of this gene cluster is under tight regulatory control and gene expression is mainly induced when cells are approaching stationary phase under oxygen-limiting conditions. Transcriptional activation occurs when the stationary phase sigma factor, RpoS, promotes the expression of the AraC-family transcriptional activator PhbR[36,37] which binds to specific sequences upstream of *phbB* and recruits RNA polymerase to drive transcription[37,38]. For transcriptional repression, *A. vinelandii* utilizes CydR, an FNR-like global regulator, which contains oxygen-responsive Fe-S metal clusters and acts as a repressor to *phbB*

and *phbA* transcription[24,38,39]. There are also several post-transcriptional repression systems that are known to be active in *A. vinelandii* including: the Gac/Rsm system[40,41] and the iron-responsive small RNA ArrF system[42-44].

Throughout the PHB synthesis process, the PHB synthase protein (PhbC) remains physically bound to its own product, which self-assembles under sufficiently high concentrations to form the PHB nanobead. After polymer formation, PhbC remains on the assembled bead surface and can act as a translational fusion partner. Thus stable nanobeads containing chimeric proteins are produced and accumulate intracellularly in a one-step biosynthesis process[238,239]. To date, *A. vinelandii* has not been evaluated for the production of these chimeric protein nanobeads because of its difficulty hosting plasmids[64], which are traditionally used during genetic complementation experiments to express recombinant translational fusion cassettes in trans[238,239]. The production of these chimeric protein nanobeads by *A. vinelandii* is desirable because this microorganism can be cultured in minimal media with cost-effective sources of carbon while co-producing industrially-relevant compounds such as hydrogen, ammonium, alginate, and ethylene[91,129,182,216,249]. To overcome the strains' inability to host plasmids in a stable manner, we performed site-specific chromosomal integrations of a *phbC* translational fusion cassette in *A. vinelandii* to obtain recombinant bio-functional nanobeads.

In particular, we were interested in expressing a protein chimera composed of PhbC and the ethylene-forming enzyme EFE, originally isolated from *Pseudomonas syringae*. This protein is a 2-oxoglutarate dioxygenase that converts 2-oxoglutarate and L-arginine into ethylene and succinate in a dual-circuit mechanism (Equation 1)[167,170,171].

Equation 1: 2-OG + 3 O_2 + L-arginine → 2 C_2H_4 + succinate + 7 CO_2 + guanidine + P5C

In nature, it is thought that EFE is utilized by microbial plant pathogens to initiate plant decay and make access to plant-derived carbohydrates easier[250]. Recombinant expression of active EFE has been successful in several different hosts including: *Escherichia coli*, *Saccharomyces cerevisiae*, and *Synechocystis sp.*; producing up to 600 µg C_2H_4 g^{-1} dry biomass h^{-1} [169,172,251,252]. However, achievement of these production values requires intense aeration of the culture, expensive reagent supplements, and high rates of cellular respiration[174,175,251]. Furthermore, the native enzyme is highly thermosensitive and loses nearly all activity above 30°C[175]. These enzymatic constraints make *A. vinelandii* an ideal host to express this enzyme since it is an obligate aerobe capable of sustaining high rates of respiration during mesophilic

optimal growth conditions[91,216]. Additionally, this organism is already known to convert carbon monoxide into ethylene using its vanadium nitrogenase[148,249] and therefore, the production of PHB-bound EFE (PHB-EFE) would provide *A. vinelandii* with an additional metabolic pathway for *in vivo* ethylene generation while, at the same time, providing proof-of-concept data for the production of PHB nanobeads containing functional chimeric proteins.

Materials and Methods

Strains and media

The strains utilized in this study are listed in Table 4.1, along with the plasmids and primers. *E. coli* strains were cultured in lysogeny broth (LB) while *A. vinelandii* strains were cultured in modified Burks medium containing (per liter): 10 g glucose, 0.2 g magnesium sulfate, 90 mg calcium chloride, 0.2 g potassium phosphate monobasic, 0.8 g potassium phosphate dibasic, 15 mg iron sulfate, 0.5 g sodium citrate, and 3 g yeast extract. Antibiotics were added to the media as needed: ampicillin (50 μg mL^{-1} for both organisms) and spectinomycin (50 μg mL^{-1} for *E. coli* and 20 μg mL^{-1} for *A. vinelandii*).

Table 4.1. List of strains, plasmids, and primers used in this study. Underlined sequence indicates sites for restriction enzymes.

Strain, plasmid, or primer	**Relevant Characteristics**	**Source**
Strains		
Azotobacter vinelandii		
CA11.6	CA11 (Δ*nifHDK*, knockout of molybdenum nitrogenase) with CA6 mutation (42-kb natural deletion) that disrupts nitrogenase regulation	81
CA11.6 Δ*phbC*	CA11.6 with *phb*C knockout, does not produce PHB, amp^r	216
CA11.6 Δ*phbC* Δ*cydR*	CA11.6 *ΔphbC* with *cydR* knockout, does not express a functional CydR, sp^r	This study
CA11.6 *ΔphbC ΔcydR::phbC*	CA11.6 *ΔphbC ΔcydR* + *phbC* genomic region inserted into middle of the *cydR* gene, complemented *phbC* restores PHB production (Table 4.2)	This study
CA11.6 *ΔphbC ΔcydR::phbC-efe*	CA11.6 *ΔphbC ΔcydR::phbC* + *efe-Flag* translationally fused to C terminal end of *phbC*, provides secondary pathway for ethylene production	This study

Table 4.1 (continued).

Escherichia coli		
DH5α	*supE*44 Δ*lacU*169 *hsdR*17 *end*A1 *rec*A1 *gyrA*96 *hi*-1 *relA*1	Invitrogen
Plasmids		
pUC19	Amp^r, *lacZ* α-subunit, pMB1 origin	New England BioLabs
pUC-*PpsbA*-*efe*-FLAG	Source of the *efe-Flag* gene	174
pUC*cydR*	pUC19 + partial region of *A. vinelandii* genomic *cydR* DNA inserted at multi-cloning site	This study
pUC*cydR*mcs	PCR generated pUC*cydR* with multi-cloning site (mcs) added into center of the *cydR* gene fragment	This study
pUCA	pUC*cydR*mcs + *aadA* gene inserted into the mcs within the *cydR* gene fragment	This study
pUCAP	pUCA + *A. vinelandii* genomic *phbC* gene inserted into the mcs within the *cydR* region	This study
pUCAPL	PCR generated pUCAP + removal of *phbC* stop codon + introduction of C terminal linker sequence[239]	This study
pUCAPLE	pUCAPL + *efe-Flag* gene translationally fused in-frame to C terminal end of the *phbC* linker sequence + TEV protease site added between linkers and the *efe-Flag* gene	This study
Primers		
cydR gDNA Fwd	AAGGATCCACCTGCCAGGGAGCATAATTC	This study
cydR gDNA Rev	CCTAAGCTTGCCTACCGATTTCGCTCAAC	This study
pUC*cydR* mcs Fwd	GAAGATCTCCATGGCTCGAGTCCGCGGTCGACAGCAGCAGCATCATC	This study
pUC*cydR* mcs Rev	GAAGATCTACGAACGCATCGCCACCTTC	This study
phbC gDNA Fwd	CATGCCATGGTCTGACATCGCTTGGTAGGG	This study
phbC gDNA Rev	CCGCTCGAGAGGCAGCCAAAGTCTTCATC	This study
pUCAP Linkers Fwd	GCTCTAGATCCTCCTCCTCCTCCACGCTTGTCGATCACTGCCAACACGCCTTTCACGTAACGGCCTGGTGC	This study

Table 4.1 (continued).

pUCAP Linkers Rev	GCTCTAGATCTGGAGGAGGATCTGGAGGAGGATCTGGAGGAGGAGGATCTACTAGTGCCCTACCAAGCGATGTCAG	This study
efe-Flag Fwd	GGACTAGTGAGAACCTGTACTTCCAAGGAATGACCAATTTGCAAACTTTTG	This study
efe-Flag Rev	CATGCCATGGCGCAATTAACCCTCACTAAAG	This study

Plasmid construction

Construction of the final plasmid that would contain the full *phbC-efe* translational fusion cassette occurred in six stages and resulted in six independent plasmids. First, a partial region of the *cydR* open reading frame (ORF) from *A. vinelandii* CA11.6 Δ*phbC* was amplified via colony PCR and introduced into the multi-cloning site (mcs) of the pUC19 plasmid generating pUC*cydR*. Next, a new mcs was introduced in the center of the partial *cydR* ORF via PCR generating pUC*cydR*mcs. A spectinomycin resistance gene, *aadA*, was then introduced into the mcs of the partial *cydR* ORF generating pUCA (Figure 4.2A). This was followed by the PCR amplification of the *phbC* gene (including 100 bp of the upstream region) from *A. vinelandii* CA11.6 which was then introduced into the mcs of the partial *cydR* ORF generating pUCAP (Figue 4.2B). Special care was taken to ensure that the *phbC* gene would not be in-frame of the *cydR* gene once integrated into the chromosome (eliminating the possibility of polar effects). The stop codon of *phbC* was then removed via PCR followed by the addition of a linker sequence, containing the TEV protease recognition sequence and specific sequences to ensure the eventual surface display of EFE-Flag[239], generating pUCAPL. Finally, the *efe*-Flag ORF was amplified via PCR and inserted, in-frame, at the 3' end of the linker region generating pUCAPLE (Figure 4.2C). This final version of the plasmid contained the *cydR* ORF interrupted by a *phbC-efe* translational fusion cassette and a spectinomycin resistance gene.

Transforming Azotobacter vinelandii

Competent *A. vinelandii* cells were prepared and transformed as previously described[216]. Briefly, *A. vinelandii* CA11.6 Δ*phbC* cells were cultured for 3-5 days on solid TF agar medium containing per liter 10 g sucrose, 2 g magnesium sulfate, 90 mg calcium chloride, 0.2 g

potassium phosphate monobasic, 0.8 g potassium phosphate dibasic, 2.2 g ammonium acetate, and 15 g agar. Once the culture began to produce siderophores, indicated by the colonies turning a bright green color, the plate was flushed with 1 mL of 1x Burks Buffer (0.2 g L^{-1} potassium phosphate monobasic and 0.8 g L^{-1} potassium phosphate dibasic) and the cells were transferred to a sterile 1.5 mL Eppendorf tube containing approximately 5 µg of BamHI-linearized plasmid. This mixture was then incubated at 30°C for 1 hour to allow for double homologous recombination. Successful mutants were selected based on both ampicillin resistance (indicating the original *phbC* deletion was maintained) and spectinomycin resistance (indicating the *aadA* gene was integrated into the *cydR* ORF). Furthermore, we performed PCR on these mutants to confirm integration at the correct location site and utilized microscopy to check for visible PHB nanobead accumulation; which was apparent under phase-contrast.

PHB quantification

PHB was quantified using a modified method previously described[253]. Briefly, *A. vinelandii* cells were cultured in modified Burks media under oxygen-limiting conditions for 48 h. Dry biomass concentration was then quantified by filtering (using vacuum suction) a fixed sample volume through a 0.2 µm-pore-size filter of a known mass. The filter was then dried until a constant weight was reached to determine the dry weight of biomass per unit filtered volume. The cells were then harvested using centrifugation (4,000 rpm for 15 min at 4ºC), re-suspended in 10 mL of 20 mM Tris-HCl (pH 8.0), and lysed via sonication using a Misonix Sonicator 3000 (Misonix Inc, USA). Approximately 25 mg of lysed cell debris was then added to a 15 mL Corning centrifuge tube and exposed to 1 mL of concentrated sulfuric acid for 1 h at 90°C. This acid-hydrolyzed cell debris was then cooled on ice for 10 min followed by addition of 4 mL of 5 mM sulfuric acid. This mixture was then filtered through a 0.45 µm-pore size HAWP filter and diluted 1:10 in water. This final dilution was then analyzed via high-performance liquid chromatography (HPLC) operated under isocratic conditions at 65°C using a 5 mM sulfuric acid mobile phase flowing at rate of 0.5 mL min^{-1} through a Rezex™ ROA-Organic Acid H+ column (Phenomenex, USA). The column was coupled to a variable wavelength detector (Agilent) operated at a 254 nm wavelength. Absolute values for PHB were obtained by measuring known quantities of trans-crotonic acid processed under the same conditions to generate a standard curve.

Western blotting

Determination of the localization of the EFE-Flag protein was done by Western blotting. Briefly, cells were cultured, harvested, and lysed as previously described. The lysed cell debris was then washed three times with 20 mM Tris-HCl (pH 8.0). After the third wash, the cell debris pellet was re-suspended in TEV-protease buffer (50 mM Tris-HCl, 0.5 mM EDTA, 1 mM DTT, pH 8.0) and TEV protease was added to a final concentration of 20 µg protein mL^{-1}. This mixture was then incubated at room temperature for 3 hours with gentle mixing. Supernatant samples were taken from each step of this process (directly after cell lysis, after washing, and after TEV treatment) in order to visualize any release of chimeric EFE-Flag from the PHB nanobead surface. Protein concentration in these supernatant samples was determined by Bradford assay (Bio-Rad) and the levels of each sample were adjusted to ~0.5 µg protein $µL^{-1}$. Each sample was then prepared for SDS-PAGE by boiling 4 µg of soluble protein in 1x Laemmli sample buffer (Bio-Rad) for 10 minutes at 80ºC. These samples were then loaded onto a SDS-PAGE (10%) gel and ran for 1 hour at 150V. The separated proteins were then transferred to a PVDF membrane by western blotting for 1 hour at 300 mA. Membranes were blocked in 1% BSA, 1 x PBST, and primary and secondary antibodies were diluted in 1% BSA, 1 x PBST. For primary incubation, antibodies against the 3XFlag tag on EFE (GenScript THE^{TM}DYKDDDDK Tag) were diluted 1:10000 and left rocking for 1 hour. For secondary incubation, goat anti-mouse IgG antibodies were diluted 1:5000 and left rocking for 1 hour. Signal development was accomplished using the 1-Step NBT/BCIP treatment (Thermo Scientific).

In vitro ethylene production assays

In vitro measurement of PHB-bound EFE-Flag activity was performed in the same way as soluble, purified EFE[254]. Briefly, *A. vinelandii* strains were cultured, harvested, lysed, and washed as previously described. PHB concentration was quantified and approximately 5.4 mg of PHB was added to 30 mL of EFE Reaction Buffer containing (per liter) 19.1 g HEPES/NaOH (pH 8.0), 0.04 g iron sulfate, 0.31 g dithiothreitol, 0.35 g L-arginine, 3.1 g L-histidine, and 0.29 g 2-oxoglutarate. These vials, containing 10 mL of headspace, were immediately sealed after PHB addition and incubated at 30°C with light agitation for 24 hours. Samples from the headspace were taken using a gas-tight syringe and injected into a Shimadzu 8A-FID gas chromatograph with prior separation using a 6-foot Restek Porapak Q80/100 stainless steel packed column. The

split/splitless injector and the FID were held at 200°C with an oven temperature maintained at 50°C while using nitrogen as a carrier gas at a constant flow rate of 10 mL min^{-1}. Absolute values of ethylene were obtained by measuring known quantities of pure ethylene gas (Airgas, USA) to generate a standard curve which had a limit of detection of 1 ppm.

In vivo ethylene production assays

In order to confirm *in vivo* ethylene production, we grew 8 independent cultures of *A. vinelandii* CA11.6 Δ*phbC* Δ*cydR::phbC-efe* in modified Burks media under oxygen-limiting conditions. Every six hours, one of the cultures would be pulled from the incubator and would be processed using the following steps: measure optical density, measure cell dry weight, concentrate the cells via centrifugation, quantify PHB production (without prior sonication), and re-suspension of the concentrated whole cells in 30 mL of the media supernatant. This concentrated whole cell suspension was then sealed in vials, containing a 10 mL headspace, and ethylene accumulation was monitored as previously described. This entire process was repeated three times at each time point to ensure statistical accuracy.

Results

Methodological design and analysis of the PHB biosynthetic gene cluster, phbBAC

As previously reported by our group, interrupting the *phbC* open reading frame completely eliminates PHB production by *A. vinelandii* CA11.6 and other strains[216]. To generate recombinant, bio-functional PHB nanobeads, the previously characterized strain CA11.6 Δ*phbC* was used as host throughout this study because it would allow for the transformation and complementation of a *phbC* translational fusion cassette to restore PHB nanobead production containing chimeric EFE proteins.

For site-directed integration of a translational fusion cassette, the *cydR* open reading frame was targeted in particular because its product, CydR, acts as a master regulator known to repress transcription of the genes responsible for PHB production by *A. vinelandii*[39]. Furthermore, CydR controls expression of the cytochrome *bd* branch of the electron transport chain, which is correlated with higher rates of respiration[24-27]. Therefore, a concurrent *cydR* knock-out and complementation mutant could be ideal for restoring production of PHB since it is

predicted to increase expression of acetoacetyl-CoA reductase and β-ketothiolase[39] while increasing flux of carbon through the TCA cycle[216].

In *A. vinelandii*, the PHB biosynthetic gene cluster, *phbBAC*, has been predicted as an operon[31,37,38,41,255]; implying that transcription of *phbC* is controlled by promoters upstream of the *phbB* gene. If this was true, then any *phbC-efe* translational fusion cassette integrated into the *cydR* region would need a synthetic promoter to be added upstream; which can sometimes have unintended consequences. However, after examining unrelated transcriptomic experiments conducted by independent research groups we noticed that while the number of transcripts was nearly identical between *phbB* and *phbA* across multiple conditions, the number of transcripts for *phbC* was always significantly different[112,256]. Additionally, the intergenic space between *phbA-C* is four times larger than the space between *phbB-A* (246 bp versus 62 bp), which is unusual for traditional operons[257]. Therefore, we decided to quickly analyze these intergenic regions to determine if there were any putative promotors or terminators in existence that might help explain the previously observed expression differences. Initial examination using Clone Manager software revealed the *phbA-C* intergenic region comprised a predicted rho-independent transcriptional terminator sequence downstream of the *phbA* stop codon. This putative terminator had an estimated Gibbs free energy (ΔG) of -11.7 kcal/mole which is consistent with experimentally identified terminators in other microorganisms[258]. Furthermore, this region contained sequence that was identified by the Softberry BProm software[259] as a putative promoter upstream of the *phbC* start codon (Figure 4.). If active, this putative terminator/promoter combination could explain the difference in gene expression between *phbBA* and *phbC*. Furthermore, if *phbC* is under the control of an independent promoter in *A. vinelandii*, then a functional *phbC-efe* translational fusion cassette could be possible without the need for the addition of an alternative, synthetic promoter.

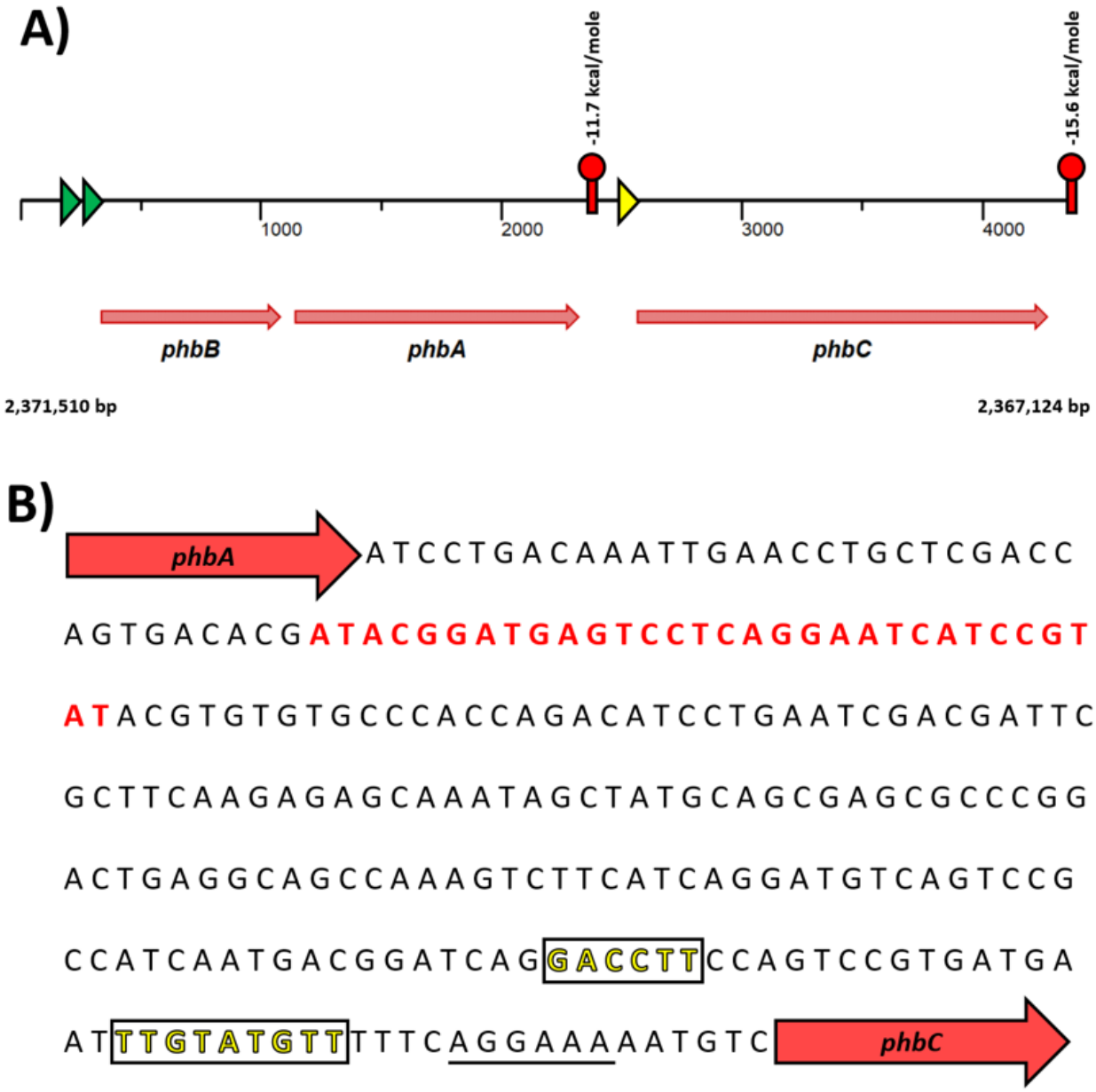

Figure 4.1. Analysis of the PHB biosynthetic gene cluster in *A. vinelandii*. A) Coding strand of the full *phb*BAC biosynthetic gene cluster. The green triangles indicate the two confirmed *phb*B overlapping promoters, the red loops indicate predicted terminator sequences (Clone Manager, minimum energy threshold of -11 kcal/mole), and the yellow arrow indicates the predicted promoter upstream of *phb*C (Softberry BProm software). B) Intergenic coding sequence between *phb*A and *phb*C in *A. vinelandii*. Red base pairs indicate the predicted stem-and-loop terminator sequence. Boxed, yellow base pairs indicate the location of the putative promoter and the underlined base pairs indicate a possible Shine-Dalgarno sequence.

Complementation of phbC into a ΔphbC strain fully restores PHB production

Initial disruption of the *cydR* ORF in the *A. vinelandii* CA11.6 Δ*phbC* genome was achieved via homologous recombination mediated by plasmid pUCA which harbors a spectinomycin resistance gene *aadA* flanked by *cydR* ORF fragments (Figure 4.2.A). The resulting strain, *A. vinelandii* CA11.6 Δ(*phbC, cydR)* exhibited no significant differences in specific growth rate under oxygen-limiting conditions and had no changes on overall biomass accumulation over 48 h (Table 4.2).

Based on pUCA, a second plasmid, pUCAP, harboring the *phbC* gene (including the 100 bp upstream region containing the putative promoter sequence) in antisense direction downstream of the *aadA* gene (Figure 4.2.B) was constructed. This cassette, when integrated into the *A. vinelandii* CA11.6 Δ*phbC* genome, resulted in a *phbC* complemented strain (Δ*phbC* Δ*cydR::phbC*) that regained its PHB production capabilities and had accumulated nearly twice the biomass (after 48 h) compared to the PHB-deficient strains (Table 4.2). We therefore could experimentally confirm that the direct upstream region of *phbC* does harbor a promoter capable of independently driving transcription.

After confirming the functionality of a promoter and the restoration of PHB biosynthesis, a third plasmid, pUCAPLE, bearing the *phbC-efe* translational fusion cassette was constructed (Figure 4.2.C). This fusion cassette comprised the following important characteristics (in order): the *phbC* open reading frame (+100 bp upstream region) with the stop codon removed, in-frame PHB surface display linker (amino acids: VLAVIDKRGGGGG), in-frame SG linker (amino acids: SRSGGGSGGGSGGGGSTS), in-frame tobacco etch virus (TEV) protease cleavage site (amino acids: ENLYFQ/G), and the in-frame *efe-Flag* open reading frame. The two linker sequences have previously been identified as being important in other microorganisms for maintaining PHB-bound enzyme activity[239]. The TEV protease cleavage site was added to allow for eventual removal of the EFE-Flag protein from the PHB nanobead surface with minimal added amino acids to its N-terminal region (leaving only a single G residue)[260]. Once complete, linearized pUCAPLE was transformed into *A. vinelandii* CA11.6 Δ*phbC* and chromosomal integration resulted in a *phbC-efe* complemented strain (*A. vinelandii* CA11.6 Δ*phbC* Δ*cydR*::*phbC-efe)* that, again, restored PHB biosynthesis capabilities, and hence, PHB nanobead production. *A. vinelandii* CA11.6 Δ*phbC* Δ*cydR*::*phbC-efe* showed a significant decrease in overall biomass accumulation over 48 hours compared to the other *phbC* complemented strain

(Δ*phbC* Δ*cydR::phbC*) (Table 4.2). This reduction of biomass accumulation is a clear indication of *in vivo* EFE-Flag activity as this enzyme would divert 2-oxoglutarate away from the 2-oxoglutarate dehydrogenase / succinyl-CoA synthetase branch of the TCA cycle and shunt that carbon towards ethylene production.

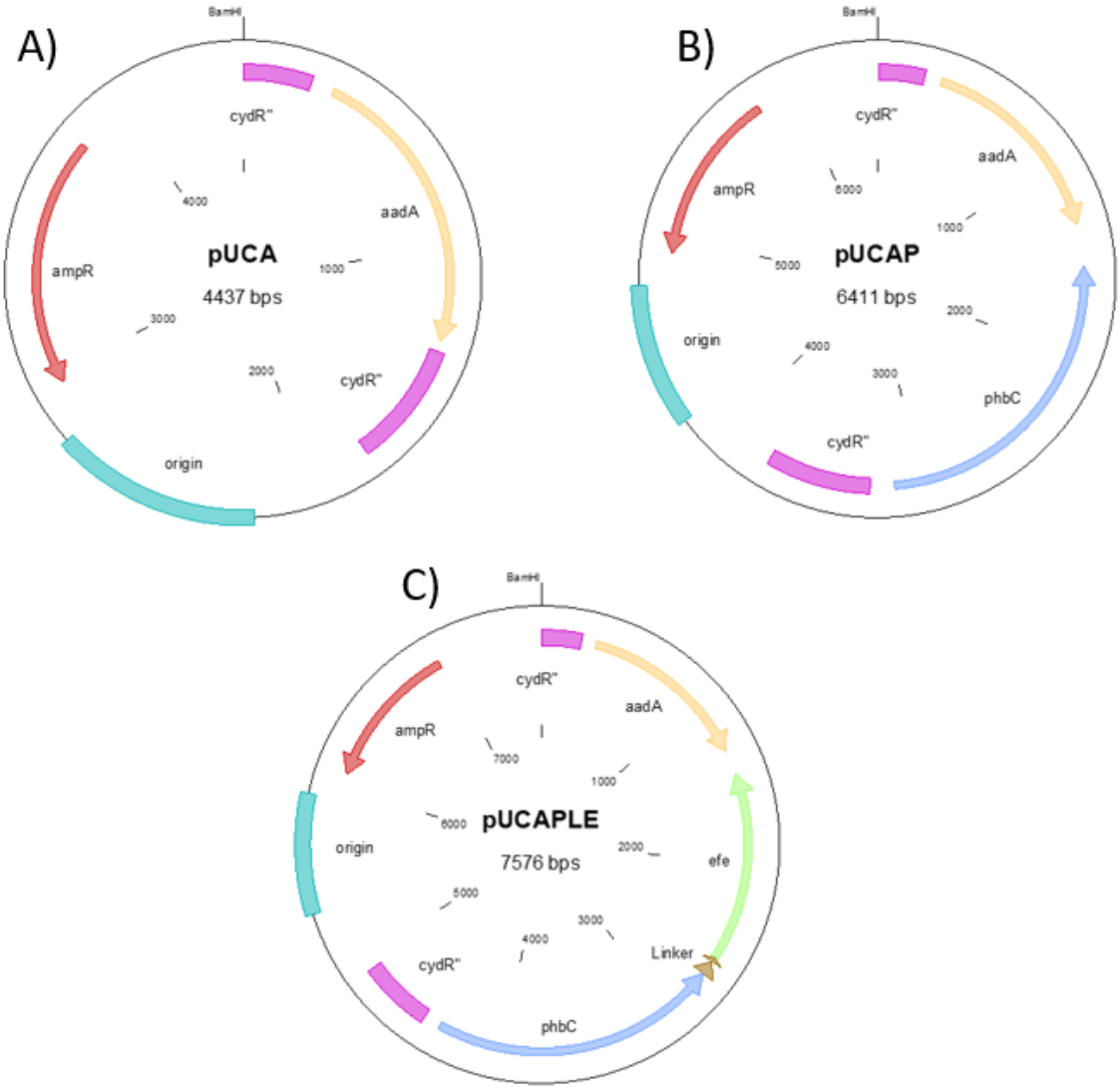

Figure 4.2. Plasmids, hosted in *E. coli* DH5α, containing various translational fusion cassettes targeting *cyd*R site specific integration. The final construct, pUCAPLE, consisted of the *cyd*R ORF (purple boxes) interrupted by a spectinomycin resistance gene (*aad*A, yellow arrow) and the *phb*C-*efe* translational fusion cassette (blue arrow *phb*C lacking a stop codon > brown arrow linker regions > green arrow *efe*-Flag). These plasmids were linearized using the BamHI restriction enzyme and transformed into competent *A. vinelandii* CA11.6 Δ*phb*C cells in order to generate new chromosomic integrants with characteristics important for this study.

Table 4.2. Growth kinetics and PHB yield values obtained from various *A. vinelandii* CA11.6 strains cultured in modified Burks media under oxygen-limiting conditions. Maximum specific growth rate values were calculated during exponential growth (between 6 and 12 hours) while final biomass concentration and specific PHB yield were measured after 48 hours. All experiments were performed in triplicate.

***A. vinelandii* strain**	**Maximum specific growth rate (h^{-1})**	**Biomass ($g\ L^{-1}$)**	**PHB yield ($mg\ g^{-1}$ biomass)**
CA11.6	0.19 ± 0.00	3.3 ± 0.5	34 ± 19
Δ*phbC*	0.15 ± 0.01	2.4 ± 0.2	ND
Δ*phbC* Δ*cydR*	0.18 ± 0.00	2.4 ± 0.1	ND
Δ*phbC* Δ*cydR*::*phbC*	0.17 ± 0.01	4.0 ± 0.4	51 ± 17
Δ*phbC* Δ*cydR*::*phbC-efe*	0.16 ± 0.01	2.0 ± 0.4	45 ± 8

EFE-Flag is bound to the PHB nanobead surface

Once complementation of the *phbC* gene proved to be an effective strategy for restoring PHB nanobead production in *A. vinelandii* Δ*phbC*, we needed to demonstrate that the PhbC-EFE-Flag protein chimera was displayed on the PHB nanobead surface. To accomplish this, *A. vinelandii* CA11.6 Δ*phbC* Δ*cydR::phbC-efe* was cultured in modified Burks media under oxygen-limiting conditions for 48 hours; generating approximately 45 mg PHB g^{-1} dry biomass (Table 4.2). Cells were then recovered, lysed, washed, and resuspended in buffer containing TEV protease which releases the EFE-Flag protein from the PHB nanobead surface. The protein release was estimated by measuring the protein concentration in the cell free extracts/supernatant (after centrifugation) at the beginning and end of TEV protease treatment. The results showed that approximately 33 µg protein mg^{-1} PHB was released after TEV addition.

To confirm the identity of the released protein, supernatant fractions (cell free extract, washed cell debris, and washed cell debris + TEV) were subjected to Western Blot. A positive signal for the released EFE-Flag protein was found exclusively in the TEV-treated fraction of the *A. vinelandii* CA11.6 Δ*phbC* Δ*cydR::phbC-efe* washed cell debris supernatant (Figure 4.1); confirming the identity and presence of the EFE-Flag protein on the surface of the PHB nanobead. As expected, no FLAG proteins were found in the supernatant fractions of the control.

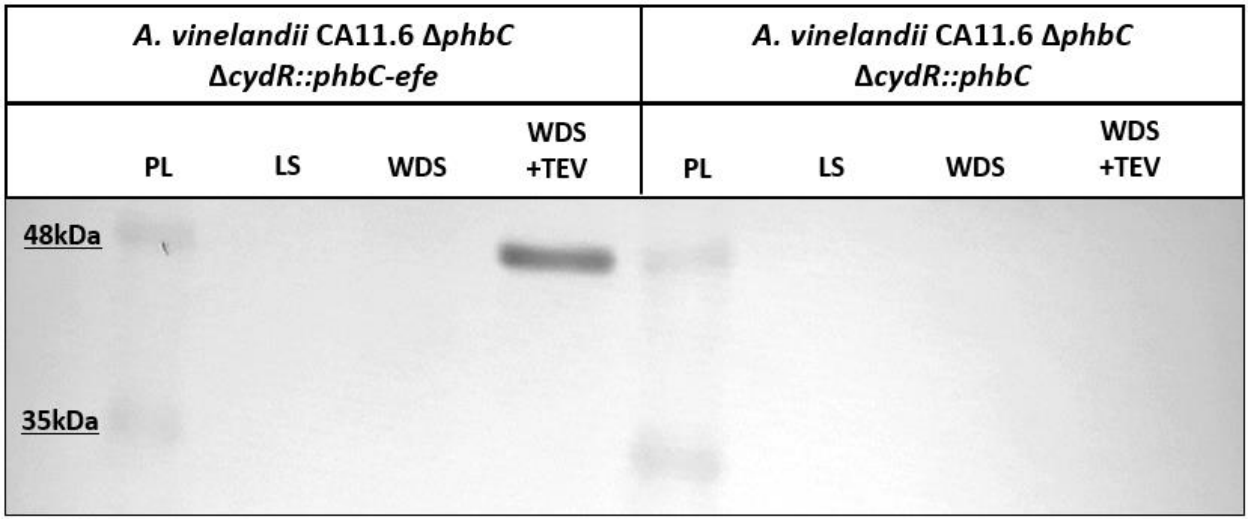

Figure 4.1. SDS-PAGE (10%) separation followed by Western Blot targeting for the presence of Flag proteins from two strains of *A. vinelandii*. Soluble protein (4 µg) was loaded into each lane PL protein ladder; LS cell lysate supernatant; WDS washed cell debris supernatant; WDS+TEV washed cell debris supernatant with TEV protease addition. All fractions were incubated at room temperature for 3 h prior to centrifugation, Bradford, and sample loading.

Integration of a translational phbC-efe fusion cassette results in ethylene-forming nanobeads

After confirming EFE-Flag surface display, enzymatic activity of the recombinant PHB nanobeads was evaluated. Previously reported data using purified, free EFE enzymes have shown a maximum specific activity of 670 units mg^{-1} EFE (defining a unit as 1 nmol ethylene produced per minute)[167,175]. In order to test the activity of the PhbC-EFE-Flag nanobeads, we added approximately 5.4 mg of either PHB or PHB-EFE-Flag nanobeads (containing approximately 0.18 mg of surface-displayed EFE-Flag) into sealed vials containing 30 mL EFE reaction buffer and 10 mL of headspace. Ethylene accumulation was quantified using gas chromatography. Through this process, the purified PHB-EFE-Flag nanobeads produced ethylene at a rate of 42 µg C_2H_4 mg^{-1} PHB h^{-1}; which translates to an approximate specific activity of 464 units mg^{-1} EFE-Flag. As expected, unmodified PHB nanobeads showed no evidence of *in vitro* ethylene production (Figure 4.2).

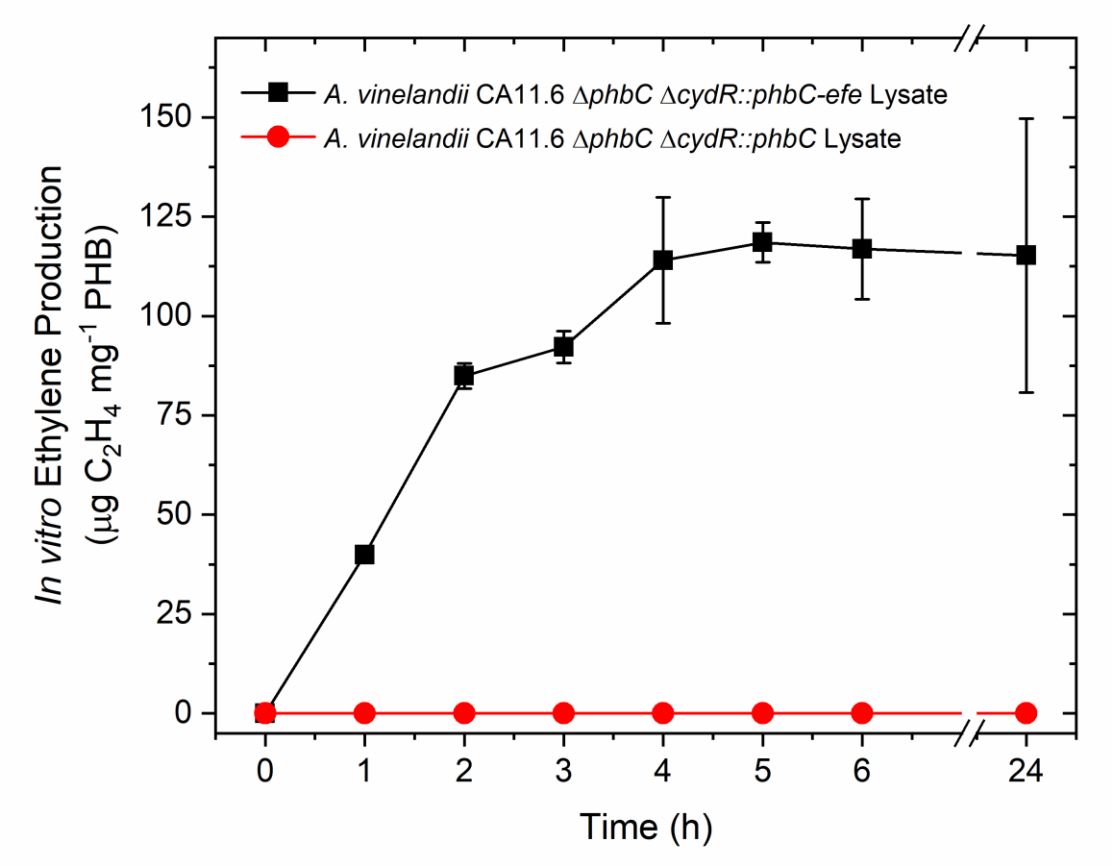

Figure 4.2. *In vitro* ethylene production from concentrated nanobeads of *A. vinelandii* CA11.6 Δ*phb*C Δ*cyd*R::*phb*C (red circles) and *A. vinelandii* CA11.6 Δ*phb*C Δ*cyd*R::*phb*C-*efe* (black squares). Ethylene accumulation in the headspace was monitored by GC-FID. Experiments were performed in triplicate.

PHB-EFE-Flag nanobeads generate ethylene in vivo

While *in vitro* experiments utilizing purified nanobeads and expensive reaction buffers is effective for generating proof-of-concept data for PHB-bound EFE activity, it does not provide a realistic assessment of the full metabolic ethylene production potential by the new *A. vinelandii* strain. In order to be economically feasible, the EFE enzyme would need to be capable of converting naturally produced 2-oxoglutarate from central metabolism into ethylene under physiological conditions. However, culturing the strictly aerobic *A. vinelandii* in a sealed system in order to monitor ethylene accumulation is not possible. Therefore, *A. vinelandii* CA11.6 Δ*phbC* Δ*cydR::phbC-efe* was cultured under open batch conditions containing modified Burks media, as previously described. In order to measure ethylene, live cell concentrates, derived from

the same inoculant, were harvested at different time points and added to sealed flasks containing media supernatant. Headspace accumulation was then monitored over a one-hour time period.

As expected, cultures showed no evidence of PHB nanobead production or ethylene generation during early logarithmic growth (0 – 6 h). However, as the cultures entered the mid- to late-logarithmic growth phase (12 - 18 h) ethylene generation became detectable while PHB accumulation had not. After 24 hours, the specific growth rate decreased, indicating transition into stationary phase, accompanied by production of 10 mg PHB g^{-1} dry biomass. Between 12 to 24 hours, specific ethylene productivity continued to increase linearly, reaching a rate of 426 µg C_2H_4 g^{-1} dry biomass h^{-1} after 36 hours corresponding to a PHB yield of 12 mg PHB g^{-1} dry biomass (Figure 4.3).

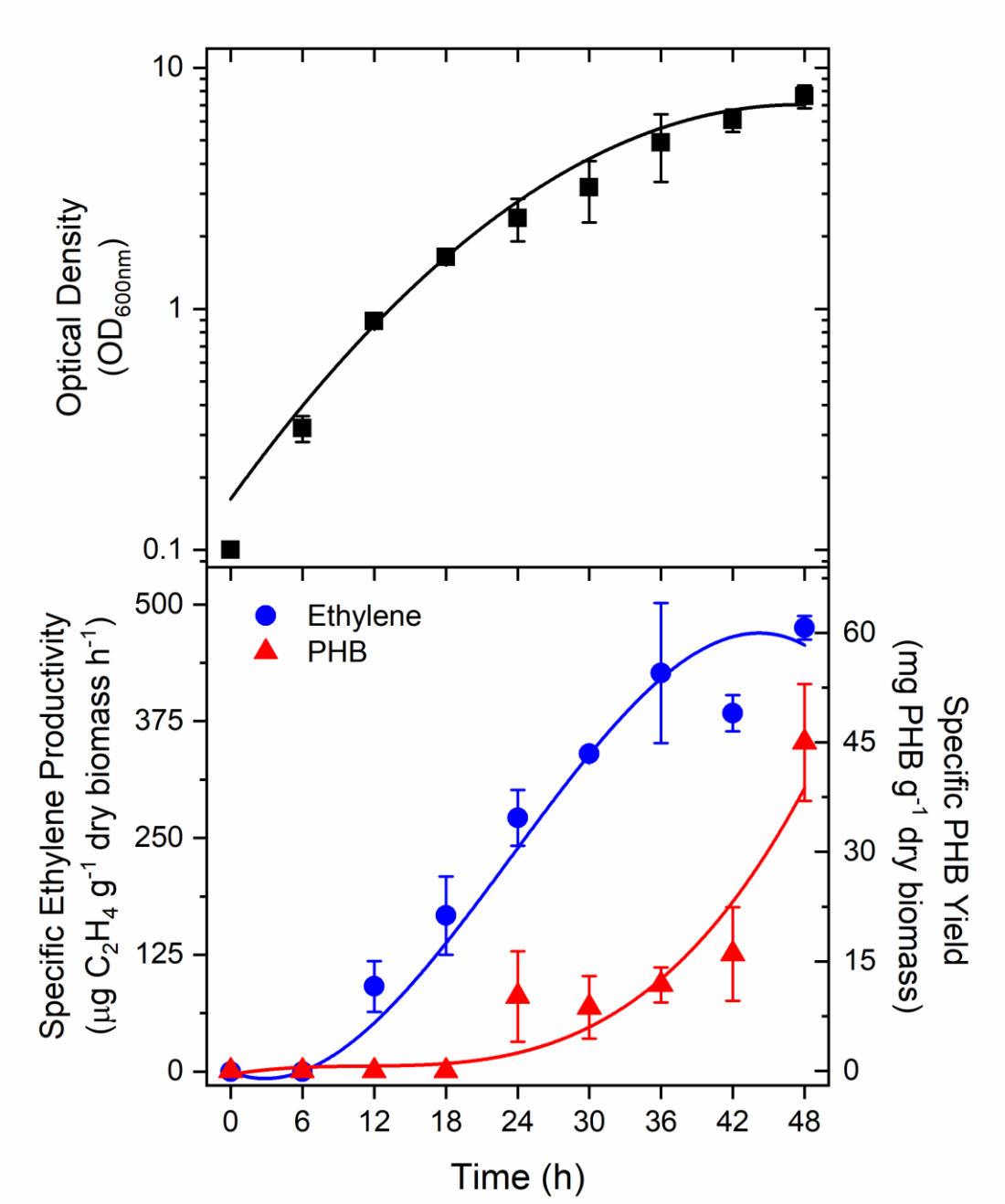

Figure 4.3. Batch cultures of *A. vinelandii* CA11.6 Δ*phb*C Δ*cyd*R::*phb*C-*efe* in modified Burks medium at 30ºC. Values for each point depicted on the graphs was measure after harvest and/or incubation of samples obtained from independent cultures. Optical density (black squares, top), specific ethylene productivity (blue circles, bottom), and specific PHB yield (red triangles, bottom). Experiments were performed in triplicate.

Discussion

This work provides proof-of-concept data for both heterologous enzyme expression linked to PHB nanobead production as well as a new metabolic pathway for *in vivo* ethylene generation by *Azotobacter vinelandii*. Furthermore, we functionally validated that the *phbC* gene has an independent promoter upstream of the start codon (Figure 4., Table 4.2), challenging the accepted viewpoint that the PHB biosynthetic gene cluster in *A. vinelandii* (*phbBAC*) is a true operon[38].

Once integration of a *phbC-efe* translational fusion cassette into the *A. vinelandii* chromosome was achieved, the presence and abundance of the nanobead-displayed EFE-Flag protein was evaluated. The recombinant PHB nanobeads contained approximately 33 µg of surface-displayed EFE-Flag mg^{-1} PHB and the specific activity of the bound enzyme was not majorly affected (Figure 3, Figure 4). These values are promising and consistent with other groups[248], but the overall titer of the heterologous expressed fusion enzyme still needs to be improved. A first step could be expressing the translational fusion cassette into different genetic backgrounds conducive to hyper PHB production. For example, *A. vinelandii* UWD is a genetically modified strain with significant impairments in NADH oxidation, resulting in the overproduction of PHB[29]; with reported values up to 730 mg PHB g^{-1} dry biomass[261]. Alternatively, *A. vinelandii* lacking *arrF* has been reported to accumulate up to 300-fold more PHB than the wild-type[43,44]. If the chimeric protein yield is maintained, then the increased PHB production should translate into increased protein production.

In addition to the generation of bio-functional PHB nanobeads, this work also provides physiological evidence that the addition of an ethylene-forming gene (*efe*) from *Pseudomonas syringae* implements a new pathway in *A. vinelandii*, rendering it capable of generating metabolic ethylene (Figure 4.3). Once expressed, EFE draws 2-oxoglutrarate away from the TCA cycle (skipping GTP and NADH producing steps) and produces succinate, P5C, ethylene, and CO_2. The gaseous carbon-containing compounds escape the cell which, along with the loss of energy and reducing equivalents, results in a significant decrease in end-point biomass accumulation (Table 4.2). Furthermore, a decrease in specific ethylene productivity was observed as the cells entered stationary phase, which may be due to critical substrate limitations of either 2-oxoglutarate or L-arginine (Figure 4.3). While expected, it would likely be beneficial to evaluate new genetic modifications of *A. vinelandii* allowing for increased intracellular pools

of these two substrates. As example, previous work has shown that overexpression of isocitrate dehydrogenase in an EFE-expressing strain of *E. coli* resulted in a two-fold increase in 2-oxoglutarate levels, while inactivating genes involved in L-arginine metabolism (*argR* and *gltBD*) resulted in a substantial increase in ethylene production (presumably due to an increase in L-arginine availability)[174]. Additionally, the experiments herein were conducted under oxygen-limiting conditions in order to promote PHB production, which is not optimal for EFE activity. Therefore, decoupling *efe-Flag* expression from PHB biosynthesis and producing soluble EFE enzymes under a higher mass oxygen transfer rate could significantly improve the ethylene production metrics observed in this work.

Finally, it may be worth exploring the possibility of implementing additional ethylene generating pathways in *A. vinelandii* in order to increase overall production metrics. Recently, a methylthio-alkane reductase (*marBDHK*) was discovered in *Rhodospirillum rubrum* that has the capability to convert (2-methylthio)ethanol into ethylene as a part of methionine biosynthesis. Under initial examination, with no bioprocess optimization, cells expressing *marBDHK* produced approximately 20 µg C_2H_4 g^{-1} biomass h^{-1} under sulfate limiting conditions[166]. Furthermore, this enzyme is related to the nitrogenase isoenzymes found in *A. vinelandii*, making it a good candidate for heterologous expression and, if functional, would provide *A. vinelandii* with three independent ethylene biosynthesis pathways (EFE, vanadium nitrogenase[249], and methylthio-alkane reductase).

Overall, this study demonstrates that PHB-mediated chimeric protein immobilization is a possibility for *A. vinelandii* researchers. While this paper focused on the heterologous expression of the EFE-Flag protein in particular, it is important to note that many other enzymes could take its place in order to add value to a process or build alternative pathways for the synthesis of many complex molecules. Ultimately, the hope of this work is to increase the industrial utility of this microorganism by providing it with multiple profit streams that can later be exploited when cultured at-scale.

Chapter 5. General Conclusions and Future Directions of *Azotobacter vinelandii* as a Microbial Bio-factory

Over the past four years, we have provided proof-of-concept data for several new biotechnological capabilities by *A. vinelandii* in the hopes of furthering its potential as an industrial biocatalyst. In the process of these investigations, we also developed a novel alternative to the acetylene reduction assay, which was the traditional standard for measuring nitrogenase activity. Our new method relies upon an in-line quadrupole mass spectrometer to continually track H_2 production from diazotrophically growing, uptake hydrogenase-deficient mutants of *A. vinelandii*; eliminating the need to remove cells from their culture conditions and perform invasive cellular disruptions that impact enzyme performance. Furthermore, the CA6 and CA11.6 strains we utilized are capable of expressing each nitrogenase isoenzyme independently; depending on which metal cofactor is added to the culture media. Through this work we confirmed that the less-efficient alternative nitrogenases, which produce more H_2 *in vitro*, are less active under physiological conditions and, as a result, produce less H_2 *in vivo* across different oxygen exposure conditions (Chapter 2)[216].

After validating our method for real-time nitrogenase activity monitoring, we began to investigate the potential for *A. vinelandii* to continuously convert molecules of carbon monoxide into ethylene using its vanadium nitrogenase. Previous experiments with *A. vinelandii* cultured in sealed, batch environments demonstrated the possibility of this reaction but reported critical inhibitory effects of CO on diazotrophic growth. In order to overcome this, we developed and optimized a two-stage culturing system in which a seed tank, focused on generating dense biomass with maximal nitrogenase activity, was linked in-tandem with a reaction vessel that was exposed to a constant flow of air enriched in 5% CO. This setup provided a consistent supply of catalytically active cells to the reaction vessel where CO could be catalytically reduced to ethylene; generating a steady-state culture capable of generating ethylene at a specific productivity rate of 90 μg C_2H_4 g^{-1} dry biomass h^{-1} [262]. This production value represented a substantial increase over the previous methodology (Figure 5.1). Furthermore, this system required a lower concentration of input CO (5% versus 15%) and was capable of operating continuously without the need for long, intermittent periods of recovery (Chapter 3).

In addition to nitrogenase-mediated CO reductive coupling, we were also successful in achieving heterologous expression of the ethylene-forming enzyme, isolated from *P. syringae*, in *A. vinelandii*. The presence of this enzyme provided *A. vinelandii* with a second, independent pathway for *in vivo* ethylene production that relied on oxygen, 2-oxoglutarate, and L-arginine instead of CO. The expression of EFE was linked with PHB granule formation, through a translational fusion to *phbC*, which acted as a proof-of-concept for the production of bio-functional PHB nanobeads in *A. vinelandii* (Chapter 4). These recombinant nanobeads could theoretically be utilized to express a wide variety of other proteins with economic values greater than EFE (Chapter 4). For example, by creating a translational fusion cassette between *phbC* and a super oxide dismutase gene, you could get recombinant expression and column-free purification of an industrially relevant enzyme that retails between $30 - $150 per kg (www.alibaba.com).

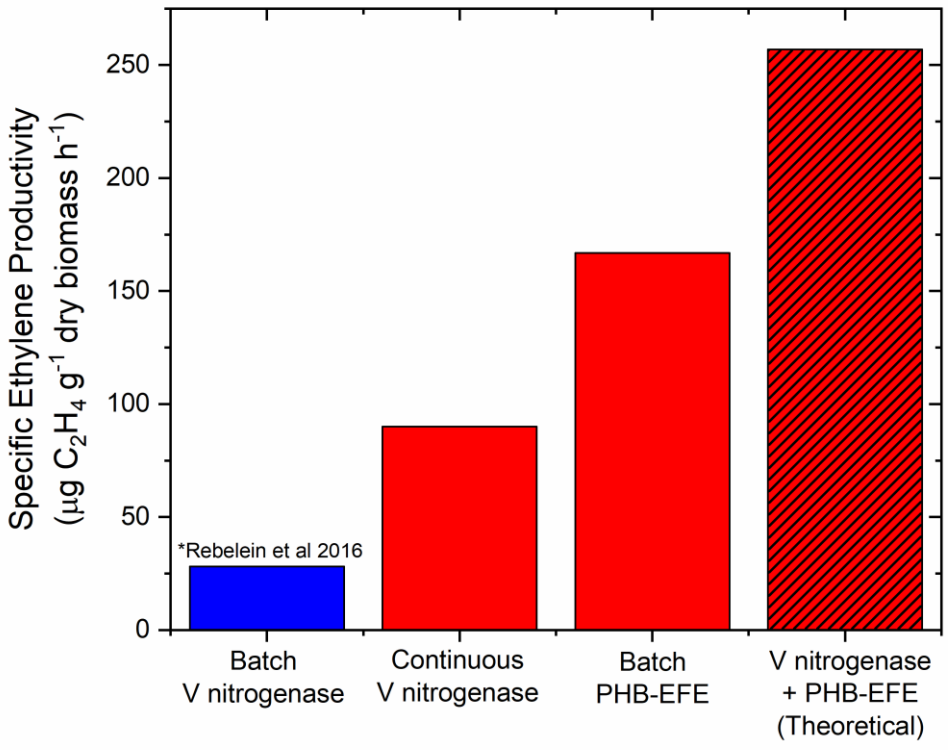

Figure 5.1 Advances in specific ethylene productivity rates from *A. vinelandii*.

While the increases in *in vivo* ethylene productivity made by our group was significant, there is still a need for major improvements if this technology is to ever be adopted by industry

for this purpose. The main reason for this is the value of ethylene has gone down over the past decade due to advances in fracking and cracking technologies, which have increased the supply of non-renewable ethylene substantially. Therefore, any future renewable bio-ethylene production strategy needs to be conscience of this new reality and make low cost of operation a central focus.

For *A. vinelandii*, the cost of production should be relatively cheap, compared to other candidate microorganisms, like *E. coli* or *S. cerevisiae*, because of the aforementioned low-cost substrate requirements (no complex media ingredients required like yeast extract). This is important because, for microbial bio-refineries, media composition is considered to be one of the largest recurring operating costs a business will need to absorb[8,263]. Table 5.1 provides a rough estimate of the raw material media costs of operating a system, similar to our two-stage system in Chapter 3, at industrial scale. The amount of each raw material was extrapolated to represent a bio-refinery operating a 60,000 L seed tank and a 150,000 L reaction vessel continuously with a flow rate of 4,650 L h^{-1}. Bulk material prices were sourced from www.alibaba.com and should be viewed as an approximation of the real value of these commodity chemicals.

Table 5.1 Theoretical annual media cost of operating a 150,000 L reaction vessel at an overall dilution rate of 0.022h^{-1}. Bulk material prices were sourced from www.alibaba.com on September 16th, 2020.

Raw Materials	**Unit cost ($/kg)**	**Quantity used per year (kg)**	**Annual Cost ($)**
Glucose	0.40	809,424	323,770
Magnesium sulfate	0.11	8,094	890
Calcium chloride	0.10	3,642	364
Sodium vanadate	20.00	134	2,671
Iron sulfate	0.13	607	80
Sodium citrate	0.60	20,236	12,160
Potassium phosphate	1.30	40,471	52,653
Water	0.0012	40,471,200	48,565
Total Annual Cost	-	-	**441,153**

From this approximation, it is clear that most of the raw material costs associated with culturing *A. vinelandii* are quite low, even at scale. Glucose is by far the most expensive substrate in the process and would likely be replaced with cheaper plant biomass substitutes later on; assuming some key technical challenges related to nitrogenase regulation can be solved. The

reason *A. vinelandii* can be cultured in such minimal media is that it is capable of generating all of its' required amino acids independently and does not need an external supply of fixed nitrogen or vitamins in order to proliferate[14]. However, in order to know if this process is economical, we would need to know the amount of product that could be produced under these conditions in a given year.

Using the yield and productivity metrics obtained in our work, we could expect this theoretical process to annually produce roughly 250 Mg of hydrogen, 180 Mg of ethylene, 67 Mg of PHB, and 2.2 Mg of heterologous protein (Table 5.2). At the current commodity prices, this would translate to an approximate unit value of $1.44 per kg product, which is well below the estimated unit production cost of $3.03 per kg product (which includes rough estimates for labor, utilities, and other miscellaneous operating costs). The only way to bridge this gap between unit cost and unit value would either be a dramatic change in commodity prices (either substrate cost reduction or product price increase) or a change to the microbial host that increases overall productivity at least 3-fold without increasing cost (Figure 5.2).

Table 5.2 Estimated annual production values and expected revenue from our theoretical industrial-scale *A. vinelandii* 'bio-factory'. Bulk commodity prices were sourced from www.alibaba.com on September 16th, 2020.

Product	**Expected Quantity (kg yr^{-1})**	**Unit Price (US$ kg^{-1})**	**Expected Revenue (US$ yr^{-1})**
Hydrogen	251,000	0.80	199,000
Ethylene	179,000	0.58	104,000
PHB	67,000	3.20	215,000
Protein (SOD)	2,200	90.00	199,000
Total	**499,200**	**1.44**	**717,000**

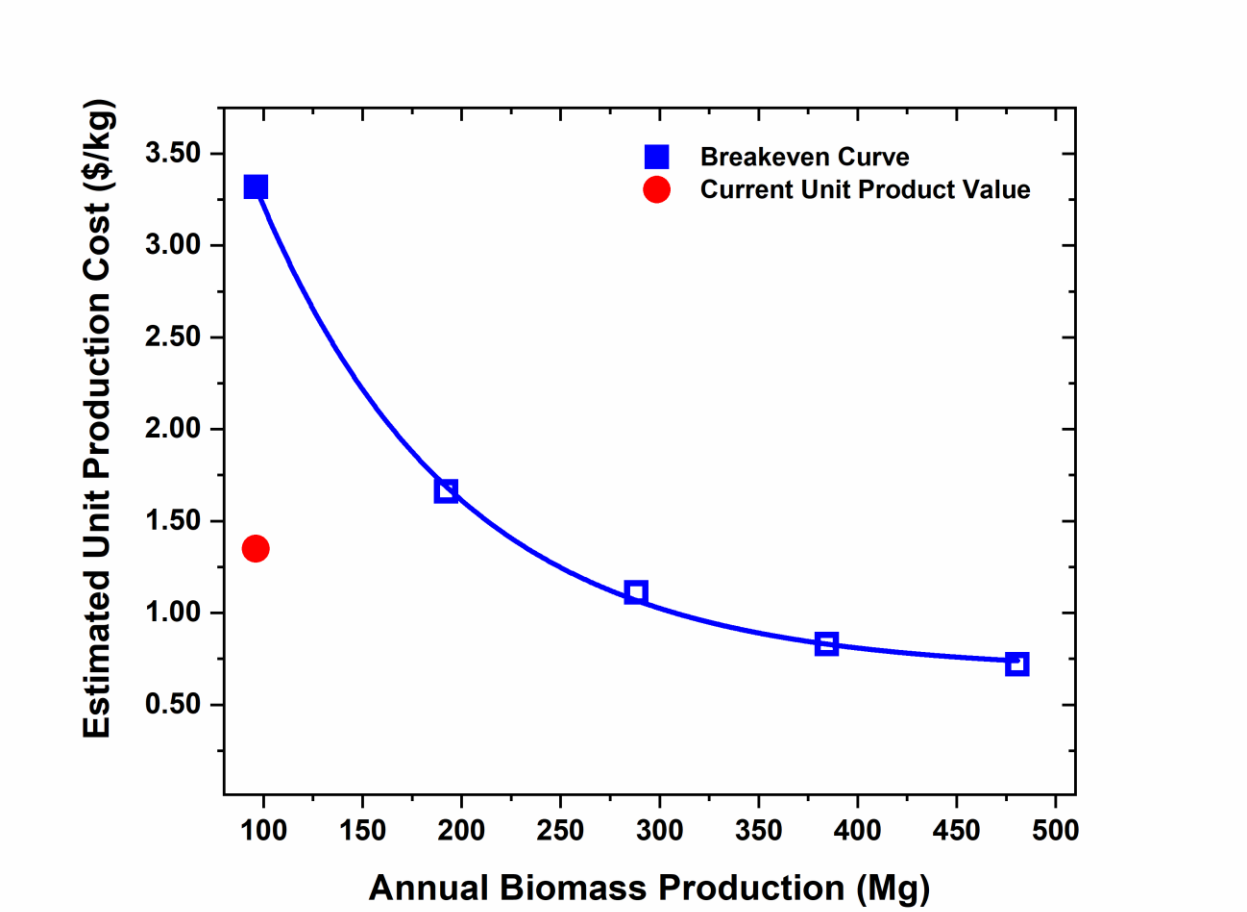

Figure 5.2. Theoretical breakeven curve and sensitivity analysis for an *A. vinelandii* bio-factory.

For our system, an ideal way to boost overall production metrics would be to substantially increase the biomass production in the reaction vessel without sacrificing productivity, which is likely limited by the need to fix atmospheric dinitrogen in the presence of carbon monoxide (Chapter 3). Evidence for this can be seen when looking at the growth characteristics of our CODH-deficient mutant when exposed to 5% CO: which displayed a transient increase in ethylene productivity (due to an increase in soluble CO reaching the V nitrogenase active site) followed by cell death and culture washout (due to the CO outcompeting N_2 for the active site of the V nitrogenase) (Figure 3.3). Therefore, a hypothetical mutant that does not need its nitrogenase for ammonium production should maintain CO reductive coupling under elevated intracellular CO concentrations and thus produce higher ethylene and biomass molar yields. Additionally, such a mutant would allow for cheaper plant biomass residues to be used as a carbon source instead of glucose. These agricultural residues inherently contain fixed

nitrogen compounds and would provide the double benefit of acting as both a carbon and nitrogen source. Finally, the economics of the process could be boosted by government-derived carbon credits, which have been used to incentivize the capture of carbon dioxide from other industrial processes[264]. If these credits can be applied to the reduction of CO in industrial waste gas streams, then this could add another potential revenue stream for this technology.

In addition to strain improvements, certain system modifications may provide additional benefits as well. In Chapter 3 we identified CO mass transfer as a key reaction-limiting factor and found that decreasing the input gas bubble size, by switching to a 0.5 µm microsparger, resulted in significantly higher ethylene productivity rates (Table 3.2). Simply put, the more soluble CO you have, the more ethylene you can produce (up to a certain point). Therefore, a system that promotes the solubilization of gasses would likely be an effective strategy for increasing ethylene and hydrogen yields. For example, researchers in the biotechnology field have long utilized pressurized reactor systems in order to drive the gas-to-liquid condensation reaction and boost oxygen transfer rates and product molar yields[265,266]. Furthermore, these pressurized systems have already been used *in vitro* with purified nitrogenases and CO; resulting in increased ethylene productivity and a shift in product distribution to higher order hydrocarbons; which have more economic value[177]. Therefore, it may be beneficial to culture whole cells of *A. vinelandii* in a pressurized reaction vessel; although another round of growth optimization studies would be needed in order to assess the effects.

In conclusion, I believe we are just scratching the surface of the potential for bio-ethylene production in *A. vinelandii* and future advances could result in this microorganism being utilized in a new green economy.

REFERENCES

1 Bodansky, D. The Paris climate change agreement: a new hope? *The American Journal of International Law* **110**, 288-319 (2016).

2 Maitlis, P. & Zanotti, V. The role of electrophilic species in the Fischer–Tropsch reaction. *Chemical Communications* **0**, 1619-1634, doi:10.1039/B822320N (2009).

3 Le, T.-H., Chang, Y. & Park, D. Renewable and nonrenewable energy consumption, economic growth, and emissions: international evidence. *The Energy Journal* **41** (2020).

4 Sicotte, D. M. From cheap ethane to a plastic planet: Regulating an industrial global production network. *Energy Research & Social Science* **66**, 101479 (2020).

5 Purvis, R. M. *et al.* Effects of 'pre-fracking' operations on ambient air quality at a shale gas exploration site in rural North Yorkshire, England. *Science of the Total Environment* **673**, 445-454 (2019).

6 Black, K., McCoy, S. & Weber, J. The causal impact of fracking on indoor radon levels: a difference-in-difference approach. *Environmental Epidemiology* **3**, 31 (2019).

7 Xu, M. & Xu, Y. Fraccidents: the impact of fracking on road traffic deaths. *Journal of Environmental Economics and Management*, 102303 (2020).

8 Gustavsson, M. & Lee, S. Y. Prospects of microbial cell factories developed through systems metabolic engineering. *Microbial Biotechnology* **9**, 610-617, doi:10.1111/1751-7915.12385 (2016).

9 Lee, S. Y. & Kim, H. U. Systems strategies for developing industrial microbial strains. *Nat. Biotechnol.* **33**, 1061-1072, doi:10.1038/nbt.3365 (2015).

10 Seth-Smith, H. A more convenient truth. *Nature Reviews Microbiology* **5**, 248-250, doi:10.1038/nrmicro1644 (2007).

11 Tchan, Y., New, P. & Genus, I. *Azotobacter beijerinck. Bergey's Manual of Systematic Bacteriology*, 220 (1984).

12 Alden, L., Demoling, F. & Baath, E. Rapid method of determining factors limiting bacterial growth in soil. *Applied and Environmental Microbiology* **67**, 1830-1838, doi:10.1128/aem.67.4.1830-1838.2001 (2001).

13 Page, W. J. Production of poly-β-hydroxybutyrate by *Azotobacter vinelandii* UWD in media containing sugars and complex nitrogen sources. *Appl Microbiol Biotechnol* **38**, 117-121, doi:10.1007/BF00169430 (1992).

14 Revillas, J. J., Rodelas, B., Pozo, C., Martínez-Toledo, M. V. & López, J. G. Production of amino acids by *Azotobacter vinelandii* and *Azotobacter chroococcum* with phenolic compounds as sole carbon source under diazotrophic and adiazotrophic conditions. *Amino Acids* **28**, 421-425, doi:10.1007/s00726-004-0153-x (2005).

15 Wu, F. J., Moreno, J. & Vela, G. R. Growth of *Azotobacter vinelandii* on soil nutrients. *Appl. Environ. Microbiol.* **53**, 489-494 (1987).

16 Kim, B. S. & Chang, H. N. Production of poly (3-hydroxybutyrate) from starch by *Azotobacter chroococcum*. *Biotechnology letters* **20**, 109-112 (1998).

17 Tauchert, K., Jahn, A. & Oelze, J. Control of diauxic growth of *Azotobacter vinelandii* on acetate and glucose. *Journal of Bacteriology* **172**, 6447-6451 (1990).

18 Quiroz-Rocha, E. *et al.* Glucose uptake in *Azotobacter vinelandii* occurs through a GluP transporter that is under the control of the CbrA/CbrB and Hfq-Crc systems. *Scientific Reports* **7**, 1-15 (2017).

19 Conway, T. The Entner-Doudoroff pathway: history, physiology and molecular biology. *FEMS Microbiology Letters* **103**, 1-28, doi:10.1111/j.1574-6968.1992.tb05822.x (1992).

20 Flamholz, A., Noor, E., Bar-Even, A., Liebermeister, W. & Milo, R. Glycolytic strategy as a tradeoff between energy yield and protein cost. *Proceedings of the National Academy of Sciences* **110**, 10039-10044 (2013).

21 Bresters, T. W., De Abreu, R. A., De Kok, A., Veeger, C. & Visser, J. The pyruvate-dehydrogenase complex from *Azotobacter vinelandii*: 1. purification and properties. *European Journal of Biochemistry* **59**, 335-345 (1975).

22 Downs, A. & Jones, C. Respiration-linked proton translocation in *Azotobacter vinelandii*. *FEBS Letters* **60**, 42-46 (1975).

23 Poole, R. K. & Hill, S. Respiratory protection of nitrogenase activity in *Azotobacter vinelandii*—roles of the terminal oxidases. *Bioscience Reports* **17**, 303-317 (1997).

24 Wu, G., Hill, S., Kelly, M. J., Sawers, G. & Poole, R. K. The *cydR* gene product, required for regulation of cytochrome *bd* expression in the obligate aerobe *Azotobacter vinelandii*, is an Fnr-like protein. *Microbiology* **143**, 2197-2207 (1997).

25 Bertsova, Y. V., Bogachev, A. V. & Skulachev, V. P. Two NADH:ubiquinone oxidoreductases of *Azotobacter vinelandii* and their role in the respiratory protection. *Biochimica et Biophysica Acta (BBA) - Bioenergetics* **1363**, 125-133, doi:10.1016/s0005-2728(97)00094-7 (1998).

26 Bertsova, Y. V., Bogachev, A. V. & Skulachev, V. P. Noncoupled NADH: ubiquinone oxidoreductase of *Azotobacter vinelandii* is required for diazotrophic growth at high oxygen concentrations. *Journal of Bacteriology* **183**, 6869-6874 (2001).

27 D'mello, R., Purchase, D., Poole, R. K. & Hill, S. Expression and content of terminal oxidases in *Azotobacter vinelandii* grown with excess NH_4^+ are modulated by O_2 supply. *Microbiology* **143**, 231-237 (1997).

28 Post, E., Kleiner, D. & Oelze, J. Whole cell respiration and nitrogenase activities in *Azotobacter vinelandii* growing in oxygen controlled continuous culture. *Archives of Microbiology* **134**, 68-72 (1983).

29 Page, W. J. & Knosp, O. Hyperproduction of poly-β-hydroxybutyrate during exponential growth of *Azotobacter vinelandii* UWD. *Appl. Environ. Microbiol.* **55**, 1334-1339 (1989).

30 Anderson, A. J. & Dawes, E. A. Occurrence, metabolism, metabolic role, and industrial uses of bacterial polyhydroxyalkanoates. *Microbiology and Molecular Biology Reviews* **54**, 450-472 (1990).

31 Segura, D., Guzmán, J. & Espín, G. *Azotobacter vinelandii* mutants that overproduce poly-β-hydroxybutyrate or alginate. *Appl Microbiol Biotechnol* **63**, 159-163 (2003).

32 Senior, P. J. & Dawes, E. A. The regulation of poly-β-hydroxybutyrate metabolism in *Azotobacter beijerinckii*. *Biochemical Journal* **134**, 225-238 (1973).

33 Hermawan, S. & Jendrossek, D. Microscopical investigation of poly(3-hydroxybutyrate) granule formation in *Azotobacter vinelandii*. *FEMS Microbiology Letters* **266**, 60-64, doi:10.1111/j.1574-6968.2006.00506.x (2007).

34 Saha, S. P. & Paul, A. Intracellular degradation of poly (3-hydroxybutyric acid) accumulated by *Azotobacter chroococcum* MAL-201. *Romanian Archives* **65**, 50 (2005).

35 Yan, Y.-B., Wu, Q. & Zhang, R.-Q. Dynamic accumulation and degradation of poly(3-hydroxyalkanoate)s in living cells of *Azotobacter vinelandii* UWD characterized by ^{13}C NMR. *FEMS Microbiology Letters* **193**, 269-273, doi:10.1111/j.1574-6968.2000.tb09435.x (2000).

36 Sandercock, J. R. & Page, W. J. RpoS expression and the general stress response in *Azotobacter vinelandii* during carbon and nitrogen diauxic shifts. *Journal of Bacteriology* **190**, 946-953, doi:10.1128/jb.01571-06 (2008).

37 Hernandez-Eligio, A., Castellanos, M., Moreno, S. & Espín, G. Transcriptional activation of the *Azotobacter vinelandii* polyhydroxybutyrate biosynthetic genes *phbBAC* by PhbR and RpoS. *Microbiology* **157**, 3014-3023, doi:10.1099/mic.0.051649-0 (2011).

38 Peralta-Gil, M., Segura, D., Guzmán, J., Servín-González, L. & Espín, G. Expression of the *Azotobacter vinelandii* poly-β-hydroxybutyrate biosynthetic *phbBAC* operon is driven by two overlapping promoters and is dependent on the transcriptional activator PhbR. *J. Bacteriol.* **184**, 5672-5677, doi:10.1128/JB.184.20.5672-5677.2002 (2002).

39 Wu, G., Moir, A. J. G., Sawers, G., Hill, S. & Poole, R. K. Biosynthesis of poly-β-hydroxybutyrate (PHB) is controlled by CydR (Fnr) in the obligate aerobe *Azotobacter vinelandii*. *FEMS Microbiology Letters* **194**, 215-220, doi:10.1111/j.1574-6968.2001.tb09472.x (2001).

40 Castañeda, M., Guzmán, J., Moreno, S. & Espín, G. The GacS sensor kinase regulates alginate and poly-β-hydroxybutyrate production in *Azotobacter vinelandii*. *J. Bacteriol.* **182**, 2624-2628, doi:10.1128/JB.182.9.2624-2628.2000 (2000).

41 Hernandez-Eligio, A. *et al.* RsmA post-transcriptionally controls PhbR expression and polyhydroxybutyrate biosynthesis in *Azotobacter vinelandii*. *Microbiology* **158**, 1953-1963, doi:10.1099/mic.0.059329-0 (2012).

42 Jung, Y.-S. & Kwon, Y.-M. Small RNA ArrF regulates the expression of *sodB* and *feSII* genes in *Azotobacter vinelandii*. *Current Microbiology* **57**, 593-597, doi:10.1007/s00284-008-9248-z (2008).

43 Pyla, R., Kim, T.-J., Silva, J. L. & Jung, Y.-S. Overproduction of poly-β-hydroxybutyrate in the *Azotobacter vinelandii* mutant that does not express small RNA ArrF. *Appl Microbiol Biotechnol* **84**, 717-724, doi:10.1007/s00253-009-2002-z (2009).

44 Pyla, R., Kim, T.-J., Silva, J. L. & Jung, Y.-S. Proteome analysis of *Azotobacter vinelandii* Δ*arrF* mutant that overproduces poly-β-hydroxybutyrate polymer. *Appl Microbiol Biotechnol* **88**, 1343-1354, doi:10.1007/s00253-010-2852-4 (2010).

45 Flores, C., Díaz-Barrera, A., Martínez, F., Galindo, E. & Peña, C. Role of oxygen in the polymerization and de-polymerization of alginate produced by *Azotobacter vinelandii*. *Journal of Chemical Technology & Biotechnology* **90**, 356-365 (2015).

46 Lin, L. & Sadoff, H. Encystment and polymer production by *Azotobacter vinelandii* in the presence of β-hydroxybutyrate. *Journal of Bacteriology* **95**, 2336-2343 (1968).

47 Socolofsky, M. & Wyss, O. Cysts of *Azotobacter*. *Journal of Bacteriology* **81**, 946 (1961).

48 Sutherland, I. W. Biosynthesis and composition of Gram-negative bacterial extracellular and wall polysaccharides. *Annual Reviews in Microbiology* **39**, 243-270 (1985).

49 Socolofsky, M. & Wyss, O. Resistance of the *Azotobacter* cyst. *Journal of Bacteriology* **84**, 119-124 (1962).

50 Bush, J. & Wilson, P. A non-gummy chromogenic strain of *Azotobacter vinelandii*. *Nature* **184**, 381-381 (1959).

51 Page, W. & Sadoff, H. Physiological factors affecting transformation of *Azotobacter vinelandii*. *Journal of Bacteriology* **125**, 1080-1087 (1976).

52 Galindo, E., Peña, C., Núñez, C., Segura, D. & Espín, G. Molecular and bioengineering strategies to improve alginate and polydydroxyalkanoate production by *Azotobacter vinelandii*. *Microbial Cell Factories* **6**, 7 (2007).

53 Pacheco-Leyva, I., Guevara Pezoa, F. & Díaz-Barrera, A. Alginate biosynthesis in *Azotobacter vinelandii*: overview of molecular mechanisms in connection with the oxygen availability. *International Journal of Polymer Science* **2016** (2016).

54 Sabra, W., Zeng, A.-P., Lünsdorf, H. & Deckwer, W.-D. Effect of oxygen on formation and structure of *Azotobacter vinelandii* alginate and its role in protecting nitrogenase. *Appl. Environ. Microbiol.* **66**, 4037-4044 (2000).

55 Díaz-Barrera, A., Maturana, N., Pacheco-Leyva, I., Martínez, I. & Altamirano, C. Different responses in the expression of alginases, alginate polymerase and acetylation genes during alginate production by *Azotobacter vinelandii* under oxygen-controlled conditions. *Journal of Industrial Microbiology & Biotechnology* **44**, 1041-1051 (2017).

56 Rehman, Z. U., Wang, Y., Moradali, M. F., Hay, I. D. & Rehm, B. H. Insights into the assembly of the alginate biosynthesis machinery in *Pseudomonas aeruginosa*. *Appl. Environ. Microbiol.* **79**, 3264-3272 (2013).

57 Rehm, B., Boheim, G., Tommassen, J. & Winkler, U. Overexpression of *algE* in *Escherichia coli*: subcellular localization, purification, and ion channel properties. *Journal of Bacteriology* **176**, 5639-5647 (1994).

58 Ertesvag, H. Alginate-modifying enzymes: biological roles and biotechnological uses. *Frontiers in Microbiology* **6**, doi:10.3389/fmicb.2015.00523 (2015).

59 Moreno, S., Nájera, R., Guzmán, J., Soberón-Chávez, G. & Espín, G. Role of alternative sigma factor AlgU in encystment of *Azotobacter vinelandii*. *Journal of Bacteriology* **180**, 2766-2769 (1998).

60 Gaona, G. *et al.* Characterization of the *Azotobacter vinelandii algC* gene involved in alginate and lipopolysaccharide production. *FEMS Microbiology Letters* **238**, 199-206, doi:10.1111/j.1574-6968.2004.tb09756.x (2004).

61 Martinez-Salazar, J. M. *et al.* Characterization of the genes coding for the putative sigma factor AlgU and its regulators MucA, MucB, MucC, and MucD in *Azotobacter vinelandii* and evaluation of their roles in alginate biosynthesis. *Journal of Bacteriology* **178**, 1800-1808 (1996).

62 Núñez, C., León, R., Guzmán, J., Espín, G. & Soberón-Chávez, G. Role of *Azotobacter vinelandii mucA* and *mucC* gene products in alginate production. *Journal of Bacteriology* **182**, 6550-6556 (2000).

63 Glick, B. R., Brooks, H. E. & Pasternak, J. Transformation of *Azotobacter vinelandii* with plasmid DNA. *Journal of Bacteriology* **162**, 276-279 (1985).

64 Glick, B. R., Brooks, H. E. & Pasternak, J. J. Physiological effects of plasmid DNA transformation on *Azotobacter vinelandii*. *Canadian Journal of Microbiology* **32**, 145-148, doi:10.1139/m86-028 (1986).

65 Doran, J., Bingle, W., Roy, K., Hiratsuka, K. & Page, W. Plasmid transformation of *Azotobacter vinelandii* OP. *Microbiology* **133**, 2059-2072 (1987).

66 Glick, B. R. Metabolic load and heterologous gene expression. *Biotechnology Advances* **13**, 247-261 (1995).

67 Summers, D. The kinetics of plasmid loss. *Trends in Biotechnology* **9**, 273-278, doi:10.1016/0167-7799(91)90089-z (1991).

68 Trevors, J. & Starodub, M. Electroporation and expression of the broad host-range plasmid pRK2501 in *Azotobacter vinelandii*. *Enzyme and Microbial Technology* **12**, 653-655 (1990).

69 Kahn, M. *et al.* in *Methods in enzymology* Vol. 68 268-280 (Elsevier, 1979).

70 Page, W. & Von Tigerstrom, M. Optimal conditions for transformation of *Azotobacter vinelandii*. *Journal of Bacteriology* **139**, 1058-1061 (1979).

71 Page, W. J. & Tigerstrom, M. v. Induction of transformation competence in *Azotobacter vinelandii* iron-limited cultures. *Canadian Journal of Microbiology* **24**, 1590-1594 (1978).

72 Renaud, C. S., Pasternak, J. & Glick, B. R. Integration of exogenous DNA into the genome of *Azotobacter vinelandii*. *Archives of Microbiology* **152**, 437-440 (1989).

73 Howard-Flanders, P., West, S. C. & Stasiak, A. Role of RecA protein spiral filaments in genetic recombination. *Nature* **309**, 215-220 (1984).

74 Anderson, D. G. & Kowalczykowski, S. C. The translocating RecBCD enzyme stimulates recombination by directing RecA protein onto ssDNA in a χ-regulated manner. *Cell* **90**, 77-86 (1997).

75 Gumbiner-Russo, L. M. & Rosenberg, S. M. Physical analyses of *E. coli* heteroduplex recombination products *in vivo*: on the prevalence of 5′ and 3′ patches. *PloS One* **2** (2007).

76 Hageman, R. V. & Burris, R. H. Nitrogenase and nitrogenase reductase associate and dissociate with each catalytic cycle. *PNAS* **75**, 2699-2702 (1978).

77 Hageman, R. V. & Burris, R. H. Electron allocation to alternative substrates of *Azotobacter* nitrogenase is controlled by the electron flux through dinitrogenase. *Biochimica et Biophysica Acta (BBA) - Bioenergetics* **591**, 63-75 (1980).

78 Lough, S., Burns, A. & Watt, G. D. Redox reactions of the nitrogenase complex from *Azotobacter vinelandii*. *Biochemistry* **22**, 4062-4066, doi:10.1021/bi00286a011 (1983).

79 Dilworth, M. J., Eldridge, M. E. & Eady, R. R. The molybdenum and vanadium nitrogenases of *Azotobacter chroococcum*: effect of elevated temperature on N2 reduction. *Biochem J* **289**, 395-400 (1993).

80 Bishop, P. E., Hawkins, M. E. & Eady, R. R. Nitrogen fixation in molybdenum-deficient continuous culture by a strain of *Azotobacter vinelandii* carrying a deletion of the structural genes for nitrogenase (*nifHDK*). *Biochem J* **238**, 437-442 (1986).

81 Chisnell, J. R., Premakumar, R. & Bishop, P. E. Purification of a second alternative nitrogenase from a *nifHDK* deletion strain of *Azotobacter vinelandii*. *J. Bacteriol.* **170**, 27-33, doi:10.1128/jb.170.1.27-33.1988 (1988).

82 Pau, R. N., Eldridge, M. E., Lowe, D. J., Mitchenall, L. A. & Eady, R. R. Molybdenum-independent nitrogenases of *Azotobacter vinelandii:* a functional species of alternative nitrogenase-3 isolated from a molybdenum-tolerant strain contains an iron-molybdenum cofactor. *Biochem J* **293**, 101-107 (1993).

83 Eady, R. R., Richardson, T. H., Miller, R. W., Hawkins, M. & Lowe, D. J. The vanadium nitrogenase of *Azotobacter chroococcum*. Purification and properties of the Fe protein. *Biochem J* **256**, 189-196 (1988).

84 Schubert, K. R. & Evans, H. J. Hydrogen evolution: A major factor affecting the efficiency of nitrogen fixation in nodulated symbionts. *Proceedings of the National Academy of Sciences* **73**, 1207-1211, doi:10.1073/pnas.73.4.1207 (1976).

85 Simpson, F. B. & Burris, R. H. A nitrogen pressure of 50 atmospheres does not prevent evolution of hydrogen by nitrogenase. *Science* **224**, 1095-1097 (1984).

86 Drummond, M., Walmsley, J. & Kennedy, C. Expression from the *nifB* promoter of *Azotobacter vinelandii* can be activated by NifA, VnfA, or AnfA transcriptional activators. *J. Bacteriol.* **178**, 788-792, doi:10.1128/jb.178.3.788-792.1996 (1996).

87 Walmsley, J., Toukdarian, A. & Kennedy, C. The role of regulatory genes *nifA*, *vnfA*, *anfA*, *nfrX*, *ntrC*, and *rpoN* in expression of genes encoding the three nitrogenases of *Azotobacter vinelandii*. *Archives of Microbiology* **162**, 422-429, doi:10.1007/bf00282107 (1994).

88 Premakumar, R., Pau, R. N., Mitchenall, L. A., Easo, M. & Bishop, P. E. Regulation of the transcriptional activators AnfA and VnfA by metals and ammonium in *Azotobacter vinelandii*. *FEMS Microbiology Letters* **164**, 63-68, doi:10.1111/j.1574-6968.1998.tb13068.x (1998).

89 Luque, F. & Pau, R. N. Transcriptional regulation by metals of structural genes for *Azotobacter vinelandii* nitrogenases. *Molecular and General Genetics* **227**, 481-487 (1991).

90 Jacobitz, S. & Bishop, P. E. Regulation of nitrogenase-2 in *Azotobacter vinelandii* by ammonium, molybenum, and vanadium. *Journal of Bacteriology* **174**, 3884-3888 (1992).

91 Noar, J. D. & Bruno-Bárcena, J. M. *Azotobacter vinelandii*: the source of 100 years of discoveries and many more to come. *Microbiology* **164**, 421-436, doi:10.1099/mic.0.000643 (2018).

92 Marks, J. A., Perakis, S. S., King, E. K. & Pett-Ridge, J. Soil organic matter regulates molybdenum storage and mobility in forests. *Biogeochemistry* **125**, 167-183, doi:10.1007/s10533-015-0121-4 (2015).

93 Sippel, D. *et al.* Production and isolation of vanadium nitrogenase from *Azotobacter vinelandii* by molybdenum depletion. *J Biol Inorg Chem* **22**, 161-168, doi:10.1007/s00775-016-1423-2 (2017).

94 Kimble, L. K. & Madigan, M. T. Evidence for an alternative nitrogenase in *Heliobacterium gestii*. *FEMS Microbiology Letters* **100**, 255-260, doi:10.1111/j.1574-6968.1992.tb14049.x (1992).

95 Drozd, J. & Postgate, J. Effects of oxygen on acetylene reduction, cytochrome content and respiratory activity of *Azotobacter chroococcum*. *Microbiology* **63**, 63-73 (1970).

96 Dixon, R. *et al.* Regulation of *nif* gene expression in free living diazotrophs: recent advances. *Biological Nitrogen Fixation for the 21st Century*, 87-92 (1998).

97 Shethna, Y., Wilson, P., Hansen, R. E. & Beinert, H. Identification by isotopic substitution of the EPR signal at g=1.94 in a non-heme iron protein from Azotobacter. *Proceedings of the National Academy of Sciences of the United States of America* **52**, 1263 (1964).

98 Lee, H. S., Narberhaus, F. & Kustu, S. *In vitro* activity of NifL, a signal transduction protein for biological nitrogen fixation. *Journal of Bacteriology* **175**, 7683-7688, doi:10.1128/jb.175.23.7683-7688.1993 (1993).

99 Austin, S., Buck, M., Cannon, W., Edymann, T. & Dixon, R. Purification and *in vitro* activities of the native nitrogen fixation control proteins NifA and NifL. *Journal of Bacteriology* **176**, 3460-3465, doi:10.1128/jb.176.12.3460-3465.1994 (1994).

100 Eydmann, T. *et al.* Transcriptional activation of the nitrogenase promoter *in vitro*: adenosine nucleotides are required for inhibition of NIFA activity by NIFL. *Journal of Bacteriology* **177**, 1186-1195, doi:10.1128/jb.177.5.1186-1195.1995 (1995).

101 Hill, S., Austin, S., Eydmann, T., Jones, T. & Dixon, R. *Azotobacter vinelandii* NIFL is a flavoprotein that modulates transcriptional activation of nitrogen-fixation genes via a redox-sensitive switch. *PNAS* **93**, 2143-2148, doi:10.1073/pnas.93.5.2143 (1996).

102 Söderbäck, E. *et al.* The redox-and fixed nitrogen-responsive regulatory protein NIFL from *Azotobacter vinelandii* comprises discrete flavin and nucleotide-binding domains. *Molecular Microbiology* **28**, 179-192 (1998).

103 Scherings, G., Haaker, H., Wassink, H. & Veeger, C. On the formation of an oxygen-tolerant three-component nitrogenase complex from *Azotobacter vinelandii*. *European Journal of Biochemistry* **135**, 591-599, doi:10.1111/j.1432-1033.1983.tb07693.x (1983).

104 Lery, L. M., Bitar, M., Costa, M. G., Rössle, S. C. & Bisch, P. M. Unraveling the molecular mechanisms of nitrogenase conformational protection against oxygen in diazotrophic bacteria. *BMC Genomics* **11**, S7, doi:10.1186/1471-2164-11-s5-s7 (2010).

105 Spatzal, T. The center of biological nitrogen fixation: FeMo-cofactor. *Zeitschrift für anorganische und allgemeine Chemie* **641** (2014).

106 Smith, B. E. Nitrogenase reveals its inner secrets. *Science* **297**, 1654-1655 (2002).

107 Crist, E., Mora, C. & Engelman, R. The interaction of human population, food production, and biodiversity protection. *Science* **356**, 260-264 (2017).

108 Harris, J. O. A study of the effect of growth substrate on the respiration of Azotobacter. *J. Biol. Chem.* **162**, 11-20 (1946).

109 Bali, A., Blanco, G., Hill, S. & Kennedy, C. Excretion of ammonium by a *nifL* mutant of *Azotobacter vinelandii* fixing nitrogen. *Appl Environ Microbiol* **58**, 1711-1718 (1992).

110 Brewin, B., Woodley, P. & Drummond, M. The basis of ammonium release in *nifL* mutants of *Azotobacter vinelandii*. *J. Bacteriol.* **181**, 7356-7362 (1999).

111 Ortiz-Marquez, J. C. F., Nascimento, M. D., Dublan, M. d. l. A. & Curatti, L. Association with an ammonium-excreting bacterium allows diazotrophic culture of oil-rich eukaryotic microalgae. *Appl Environ Microbiol* **78**, 2345-2352, doi:10.1128/AEM.06260-11 (2012).

112 Barney, B. M. *et al.* Transcriptional analysis of an ammonium-excreting strain of *Azotobacter vinelandii* deregulated for nitrogen fixation. *Applied and Environmental Microbiology* **83**, e01534-01517, doi:10.1128/AEM.01534-17 (2017).

113 Kasa, P., Modugapalem, H. & Battini, K. Isolation, screening, and molecular characterization of plant growth promoting rhizobacteria isolates of *Azotobacter* and

Trichoderma and their beneficial activities. *Journal of Natural Science, Biology, and Medicine* **6**, 360 (2015).

114 Bageshwar, U. K. *et al.* An environmentally friendly engineered *Azotobacter* strain that replaces a substantial amount of urea fertilizer while sustaining the same wheat yield. *Applied and Environmental Microbiology* **83**, e00590-00517, doi:10.1128/aem.00590-17 (2017).

115 Barney, B. M., Eberhart, L. J., Ohlert, J. M., Knutson, C. M. & Plunkett, M. H. Gene deletions resulting in increased nitrogen release by *Azotobacter vinelandii*: application of a novel nitrogen biosensor. *Appl Environ Microbiol* **81**, 4316-4328, doi:10.1128/AEM.00554-15 (2015).

116 Mano, N., Mao, F. & Heller, A. A miniature membrane-less biofuel cell operating at+ 0.60 V under physiological conditions. *ChemBioChem* **5**, 1703-1705 (2004).

117 Milton, R. D. *et al.* Bioelectrochemical Haber–Bosch process: an ammonia-producing H_2/N_2 fuel cell. *Angewandte Chemie International Edition* **56**, 2680-2683 (2017).

118 Ortiz-Medina, J. F., Grunden, A. M., Hyman, M. R. & Call, D. F. Nitrogen gas fixation and conversion to ammonium using microbial electrolysis cells. *ACS Sustainable Chemistry & Engineering* **7**, 3511-3519, doi:10.1021/acssuschemeng.8b05763 (2019).

119 Jain, I. Hydrogen the fuel for 21st century. *International Journal of Hydrogen Energy* **34**, 7368-7378 (2009).

120 Winter, C. J. Hydrogen energy - expected engineering breakthroughs. *International Journal of Hydrogen Energy* **12**, 521-546 (1987).

121 Momirlan, M. & Veziroglu, T. N. Current status of hydrogen energy. *Renewable and Sustainable Energy Reviews* **6**, 141-179, doi:10.1016/s1364-0321(02)00004-7 (2002).

122 Miyamoto, K., Hallenbeck, P. C. & Benemann, J. R. Hydrogen production by the thermophilic alga *Mastigocladus laminosus*: effects of nitrogen, temperature, and inhibition of photosynthesis. *Appl. Environ. Microbiol.* **38**, 440-446 (1979).

123 Zajic, J., Kosaric, N. & Brosseau, J. in *Advances in Biochemical Engineering, Volume 9* 57-109 (Springer, 1978).

124 Linkerhägner, K. & Oelze, J. Hydrogenase does not confer significant benefits to *Azotobacter vinelandii* growing diazotrophically under conditions of glucose limitation. *Journal of Bacteriology* **177**, 6018-6020, doi:10.1128/jb.177.20.6018-6020.1995 (1995).

125 Walker, C. C., Partridge, C. D. P. & Yates, M. G. The effect of nutrient limitation on hydrogen production by nitrogenase in continuous cultures of *Azotobacter chroococcum*. *Microbiology* **124**, 317-327, doi:10.1099/00221287-124-2-317 (1981).

126 Kow, Y. W. & Burris, R. H. Purification and properties of membrane-bound hydrogenase from *Azotobacter vinelandii*. *Journal of Bacteriology* **159**, 564-569, doi:10.1128/jb.159.2.564-569.1984 (1984).

127 Seefeldt, L. C. & Arp, D. J. Purification to homogeneity of *Azotobacter vinelandii* hydrogenase: a nickel and iron containing αβ dimer. *Biochimie* **68**, 25-34, doi:10.1016/s0300-9084(86)81064-1 (1986).

128 Walker, C. C. & Yates, M. G. The hydrogen cycle in nitrogen-fixing *Azotobacter chroococcum*. *Biochimie* **60**, 225-231, doi:10.1016/s0300-9084(78)80818-9 (1978).

129 Noar, J., Loveless, T., Navarro-Herrero, J. L., Olson, J. W. & Bruno-Bárcena, J. M. Aerobic hydrogen production via nitrogenase in *Azotobacter vinelandii* CA6. *Appl Environ Microbiol* **81**, 4507-4516, doi:10.1128/AEM.00679-15 (2015).

130 Chain, E. B., Paladino, S., Callow, D. S., Ugolini, F. & van der Sluis, J. Studies on aeration - I. *Bull. World Hlth Org.* **6**, 73-97 (1952).

131 Noar, J. D. & Bruno-Bárcena, J. M. Complete genome sequences of *Azotobacter vinelandii* wild-type strain CA and tungsten-tolerant mutant strain CA6. *Genome Announc.* **1**, e00313-00313 (2013).

132 Menon, A., Mortenson, L. E. & Robson, R. Nucleotide sequences and genetic analysis of hydrogen oxidation (*hox*) genes in *Azotobacter vinelandii*. *J Bacteriol* **174**, 4549-4557, doi:10.1128/jb.174.14.4549-4557.1992 (1992).

133 Sayavedra-Soto, L. A. & Arp, D. J. The *hoxZ* gene of the *Azotobacter vinelandii* hydrogenase operon is required for activation of hydrogenase. *J. Bacteriol.* **174**, 5295-5301, doi:10.1128/jb.174.16.5295-5301.1992 (1992).

134 Ford, C. M. *et al.* The identification, characterization, sequencing and mutagenesis of the genes (*hupSL*) encoding the small and large subunits of the H2-uptake hydrogenase of *Azotobacter chroococcum*. *Molecular Microbiology* **4**, 999-1008, doi:10.1111/j.1365-2958.1990.tb00672.x (1990).

135 Dilworth, M. Acetylene reduction by nitrogen-fixing preparations from *Clostridium pasteurianum*. *Biochimica et Biophysica Acta (BBA)-General Subjects* **127**, 285-294 (1966).

136 Seefeldt, L. C., Yang, Z.-Y., Duval, S. & Dean, D. R. Nitrogenase reduction of carbon-containing compounds. *Biochimica et Biophysica Acta (BBA) - Bioenergetics* **1827**, 1102-1111, doi:10.1016/j.bbabio.2013.04.003 (2013).

137 Chan, M. K., Kim, J. & Rees, D. The nitrogenase FeMo-cofactor and P-cluster pair: 2.2 A resolution structures. *Science* **260**, 792-794 (1993).

138 Kim, J. & Rees, D. Structural models for the metal centers in the nitrogenase molybdenum-iron protein. *Science* **257**, 1677-1682 (1992).

139 Shah, V. K. & Brill, W. J. Isolation of an iron-molybdenum cofactor from nitrogenase. *Proceedings of the National Academy of Sciences* **74**, 3249-3253 (1977).

140 Li, J., Burgess, B. K. & Corbin, J. L. Nitrogenase reactivity: cyanide as substrate and inhibitor. *Biochemistry* **21**, 4393-4402 (1982).

141 Kelly, M., Postgate, J. & Richards, R. Reduction of cyanide and isocyanide by nitrogenase of *Azotobacter chroococcum*. *Biochemical Journal* **102**, 1 (1967).

142 Harris, D. F., Yang, Z.-Y., Dean, D. R., Seefeldt, L. C. & Hoffman, B. M. Kinetic understanding of N_2 reduction versus H_2 evolution at the E4 (4H) Janus state in the three nitrogenases. *Biochemistry* **57**, 5706-5714 (2018).

143 Zheng, Y. *et al.* A pathway for biological methane production using bacterial iron-only nitrogenase. *Nature Microbiology* **3**, 281-286 (2018).

144 McRose, D. L., Zhang, X., Kraepiel, A. M. & Morel, F. M. Diversity and activity of alternative nitrogenases in sequenced genomes and coastal environments. *Frontiers in Microbiology* **8**, 267 (2017).

145 Lee, C. C., Hu, Y. & Ribbe, M. W. Vanadium nitrogenase reduces CO. *Science* **329**, 642-642, doi:10.1126/science.1191455 (2010).

146 Hu, Y., Lee, C. C. & Ribbe, M. W. Extending the carbon chain: hydrocarbon formation catalyzed by vanadium/molybdenum nitrogenases. *Science* **333**, 753-755, doi:10.1126/science.1206883 (2011).

147 Wilson, P. W. & Lind, C. J. Carbon monoxide inhibition of Azotobacter in microrespiration experiments. *J. Bacteriol.* **45**, 219-232 (1943).

148 Rebelein, J. G., Lee, C. C., Hu, Y. & Ribbe, M. W. The *in vivo* hydrocarbon formation by vanadium nitrogenase follows a secondary metabolic pathway. *Nature Communications* **7**, 13641, doi:10.1038/ncomms13641 (2016).

149 Ren, T., Patel, M. & Blok, K. Olefins from conventional and heavy feedstocks: Energy use in steam cracking and alternative processes. *Energy* **31**, 425-451, doi:10.1016/j.energy.2005.04.001 (2006).

150 Vassiliou, M. S. *Historical dictionary of the petroleum industry*. (Rowman & Littlefield, 2018).

151 Leffler, W. L. *Petroleum Refining in Nontechnical Language*. (PennWell Books, 2008).

152 Worrell, E., Phylipsen, D., Einstein, D. & Martin, N. in *Energy use and energy intensity of the US chemical industry*. (Lawrence Berkeley National Laboratory, 2015).

153 Steynberg, A. P. in *Studies in Surface Science and Catalysis* Vol. 152 *Fischer-Tropsch Technology* (eds André Steynberg & Mark Dry) 1-63 (Elsevier, 2004).

154 Maretto, C. & Krishna, R. Modelling of a bubble column slurry reactor for Fischer–Tropsch synthesis. *Catalysis Today* **52**, 279-289 (1999).

155 Khodadadi, A., Hudgins, R. & Silveston, P. Composition modulation of the Fischer-Tropsch synthesis over a supported cobalt catalyst. *The Canadian Journal of Chemical Engineering* **74**, 695-705 (1996).

156 Staffell, I. *et al.* The role of hydrogen and fuel cells in the global energy system. *Energy & Environmental Science* **12**, 463-491 (2019).

157 Laan, G. P. v. d. & Beenackers, A. A. C. M. Kinetics and selectivity of the Fischer–Tropsch synthesis: a literature review. *Catalysis Reviews* **41**, 255-318, doi:10.1081/CR-100101170 (1999).

158 Dry, M. Catalytic aspects of industrial Fischer-Tropsch synthesis. *Journal of Molecular Catalysis* **17**, 133-144 (1982).

159 Liu, G., Larson, E. D., Williams, R. H., Kreutz, T. G. & Guo, X. Making Fischer−Tropsch fuels and electricity from coal and biomass: performance and cost analysis. *Energy Fuels* **25**, 415-437, doi:10.1021/ef101184e (2011).

160 Boerrigter, H. & Calis, H. P. Green diesel from biomass via Fischer-Tropsch synthesis: new insights in gas cleaning and process design. *Pyrolysis and Gasificaiton of Biomass and Waste* **1** (2002).

161 van Vliet, O. P. R., Faaij, A. P. C. & Turkenburg, W. C. Fischer–Tropsch diesel production in a well-to-wheel perspective: a carbon, energy flow and cost analysis. *Energy Conversion and Management* **50**, 855-876, doi:10.1016/j.enconman.2009.01.008 (2009).

162 Primrose, S. Formation of ethylene by *Escherichia coli*. *Microbiology* **95**, 159-165 (1976).

163 Fukuda, H., Takahashi, M., Fujii, T., Tazaki, M. & Ogawa, T. An NADH: Fe (III) EDTA oxidoreductase from *Cryptococcus albidus*: an enzyme involved in ethylene production *in vivo*? *FEMS Microbiology Letters* **60**, 107-111 (1989).

164 Diguiseppi, J. & Fridovich, I. Ethylene from 2-keto-4-thiomethyl butyric acid: The Haber-Weiss reaction. *Arch. Biochem. Biophys.* **205**, 323-329, doi:10.1016/0003-9861(80)90114-9 (1980).

165 North, J. A., Miller, A. R., Wildenthal, J. A., Young, S. J. & Tabita, F. R. Microbial pathway for anaerobic 5′-methylthioadenosine metabolism coupled to ethylene formation. *PNAS* **114**, E10455-E10464, doi:10.1073/pnas.1711625114 (2017).

166 North, J. A. *et al.* A nitrogenase-like enzyme system catalyzes methionine, ethylene, and methane biogenesis. *Science* **369**, 1094-1098 (2020).

167 Nagahama, K. *et al.* Purification and properties of an ethylene-forming enzyme from *Pseudomonas syringae* pv. phaseolicola PK2. *Microbiology* **137**, 2281-2286, doi:10.1099/00221287-137-10-2281 (1991).

168 Fukuda, H. *et al.* Molecular cloning in *Escherichia coli*, expression, and nucleotide sequence of the gene for the ethylene-forming enzyme of *Pseudomonas syringae* pv. phaseolicola PK2. *Biochemical and Biophysical Research Communications* **188**, 826-832, doi:10.1016/0006-291X(92)91131-9 (1992).

169 Eckert, C. *et al.* Ethylene-forming enzyme and bioethylene production. *Biotechnology for Biofuels* **7**, 33, doi:10.1186/1754-6834-7-33 (2014).

170 Fukuda, H. *et al.* Two reactions are simultaneously catalyzed by a single enzyme: The arginine-dependent simultaneous formation of two products, ethylene and succinate, from

2-oxoglutarate by an enzyme from *Pseudomonas syringae*. *Biochemical and Biophysical Research Communications* **188**, 483-489, doi:10.1016/0006-291X(92)91081-Z (1992).

171 Martinez, S. *et al.* Structures and mechanisms of the non-heme Fe (II)-and 2-oxoglutarate-dependent ethylene-forming enzyme: substrate binding creates a twist. *J. Am. Chem. Soc.* **139**, 11980-11988 (2017).

172 Pirkov, I., Albers, E., Norbeck, J. & Larsson, C. Ethylene production by metabolic engineering of the yeast *Saccharomyces cerevisiae*. *Metabolic Engineering* **10**, 276-280 (2008).

173 Wang, J.-P. *et al.* Metabolic engineering for ethylene production by inserting the ethylene-forming enzyme gene (efe) at the 16S rDNA sites of *Pseudomonas putida* KT2440. *Bioresource Technology* **101**, 6404-6409, doi:10.1016/j.biortech.2010.03.030 (2010).

174 Lynch, S., Eckert, C., Yu, J., Gill, R. & Maness, P.-C. Overcoming substrate limitations for improved production of ethylene in *E. coli*. *Biotechnology for Biofuels* **9**, 3, doi:10.1186/s13068-015-0413-x (2016).

175 Ishihara, K. *et al.* Overexpression and *in vitro* reconstitution of the ethylene-forming enzyme from *Pseudomonas syringae*. *J. Ferment. Bioeng.* **79**, 205-211, doi:10.1016/0922-338X(95)90604-X (1995).

176 Dance, I. How does vanadium nitrogenase reduce CO to hydrocarbons? *Dalton Transactions* **40**, 5516-5527, doi:10.1039/C1DT10240K (2011).

177 Yang, Z.-Y., Dean, D. R. & Seefeldt, L. C. Molybdenum nitrogenase catalyzes the reduction and coupling of CO to form hydrocarbons. *J. Biol. Chem.* **286**, 19417-19421, doi:10.1074/jbc.M111.229344 (2011).

178 Hine, P. W. & Lees, H. The growth of nitrogen-fixing *Azotobacter chroococcum* in continuous culture under intense aeration. *Canadian Journal of Microbiology* **22**, 611-618, doi:10.1139/m76-091 (1976).

179 Dalton, H. & Postgate, J. R. Effect of oxygen on growth of *Azotobacter chroococcum* in batch and continuous cultures. *Journal of General Microbiology* **54**, 463-473, doi:10.1099/00221287-54-3-463 (1968).

180 Kuhla, J. & Oelze, J. Dependence of nitrogenase switch-off upon oxygen stress on the nitrogenase activity in *Azotobacter vinelandii*. *Journal of Bacteriology* **170**, 5325-5329 (1988).

181 Carter, I. S. & Dawes, E. A. Effect of oxygen concentration and growth rate on glucose metabolism, poly-β-hydroxybutyrate biosynthesis and respiration of *Azotobacter beijerinckii*. *Microbiology* **110**, 393-400 (1979).

182 Noar, J. D. & Bruno-Bárcena, J. M. Protons and pleomorphs: aerobic hydrogen production in Azotobacters. *World J Microbiol Biotechnol* **32**, 29, doi:10.1007/s11274-015-1980-5 (2016).

183 Menon, A. L., Stults, L. W., Robson, R. L. & Mortenson, L. E. Cloning, sequencing and characterization of the [NiFe] hydrogenase-encoding structural genes (*hoxK* and *hoxG*) from *Azotobacter vinelandii*. *Gene* **96**, 67-74 (1990).

184 Bishop, P. E. *et al.* Nitrogen fixation by *Azotobacter vinelandii* strains having deletions in structural genes for nitrogenase. *Science* **232**, 92-94 (1986).

185 Röckel, D., Hernando, J., Vakalopoulou, E., Post, E. & Oelze, J. Localization and activities of nitrogenase, glutamine synthetase and glutamate synthase in *Azotobacter vinelandii* grown in oxygen-controlled continuous culture. *Archives of Microbiology* **136**, 74-78 (1983).

186 Dingler, C., Kuhla, J., Wassink, H. & Oelze, J. Levels and activities of nitrogenase proteins in *Azotobacter vinelandii* grown at different dissolved oxygen concentrations. *Journal of Bacteriology* **170**, 2148-2152 (1988).

187 Ackrell, B. A. C. & Jones, C. W. The respiratory system of *Azotobacter vinelandii*. 1. Properties of phosphorylating respiratory membranes. *European Journal of Biochemistry* **20**, 22-28, doi:10.1111/j.1432-1033.1971.tb01357.x (1971).

188 Robson, R. L. Characterization of an oxygen-stable nitrogenase complex isolated from *Azotobacter chroococcum*. *Biochemical Journal* **181**, 569-575, doi:10.1042/bj1810569 (1979).

189 Kuhla, J. & Oelze, J. Dependency of growth yield, maintenance and K s-values on the dissolved oxygen concentration in continuous cultures of *Azotobacter vinelandii*. *Archives of Microbiology* **149**, 509-514 (1988).

190 Phillips, D. H. & Johnson, M. J. Aeration in fermentations. *Journal of Biochemical and Microbiological Technology and Engineering* **3**, 277-309 (1961).

191 Nagai, S., Nishizawa, Y., Onodera, M. & Aiba, S. Effect of dissolved oxygen on growth yield and aldolase activity in chemostat culture of *Azotobacter vinelandii*. *Microbiology* **66**, 197-203 (1971).

192 Nagai, S. & Aiba, S. Reassessment of maintenance and energy uncoupling in the growth of *Azotobacter vinelandii*. *Microbiology* **73**, 531-538 (1972).

193 Laane, C., Haaker, H. & Veeger, C. On the efficiency of oxidative phosphorylation in membrane vesicles of *Azotobacter vinelandii* and of *Rhizobium leguminosarum* bacteroids. *European Journal of Biochemistry* **97**, 369-377 (1979).

194 Jones, C. W. & Redfearn, E. R. The cytochrome system of *Azotobacter vinelandii*. *Biochimica et Biophysica Acta (BBA)-Bioenergetics* **143**, 340-353 (1967).

195 Ward, A. C., Rowley, B. I. & Dawes, E. A. Effect of oxygen and nitrogen limitation on poly-β-hydroxybutyrate biosynthesis in ammonium-grown *Azotobacter beijerinckii*. *Microbiology* **102**, 61-68 (1977).

196 Senior, P., Beech, G., Ritchie, G. & Dawes, E. The role of oxygen limitation in the formation of poly-β-hydroxybutyrate during batch and continuous culture of *Azotobacter beijerinckii*. *Biochemical Journal* **128**, 1193-1201 (1972).

197 Jackson, F. A. & Dawes, E. A. Regulation of the tricarboxylic acid cycle and poly-β-hydroxybutyrate metabolism in *Azotobacter beijerinckii* grown under nitrogen or oxygen limitation. *Microbiology* **97**, 303-312 (1976).

198 Senior, P. & Dawes, E. Poly-β-hydroxybutyrate biosynthesis and the regulation of glucose metabolism in *Azotobacter beijerinckii*. *Biochemical Journal* **125**, 55-66 (1971).

199 Bishop, P. E., Jarlenski, D. M. & Hetherington, D. R. Evidence for an alternative nitrogen fixation system in *Azotobacter vinelandii*. *PNAS* **77**, 7342-7346, doi:10.1073/pnas.77.12.7342 (1980).

200 Premakumar, R., Jacobitz, S., Ricke, S. C. & Bishop, P. E. Phenotypic characterization of a tungsten-tolerant mutant of *Azotobacter vinelandii*. *Journal of Bacteriology* **178**, 691-696, doi:10.1128/jb.178.3.691-696.1996 (1996).

201 Runions, J., Hawes, C. & Kurup, S. in *Protein Targeting Protocols* 239-256 (Springer, 2007).

202 Bühler, T. *et al.* Control of respiration and growth yield in ammonium-assimilating cultures of *Azotobacter vinelandii*. *Archives of Microbiology* **148**, 242-246 (1987).

203 Villa, J. A., Ray, E. E. & Barney, B. M. *Azotobacter vinelandii* siderophore can provide nitrogen to support the culture of the green algae *Neochloris oleoabundans* and *Scenedesmus sp.* BA032. *FEMS Microbiology Letters* **351**, 70-77 (2014).

204 Carroll, A. & Somerville, C. Cellulosic Biofuels. *Annual Review of Plant Biology* **60**, 165-182, doi:10.1146/annurev.arplant.043008.092125 (2009).

205 Yoo, C. G. *et al.* Significance of lignin S/G Ratio in biomass recalcitrance of *Populus trichocarpa* variants for bioethanol production. *ACS Sustainable Chemistry & Engineering* **6**, 2162-2168, doi:10.1021/acssuschemeng.7b03586 (2018).

206 Sandoval-Espinola, W. J., Chinn, M. S., Thon, M. R. & Bruno-Bárcena, J. M. Evidence of mixotrophic carbon-capture by n-butanol-producer *Clostridium beijerinckii*. *Scientific Reports* **7**, 1-13, doi:10.1038/s41598-017-12962-8 (2017).

207 Wyman, C. E. Twenty years of trials, tribulations, and research progress in bioethanol technology: selected key events along the way. *Appl. Biochem. Biotechnol.* **91-93**, 5-22, doi:10.1385/abab:91-93:1-9:5 (2001).

208 Rebelein, J. G., Lee, C. C., Newcomb, M., Hu, Y. & Ribbe, M. W. Characterization of an M-cluster-substituted nitrogenase VFe protein. *mBio* **9**, e00310-00318, doi:10.1128/mbio.00310-18 (2018).

209 Poole, R. K. & Hill, S. Respiratory protection of nitrogenase activity in *Azotobacter vinelandii* - roles of the terminal oxidases. *Bioscience Reports* **17**, 303-317 (1997).

210 Hoffmann, M.-C., Pfänder, Y., Fehringer, M., Narberhaus, F. & Masepohl, B. NifA- and CooA-coordinated *cowN* expression sustains nitrogen fixation by *Rhodobacter capsulatus* in the presence of carbon monoxide. *J. Bacteriol.* **196**, 3494-3502, doi:10.1128/JB.01754-14 (2014).

211 Hwang, J. C., Chen, C. H. & Burris, R. H. Inhibition of nitrogenase-catalyzed reductions. *Biochimica et Biophysica Acta (BBA) - Bioenergetics* **292**, 256-270, doi:10.1016/0005-2728(73)90270-3 (1973).

212 Lee, C. C., Hu, Y. & Ribbe, M. W. Unique features of the nitrogenase VFe protein from *Azotobacter vinelandii*. *PNAS* **106**, 9209-9214, doi:10.1073/pnas.0904408106 (2009).

213 Yan, L. *et al.* IR-monitored photolysis of CO-inhibited nitrogenase: a major EPR-silent species with coupled terminal CO ligands. *Chemistry – A European Journal* **18**, 16349-16357, doi:10.1002/chem.201202072 (2012).

214 Bergersen, F. The quantitative relationship between nitrogen fixation and the acetylene-reduction assay. *Australian Journal of Biological Sciences* **23**, 1015-1026, doi:10.1071/bi9701015 (1970).

215 Scott, D. J., Dean, D. R. & Newton, W. E. Nitrogenase-catalyzed ethane production and CO-sensitive hydrogen evolution from MoFe proteins having amino acid substitutions in an alpha-subunit FeMo cofactor-binding domain. *J. Biol. Chem.* **267**, 20002-20010 (1992).

216 Natzke, J., Noar, J. & Bruno-Bárcena, J. M. *Azotobacter vinelandii* nitrogenase activity, hydrogen production, and response to oxygen exposure. *Appl Environ Microbiol* **84**, doi:10.1128/AEM.01208-18 (2018).

217 Rehder, D. Vanadium nitrogenase. *Journal of Inorganic Biochemistry* **80**, 133-136, doi:10.1016/s0162-0134(00)00049-0 (2000).

218 McFarland, M. J., Vogel, C. M. & Spain, J. C. Methanotrophic cometabolism of trichloroethylene (TCE) in a two stage bioreactor system. *Water Research* **26**, 259-265, doi:10.1016/0043-1354(92)90227-U (1992).

219 Shen, H. & Wang, Y.-T. Hexavalent chromium removal in two-stage bioreactor system. *J. Environ. Eng.* **121**, 798-804, doi:10.1061/(ASCE)0733-9372(1995)121:11(798) (1995).

220 Bruno-Bárcena, J. M., Ragout, A. L., Córdoba, P. R. & Siñeriz, F. Continuous production of L(+)-lactic acid by *Lactobacillus casei* in two-stage systems. *Appl Microbiol Biotechnol* **51**, 316-324, doi:10.1007/s002530051397 (1999).

221 Fascetti, E. & Todini, O. *Rhodobacter sphaeroides* RV cultivation and hydrogen production in a one- and two-stage chemostat. *Appl Microbiol Biotechnol* **44**, 300-305, doi:10.1007/BF00169920 (1995).

222 Linkerhägner, K. & Oelze, J. Nitrogenase activity and regeneration of the cellular ATP pool in *Azotobacter vinelandii* adapted to different oxygen concentrations. *J. Bacteriol.* **179**, 1362-1367, doi:10.1128/jb.179.4.1362-1367.1997 (1997).

223 Deichmann, U., Schuster, S., Mazat, J.-P. & Cornish-Bowden, A. Commemorating the 1913 Michaelis-Menten paper *Die Kinetik der Invertinwirkung*: three perspectives. *FEBS Journal* **281**, 435-463, doi:10.1111/febs.12598 (2014).

224 Ismail, K. S. K., Najafpour, G., Younesi, H., Mohamed, A. R. & Kamaruddin, A. H. Biological hydrogen production from CO: Bioreactor performance. *Biochemical Engineering Journal* **39**, 468-477, doi:10.1016/j.bej.2007.11.003 (2008).

225 Puthli, M. S., Rathod, V. K. & Pandit, A. B. Gas–liquid mass transfer studies with triple impeller system on a laboratory scale bioreactor. *Biochemical Engineering Journal* **23**, 25-30, doi:10.1016/j.bej.2004.10.006 (2005).

226 Riggs, S. S. & Heindel, T. J. Measuring carbon monoxide gas—liquid mass transfer in a stirred tank reactor for syngas fermentation. *Biotechnol. Prog.* **22**, 903-906, doi:10.1021/bp050352f (2006).

227 Zhu, Y., Bandopadhayay, P. C. & Wu, J. Measurement of gas-liquid mass transfer in an agitated vessel—a comparison between different impellers. *J. Chem. Eng. Japan* **34**, 579-584, doi:10.1252/jcej.34.579 (2001).

228 Bredwell, M. D. & Worden, R. M. Mass-Transfer Properties of Microbubbles. 1. Experimental Studies. *Biotechnol. Prog.* **14**, 31-38, doi:10.1021/bp970133x (1998).

229 Hu, Y., Chung Lee, C. & W. Ribbe, M. Vanadium nitrogenase: A two-hit wonder? *Dalton Transactions* **41**, 1118-1127, doi:10.1039/C1DT11535A (2012).

230 Setubal, J. C. *et al.* Genome sequence of *Azotobacter vinelandii*, an obligate aerobe specialized to support diverse anaerobic metabolic processes. *J. Bacteriol.* **191**, 4534-4545, doi:10.1128/JB.00504-09 (2009).

231 Jeoung, J. H. & Dobbek, H. Carbon dioxide activation at the Ni,Fe-cluster of anaerobic carbon monoxide dehydrogenase. *Science* **318**, 1461-1464, doi:10.1126/science.1148481 (2007).

232 Pirt, J. S. *Principles of microbe and cell cultivation*. (Blackwell Scientific Publications, 1975).

233 Lim, H. C., Chen, B. J. & Creagan, C. C. An analysis of extended and exponentially-fed-batch cultures. *Biotechnology and Bioengineering* **19**, 425-433, doi:10.1002/bit.260190312 (1977).

234 Castillo, T., Heinzle, E., Peifer, S., Schneider, K. & Peña M, C. F. Oxygen supply strongly influences metabolic fluxes, the production of poly(3-hydroxybutyrate) and alginate, and the degree of acetylation of alginate in *Azotobacter vinelandii*. *Process Biochemistry* **48**, 995-1003, doi:10.1016/j.procbio.2013.04.014 (2013).

235 Steinbüchel, A. Polyhydroxyalkanoic acids. *Biomaterials* (1991).

236 Surendran, A. *et al.* Can polyhydroxyalkanoates be produced efficiently from waste plant and animal oils? *Frontiers in Bioengineering and Biotechnology* **8** (2020).

237 Sabapathy, P. C. *et al.* Recent developments in Polyhydroxyalkanoates (PHAs) production in the past decade–a review. *Bioresource Technology*, 123132 (2020).

238 Peters, V. & Rehm, B. H. *In vivo* enzyme immobilization by use of engineered polyhydroxyalkanoate synthase. *Appl. Environ. Microbiol.* **72**, 1777-1783 (2006).

239 Jahns, A. C. & Rehm, B. H. A. Tolerance of the *Ralstonia eutropha* class I polyhydroxyalkanoate synthase for translational fusions to its C terminus reveals a new mode of functional display. *Appl Environ Microbiol* **75**, 5461-5466, doi:10.1128/AEM.01072-09 (2009).

240 Rehm, F. B., Chen, S. & Rehm, B. H. Bioengineering toward direct production of immobilized enzymes: a paradigm shift in biocatalyst design. *Bioengineered* **9**, 6-11 (2018).

241 Altermann, E., Schofield, L. R., Ronimus, R. S., Beattie, A. K. & Reilly, K. Inhibition of rumen methanogens by a novel archaeal lytic enzyme displayed on tailored bionanoparticles. *Frontiers in Microbiology* **9**, 2378 (2018).

242 Robins, K. J., Hooks, D. O., Rehm, B. H. & Ackerley, D. F. *Escherichia coli* NemA is an efficient chromate reductase that can be biologically immobilized to provide a cell free system for remediation of hexavalent chromium. *PloS One* **8** (2013).

243 Grage, K. *et al.* Bacterial polyhydroxyalkanoate granules: biogenesis, structure, and potential use as nano-/micro-beads in biotechnological and biomedical applications. *Biomacromolecules* **10**, 660-669 (2009).

244 Shrivastav, A., Kim, H.-Y. & Kim, Y.-R. Advances in the applications of polyhydroxyalkanoate nanoparticles for novel drug delivery system. *BioMed Research international* **2013** (2013).

245 Yao, Y.-C. *et al.* A specific drug targeting system based on polyhydroxyalkanoate granule binding protein PhaP fused with targeted cell ligands. *Biomaterials* **29**, 4823-4830, doi:10.1016/j.biomaterials.2008.09.008 (2008).

246 Banki, M. R., Gerngross, T. U. & Wood, D. W. Novel and economical purification of recombinant proteins: Intein-mediated protein purification using *in vivo* polyhydroxybutyrate (PHB) matrix association. *Protein Science* **14**, 1387-1395, doi:10.1110/ps.041296305 (2009).

247 Barnard, G. C., McCool, J. D., Wood, D. W. & Gerngross, T. U. Integrated recombinant protein expression and purification platform based on *Ralstonia eutropha*. *Appl. Environ. Microbiol.* **71**, 5735-5742 (2005).

248 Mato, A. *et al.* Dissecting the polyhydroxyalkanoate-binding domain of the PhaF phasin: rational design of a minimized affinity tag. *Appl Environ Microbiol* **86** (2020).

249 Natzke, J. & Bruno-Bárcena, J. M. Two-stage continuous conversion of carbon monoxide to ethylene by whole cells of Azotobacter vinelandii. *Appl Environ Microbiol* **86** (2020).

250 Weingart, H. & Volksch, B. Ethylene production by *Pseudomonas syringae* pathovars *in vitro* and *in planta*. *Appl. Environ. Microbiol.* **63**, 156-161 (1997).

251 Johansson, N., Persson, K. O., Norbeck, J. & Larsson, C. Expression of NADH-oxidases enhances ethylene productivity in *Saccharomyces cerevisiae* expressing the bacterial EFE. *Biotechnol Bioproc E* **22**, 195-199, doi:10.1007/s12257-016-0602-x (2017).

252 Veetil, V. P., Angermayr, S. A. & Hellingwerf, K. J. Ethylene production with engineered *Synechocystis sp PCC 6803* strains. *Microbial Cell Factories* **16**, 34 (2017).

253 Díaz-Barrera, A., Andler, R., Martínez, I. & Peña, C. Poly-3-hydroxybutyrate production by *Azotobacter vinelandii* strains in batch cultures at different oxygen transfer rates. *Journal of Chemical Technology & Biotechnology* **91**, 1063-1071, doi:10.1002/jctb.4684 (2016).

254 Weingart, H., Völksch, B. & Ullrich, M. S. Comparison of ethylene production by *Pseudomonas syringae* and *Ralstonia solanacearum*. *Phytopathology* **89**, 360-365, doi:10.1094/PHYTO.1999.89.5.360 (1999).

255 Muriel-Millán, L. F., Castellanos, M., Hernandez-Eligio, J. A., Moreno, S. & Espín, G. Posttranscriptional regulation of PhbR, the transcriptional activator of polyhydroxybutyrate synthesis, by iron and the sRNA ArrF in *Azotobacter vinelandii*. *Appl Microbiol Biotechnol* **98**, 2173-2182 (2014).

256 Hamilton, T. L. *et al.* Transcriptional profiling of nitrogen fixation in *Azotobacter vinelandii*. *J. Bacteriol.* **193**, 4477-4486 (2011).

257 Salgado, H., Moreno-Hagelsieb, G., Smith, T. F. & Collado-Vides, J. Operons in *Escherichia coli*: genomic analyses and predictions. *PNAS* **97**, 6652-6657 (2000).

258 De Hoon, M. J., Makita, Y., Nakai, K. & Miyano, S. Prediction of transcriptional terminators in *Bacillus subtilis* and related species. *PLoS Comput Biol* **1**, e25 (2005).

259 Salamov, V. S. A. & Solovyevand, A. Automatic annotation of microbial genomes and metagenomic sequences. *Metagenomics and its applications in agriculture, biomedicine and environmental studies. Hauppauge: Nova Science Publishers*, 61-78 (2011).

260 Kapust, R. B., Tözsér, J., Copeland, T. D. & Waugh, D. S. The P1′ specificity of tobacco etch virus protease. *Biochemical and Biophysical Research Communications* **294**, 949-955 (2002).

261 Page, W. J. Suitability of commercial beet molasses fractions as substrates for polyhydroxyalkanoate production by *Azotobacter vinelandii* UWD. *Biotechnology Letters* **14**, 385-390, doi:10.1007/bf01021252 (1992).

262 Natzke, J. & Bruno-Bárcena, J. M. Two-stage continuous conversion of carbon monoxide to ethylene by whole cells of *Azotobacter vinelandii*. *Applied and Environmental Microbiology* (2020).

263 Tejayadi, S. & Cheryan, M. Lactic acid from cheese whey permeate. Productivity and economics of a continuous membrane bioreactor. *Appl Microbiol Biotechnol* **43**, 242-248 (1995).

264 Mathews, J. A. How carbon credits could drive the emergence of renewable energies. *Energy Policy* **36**, 3633-3639 (2008).

265 Knoll, A. *et al.* High cell density cultivation of recombinant yeasts and bacteria under non-pressurized and pressurized conditions in stirred tank bioreactors. *Journal of Biotechnology* **132**, 167-179 (2007).

266 Magnin, J.-P. & Deseure, J. Hydrogen generation in a pressurized photobioreactor: Unexpected enhancement of biohydrogen production by the phototrophic bacterium *Rhodobacter capsulatus*. *Applied Energy* **239**, 635-643, doi:10.1016/j.apenergy.2019.01.204 (2019).